A method for implementing performance monitoring on deep-level mine bulk air coolers

E Ezendam

orcid.org/ 0000-0001-8247-8590

Dissertation accepted in fulfilment of the requirements for the degree *Master of Engineering in Mechanical Engineering* at the North-West University

Supervisor: Dr JC Vosloo

Graduation: November 2023

ABSTRACT

Title: A method for implementing condition monitoring on deep-level mine bulk air coolers

Author: Enco Ezendam

Supervisor: Dr. Jan Vosloo

Co – Supervisor: Dr. Jean van Laar

Degree: Master of Engineering (M.Eng) in Mechanical Engineering

Keywords: Deep-level mine, Condition monitoring, Heat exchangers, Dimensional analysis, Buckingham Pi.

Deep-level mining faces significant ventilation challenges, primarily due to increased heating effects from auto-compression and geothermal heat. To address these challenges and to maintain a safe and productive working environment, tertiary spot coolers like Finned Tube Bulk Air Coolers (FBACs) are employed to cool the ventilation air before it reaches the working areas. However, FBACs become less efficient over time, leading to higher temperatures in the working areas and adversely affecting mining safety, sustainability, and productivity.

Monitoring the condition of these FBACs proves challenging due to remote installation locations and off-design operating conditions among others. Additionally, existing literature lacks effective methods to implement condition monitoring on these FBACs, with the majority of existing literature focussing mainly on heat exchangers operating at design conditions to detect fouling.

This dissertation presents an innovative condition monitoring method tailored for FBACs operating under these challenging conditions to address the identified gap in literature. The method involves using a normalised prediction model and original equipment manufacturer (OEM) data to forecast the FBAC's outlet temperature based on inlet conditions. By comparing the forecasted and measured temperatures, the condition of the FBACs can be inferred.

The method was applied to a deep-level mine with seven case study FBACs, accurately forecasting outlet temperatures within 0.35 °C of the OEM data (R^2 = 0.9678; n = 448). The analysis revealed significant temperature deviations of up to 6.09 °C in poorly performing FBACs, indicating inefficiencies and resulting in estimated production losses of up to R68 570 505, due to reduced worker efficiency. Subsequent investigations confirmed these inefficiencies, and corrective maintenance is currently underway on these FBACs.

PREFACE AND ACKNOWLEDGEMENTS

As the author of this study, I would love to express my sincere gratitude to the following parties:

My God - who has blessed me with the insight, motivation, passion, energy, and goodwill to undertake and complete this dissertation. I thank you Lord, for every moment that I had the pleasure of conducting this research and for Your continued presence in my life.

My Parents - Lida and Freddy Ezendam, for your unconditional love and support during any undertaking that I pursue. Thank you for raising me with the morals and values that I carry with me every day. I thank our Father every day for giving me the greatest gift that is the parents that I'm privileged to call my own. May this dissertation be an ode to the effort and love you both have invested in me.

My Mentors and Work Colleagues - Dr. Jan Vosloo and Dr. Jean van Laar for your valuable and wise inputs guiding this dissertation. Renier Mulder for your mentorship and guidance in my early career. Dr. Charl Cilliers for your inputs and guidance during the starting days of conducting this dissertation, in addition to my early career. And to all my other work colleagues for the support throughout the highs and lows experienced during this undertaking.

ETA Operations and IPGIP - for the opportunity and resources invested that allowed me to conduct this study and write this dissertation.

And thank you to all the remaining family, friends and colleagues not specifically mentioned for all of your support, guidance, sacrifice and belief in me.

TABLE OF CONTENTS

ABSTRACT II

PREFACE AND ACKNOWLEDGEMENTS IV

TABLE OF CONTENTS V

LIST OF FIGURES VI

LIST OF TABLES IX

NOMENCLATURE XI

LIST OF ABBREVIATIONS XII

CHAPTER 1 INTRODUCTION AND LITERATURE REVIEW 1

1.1 HISTORY AND CHALLENGES OF DEEP-LEVEL MINING 1

1.2 DEEP-LEVEL MINE VENTILATION AND REFRIGERATION 2

1.3 FINNED TUBE BULK AIR COOLERS 7

1.4 IMPACTS OF INEFFICIENCIES ON FBAC COOLING PERFORMANCE 9

1.5 CONSEQUENCES OF HIGH TEMPERATURES IN THE WORKING PLACES 10

1.6 ADDRESSING THE IMPACTS OF INEFFICIENCIES 12

1.7 REVIEW OF EXISTING CONDITION MONITORING METHODS OF INDUSTRIAL HEAT EXCHANGERS 12

1.8 PROBLEM AND NEED FOR THE STUDY 24

1.9 STUDY OBJECTIVES 25

1.10 RESEARCH APPROACH 26

1.11 STUDY CHAPTER OVERVIEW 27

CHAPTER 2 METHOD OUTLINE 29

2.1 CHAPTER PREAMBLE 29

2.2 OVERVIEW OF METHOD 29

2.3 PHASE 1: PARAMETER NORMALIZATION 31

2.4 PHASE 2: DEVELOPMENT OF PREDICTION MODEL 42

2.5 PHASE 3: IMPLEMENTATION OF PREDICTION MODEL 50

2.6 SUMMARY REVIEW OF METHOD COMPLIANCE TO STUDY OBJECTIVES 58

CHAPTER 3 METHOD IMPLEMENTATION 60

3.1 CHAPTER PREAMBLE 60

3.2 CASE STUDY BACKGROUND 60

3.3 RESULTS - PHASE 1: PARAMETER NORMALIZATION 62

3.4 RESULTS – PHASE 2: DEVELOPMENT OF PREDICTION MODEL 64

3.5 RESULTS – PHASE 3: IMPLEMENTATION OF PREDICTION MODEL 68

3.6 SUMMARY OVERVIEW OF RESULTS 81

CHAPTER 4 CONCLUSION, LIMITATIONS AND RECOMENDATIONS 83

4.1 OVERVIEW OF THE STUDY 83

4.2 REVIEW OF COMPLIANCE TO STUDY OBJECTIVES 84

4.3 STUDY LIMITATIONS AND FUTURE RECOMMENDATIONS 87

4.4 STUDY CLOSURE 90

REFERENCE LIST 91

APPENDIX A – PROCESS OF DIMENSIONAL ANALYSIS 97

APPENDIX B – FBAC MONITORING GRAPHS 100

APPENDIX C – OEM DESIGN TABLES 104

APPENDIX D – PREDICTION MODEL CHARACTERISTIC EQUATION 108

APPENDIX E – LITERATURE REVIEW SUMMARY 109

LIST OF FIGURES

Figure 1: (a) Global decline in gold ore grade (adapted from [1]) (b) Decline in South African gold ore grade from 1880 to 2005 (adapted from [2]–[4]) 1

Figure 2: Illustration of a conventional mine ventilation network (adapted from [16]) 3

Figure 3: Increase in cooling requirements as the mining depth increases (redrawn from [5]) 4

Figure 4: Mine refrigeration requirements as a function of mining depth (redrawn from [17]) 4

Figure 5: Spray tubes of an underground spray chamber bulk air cooler (Adapted from [17]) 5

Figure 6: Hierarchy of cooling infrastructure in mines used as a function of depth. (adapted from [18]) 6
Figure 7: Different tertiary spot coolers used in deep-level mines: (left) Finned tube bulk air cooler (FBAC). (right) cooling coil (adapted from [17]) 7
Figure 8: Heat exhaustion cases in a deep underground mine as a function of working place temperature condition. (adapted from [11]) 10
Figure 9: Effects of working place temperatures on work efficiency (adapted from [37]) 11
Figure 10: Operating principal behind infrared thermography for the detection of fouling (adapted from [47]) 16
Figure 11: Effect of fouling indicated by infrared thermography as found by Berce *et. al* (adapted from [46]) 17
Figure 12: Fouling growth detected by comparing the acoustic emission power to the pressure drop growth (adapted from [52]) 18
Figure 13: Accuracy of the proposed method of vibrational analysis. (adapted from [45]) 19
Figure 14: Increase in pressure drop in time over the length of a heat exchanger due to fouling. (adapted from [43]) 21
Figure 15: (a) Pressure drop increases over time due to the onset of inefficiencies in a heat exchanger in the refinery industry, with an (b) associated drop in performance of the heat exchanger seen (adapted from [29]) 21
Figure 16: Decline in overall heat transfer coefficient with subsequent rise in temperature over time in a heat exchanger due to fouling (adapted from [43]) 22
Figure 17: Overview of the case study research methodology 26
Figure 18: Holistic overview of the condition monitoring method presented (Self illustration). 30
Figure 19: Overview of the first phase of the method (Self-illustration) 31
Figure 20: The first step for Phase 1 of the method (Self-illustration) 31
Figure 21: Schematic illustration of the three primary operating sides around a general radiator-type heat exchanger (Self-illustration) 32
Figure 22: The second step for Phase 1 of the method (Self-illustration) 33
Figure 23: The third step for Phase 1 of the method (Self-illustration). 35
Figure 24: The fourth step for Phase 1 of the method (Self-illustration) 37
Figure 25: Common system parameters and their corresponding base units (adapted from [62]) 37
Figure 26: The fifth and final step for Phase 1 of the method (Self-illustration) 39
Figure 27: Overview of the second phase of the method, with each of the three respective sub-phases (Self-illustration) 42
Figure 28: First sub-phase for Phase 2 of the method (Self-illustration) 43
Figure 29: Second sub-phase for Phase 2 of the method (Self-illustration) 45
Figure 30: Use of calibration data in both dimensionless groups to obtain the characteristic equation (Adapted from [60]) 46

Figure 31 Third and final sub-phase for Phase 2 of the method (Self-illustration) 47
Figure 32: (a) Correlation between predicted vs observed outlet temperature for the jacketed shell-and-tube heat exchanger (adapted from [64]). (b) Correlation between predicted vs observed rich amine exit temperatures (adapted from [60]). 49
Figure 33: Overview of the third phase for the method (Self-illustration) 50
Figure 34: First sub-phase for Phase 3 of the method (Self-illustration) 51
Figure 35: Data acquisition process (adapted from [65]) 52
Figure 36: Second sub-phase for Phase 3 of the method (Self-illustration) 53
Figure 37: (a) Gas outlet temperatures of the HX obtained by the prediction model compared to the observed gas outlet temperatures (adapted from [64]). (b) Water outlet temperatures of the HX obtained by the prediction model compared to the observed water outlet temperatures (adapted from [60]) 54
Figure 38: Third and final sub-phase for Phase 3 of the method (Self-illustration) 55
Figure 39: Example comparison of (n) amounts of FBAC outlet temperature deviations from the predicted outlet air temperature, showing a clear hierarchy of FBAC condition, ranging from highest deviation to lowest deviation (Self illustration). 56
Figure 40: Example of FBAC condition ranking based on the deviation of outlet air temperature from the predicted outlet temperature. Adapted from Figure 38 (Self-illustration) 56
Figure 41: FBAC with the most severe condition of degradation identified from the condition ranking shown in the example in Figure 39 (Self-illustration) 57
Figure 42: Schematic layout of the four production levels with their respective FBACs located on Mine A. The production levels consist of an eastern and western side, each supplied by a FBAC. The working place areas are denoted in green (Self illustration) 60
Figure 43: Schematic layout of a FBAC found on Mine A (adapted from [23]) 61
Figure 44: Characteristic curve from the data sets obtained when applying OEM design conditions (n=448) to the respective parameters in the obtained normalised system relationship outlined in Section 2.4.2. 65
Figure 45: Correlation between the predicted outlet air temperature of the FBAC characteristic equation and the OEM specified outlet air temperature for the same set of inlet conditions (n=448). 67
Figure 46: Schematic of a FBAC cooling loop with associated sensor placements, located on Mine A (Self-illustration) 68
Figure 47: Environmental sensor located at the inlet of the FBAC loops at Mine A. (Photo taken by author) 69
Figure 48: Vane measuring wind speed of air at the entrance of the FBAC. (Photo taken by author) 69
Figure 49: Comparison obtained of the model predicted outlet temperature versus the measured outlet temperature over the initial evaluation period for FBAC 3. 72
Figure 50: Moving average trendline applied to the raw data from Figure 48 73

Figure 51: Corrosion as well as external fouling is visible on the heat transfer surfaces. Unaffected refurbished cooling banks can be seen at the bottom left (Photo taken by author) 74
Figure 52: External fouling and corrosion observed on the heat transfer surfaces (Photo taken by author) 75
Figure 53: Gaping hole in wall identified above the mainline supply piping (Photo taken by author)..... 75
Figure 54: Condition ranking of the average wet- bulb air temperature deviations obtained by implementing the prediction model over the evaluation period. 77
Figure 55: Average monthly production loss estimates due to temperature deviations from design at the respective FBACs evaluated (continued from Figure 53)..... 77
Figure 56: Two-year monitoring comparison of the outlet temperatures for FBAC 6 obtained, showcasing the impact of inefficiencies present on the cooling performance. 78
Figure 57 : (a) Inactive piping (b) Damage ,fouling and calcification on the heat transfer surface (c) Broken ventilation door leaking air past the cooling banks (d) Corrosion and external fouling present on the heat transfer surface (Photos taken by author)..... 79
Figure 58: Calcification seen on the heat transfer surface of the cooling bank (Photo taken by author).... 80

LIST OF TABLES

Table 1: Example - System parameters identified that will affect the performance and operation of a FBAC 32
Table 2: Remaining system parameters after all non-time variant parameters have been eliminated [60], [61]..... 34
Table 3: The air outlet temperature is chosen as the performance parameter 35
Table 4: Remaining system parameters with the performance parameter highlighted..... 38
Table 5: Summary of the compliance of each phase in the method to the study objectives put forth in section 1.9 58
Table 6: Remaining time-variant operating parameters around at the FBAC obtained 63
Table 7: Remaining time variant operating parameters obtained with chosen "performance parameter”. 63
Table 8: Correlation and prediction errors of each respective curve fit investigated when compared to the OEM specified outlet temperature at the same inlet conditions: 65
Table 9: Comparison of different order polynomials used as curve fits investigated with their respective correlations and prediction errors when compared to the OEM design specified outlet air temperature. 66
Table 10: Sample sise of remaining data sets used for analysis after filtering. 71
Table 11: Operating ranges (5^{th} to 95^{th} percentile) obtained after data filtering was applied to the original data set for each respective FBAC’s cooling parameters obtained. 71

Table 12: Summary of compliance for method outcomes with the set study objectives (Table re-used from Section 2.6)..... 87
Table 13: Relevance of literature considered for implementation on underground FBACs, showing lack of condition monitoring literature on finned tube heat exchangers applicable in the mining industry. . 109
Table 14: Evaluation summary of existing heat exchanger condition monitoring literature for compliance to the evaluation criteria set forth in Section 1.7.1, showing shortcomings of each and the holistic non-compliance to all methods considered. 111

NOMENCLATURE

Cooling	The process of removing heat from a substance
Downcast Shaft	Mine shaft used to route intake air downwards towards the working places
FBAC	Radiator type heat exchangers often used in mines to cool down passing ventilation air
Flatlining	Refers to a type of data quality loss where a data value is the exact same to the previous value in the series and continuous as such due to sensor faults.
kW	Equal to 1000 Watts
Level	Network of tunnels stretching laterally from the main shaft infrastructure, usually towards the working places
Return Air Way	Tunnel networks that route return air from the working places towards the upcast shaft
Upcast Shaft	Mine shaft used to route return air upwards towards surface, where it is exhausted into the ambient air
Watt	Rate of energy (or heat) transfer – denoted in Joules per second
WBGT	Wet Bulb Globe Temperature – Minimum temperature obtainable through evaporative cooling, usually determined by placing a wet bulb around the globe of a thermometer.

LIST OF ABBREVIATIONS

DMRE	South African Department of Mineral Resources
FBAC	Finned Tube Bulk Air Cooler
MW	Mega Watts
SCADA	Supervisory Control and Data Acquisition
WBGT	Wet Bulb Globe Temperature

CHAPTER 1 INTRODUCTION AND LITERATURE REVIEW

1.1 History and challenges of deep-level mining

In 2007, South Africa was the top global gold producer, but had declined to 17th place by 2017 in the global index [1], [2] . The drop in production was primarily caused by factors such as gold price volatility, low economic growth, rising production costs, labour issues, and finally a decline in shallow ore grade [1], [2]. Local ore grade had declined from 12 g/ton in 1970 to 5 g/ton in 2014 since shallow, high-grade ore was being depleted.[1]–[4].

Figure 1 below illustrates this steady decline in shallow ore grade within global and South African mines over the years:

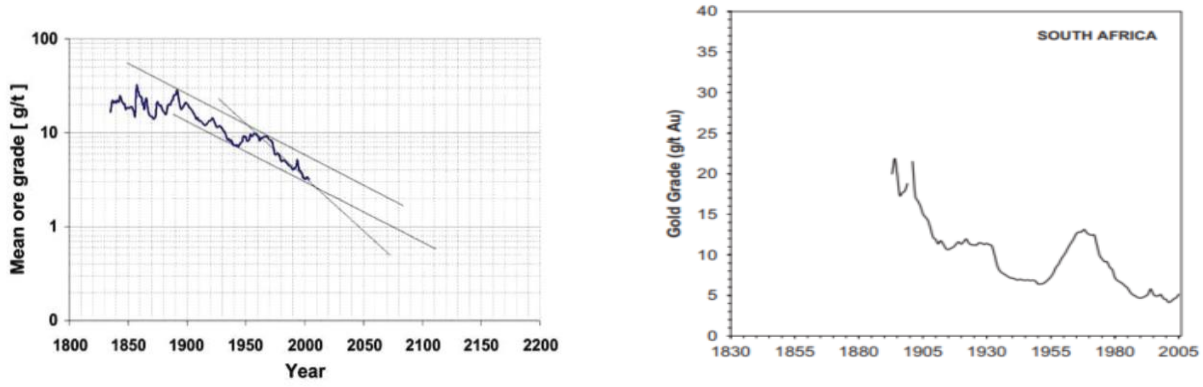

(a) (b)

Figure 1: (a) Global decline in gold ore grade (adapted from [1]) (b) Decline in South African gold ore grade from 1880 to 2005 (adapted from [2]–[4])

The decline in shallow ore grade forced South African mines to pursue higher grade ore at deeper depths, leading to some of the world's deepest mines at over 4 000 m [2], [3], [5]–[7] . These depths bring significant challenges due to enhanced heating effects to the ventilation air. In deep-level mines, ventilation air temperature is increased through enhanced heat effects from auto compression and geothermal heat from the rock, which are the primary and largest sources of heat in deep-level mines [5], [8]–[15]. Other smaller heat sources include underground fissure water, metabolic heat from workers, and heat from operational machines [5], [8]–[15].

Auto compression adds significant heat to the ventilation air in deep-level mines as a result of the extreme operating depths [5], [8], [12]–[15]. As air travels down the shaft, potential energy is converted to enthalpy which in turn heats up the ventilation air [5]. The added heat, due to auto compression, is proportional to the depth travelled at approximately 9.8 kJ/kg of heat for every 1 000 m increase in shaft depth [5], [12].

In addition, geothermal heat from the ambient rock also adds significant heat to the ventilation air [5], [8]–[13]. The virgin rock temperature - the local ambient rock temperature after exposure at a specific point - increases linearly with depth [5], [12]. The temperature gradient of the rock varies slightly depending on location, with a temperature gradient varying from 10 °C/km to 22 °C/km in South Africa [5]. Heating occurs when ventilation air exchanges heat with the hot surrounding rock, which increases temperatures.

These primary heat sources, along with the secondary heat sources discussed in the previous section, lead to significant increases in the ventilation air temperature in deep-level mines, compromising worker safety and mining sustainability - which is expanded on in later sections. Due to the large heating sources, mine refrigeration and cooling is required to reduce the temperature of the ventilation air before travelling to the working places.

1.2 Deep-level mine ventilation and refrigeration

The following sections discusses conventional mine ventilation and refrigeration, as well as the outlier case of deep-level mines in which the importance of using bulk air coolers close to the working places is emphasised.

In conventional mine ventilation systems, air travels through an open, through-flow system [16]. Air flows down a vertical shaft (referred to as a downcast shaft) to the production areas underground and is then routed through return tunnels (referred to as return airways) to be exhausted through a second shaft (referred to as an upcast shaft) [12], [16]. This system provides the necessary ventilation needed, in addition to providing air cooling power to the workers underground. Figure 2 below illustrates the ventilation system of a conventional mine:

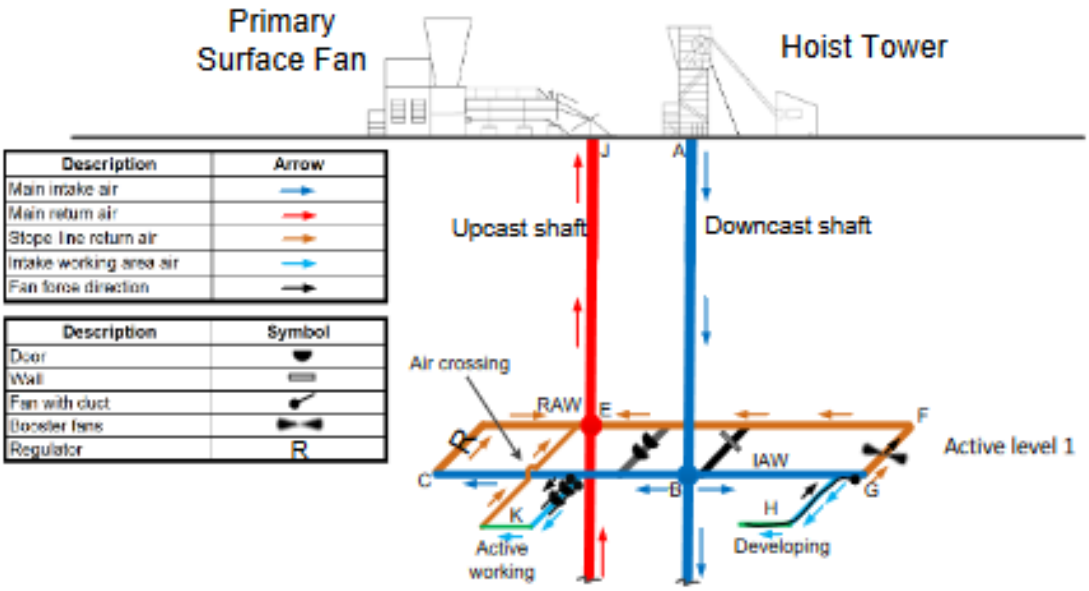

Figure 2: Illustration of a conventional mine ventilation network (adapted from [16])

As the temperature of the downcast air increases with mining depth, conventional surface-cooled air would not be sufficient. The ventilation air needs to be artificially cooled to negate the effects of various heat sources (as described in Section 1.1) from affecting the working place conditions. Shallow mines (less than 600 m in depth) use natural ventilation without refrigeration (as is the case in Figure 2) , however, deeper mines may require surface refrigeration (600 m - 1 400 m in depth) or further underground refrigeration (1 500 m - 2 000 m in depth) [5], [8], [9].

As mines deepen, the demand for refrigeration and cooling disproportionately increases with depth. Figure 3 below presents an additional estimate for the percentage increase in cooling requirements with the increase in mining depths, and Figure 4 presents the recommended refrigeration and cooling methods that are to be used at various mining depths.

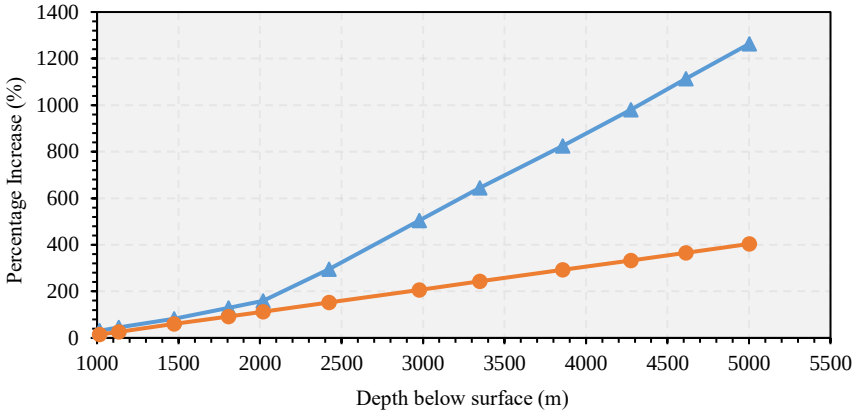

Figure 3: Increase in cooling requirements as the mining depth increases (redrawn from [5])

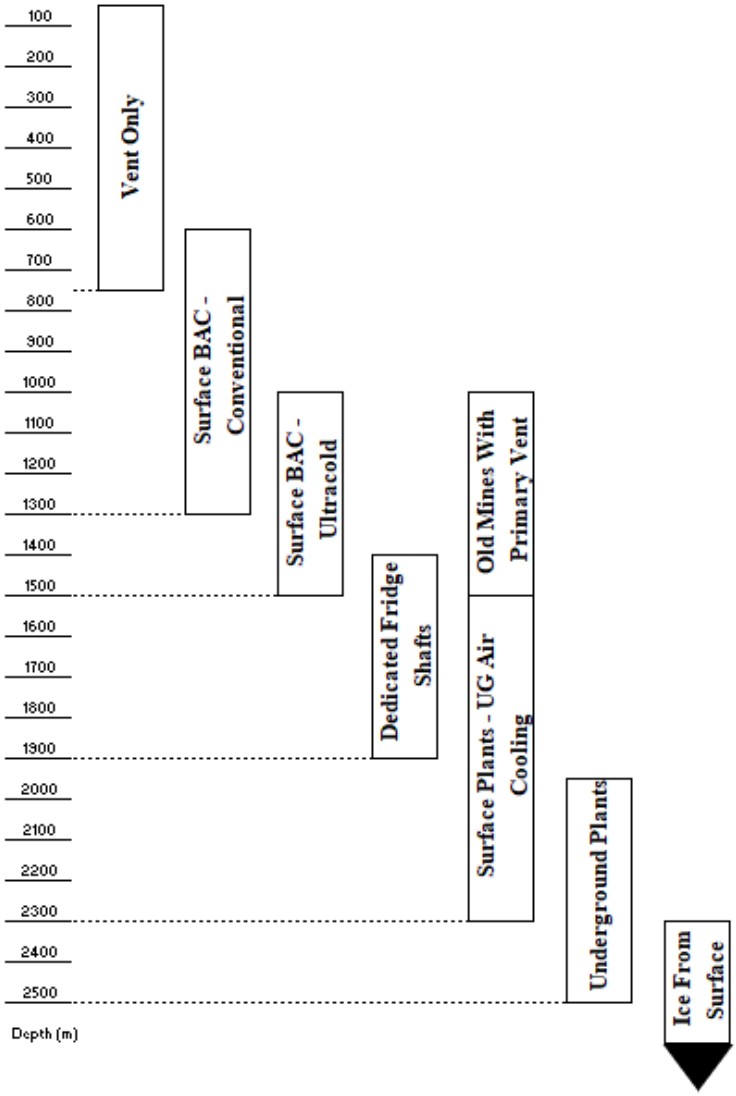

Figure 4: Mine refrigeration requirements as a function of mining depth (redrawn from [17])

Mackay *et.al* and Hooman *et. al.* estimates that conventional surface refrigeration and cooling would be insufficient past a mining depth of 1 500 m. Furthermore, a mining depth past 2 000 m underground would require refrigeration plants and bulk air coolers.[9], [17].

Underground refrigeration plants act as a secondary point of cooling for chilled service water from the surface before being sent to the underground bulk air coolers (BACs) [9], [17]. These air coolers use chilled service water from the refrigeration system to cool passing ventilation air as it travels to working places in deep-level mines [5], [9], [10], [12]–[14], [17].

Spray chamber BACs are a type of direct contact bulk air cooler, which consist of parallel tubes that spray a fine mist of chilled service water upwards into the ventilation airstream to cool and reduce the temperature thereof [12], [14]. These BACs are conventionally placed in bulk mainstream airflow, due to the high heat transfer efficiency, and magnitude of cooling that they can provide [8], [12], [14], [17]. Figure 5 below presents an example of an underground spray chamber BAC:

Figure 5: Spray tubes of an underground spray chamber bulk air cooler (Adapted from [17])

However, spray chamber BACs have a lower positional efficiency of cooling in deeper mines due to the distance they are typically installed from the working places. This is typically due to pumping requirements [17] and other factors [5], [14]. In deep-level mines,

this would mean that the effects of the cooling provided will have diminishing returns as the mining depth increases.

To offset the diminishing cooling effectiveness of larger spray chamber BACs which are placed farther away from working places, deep-level mines use smaller tertiary “spot coolers” placed closer to the working places [5], [10], [14]. Figure 6 below illustrates the type of refrigeration and bulk air-cooling infrastructure used at various mining depths, placing specific emphasis on the use of tertiary coolers:

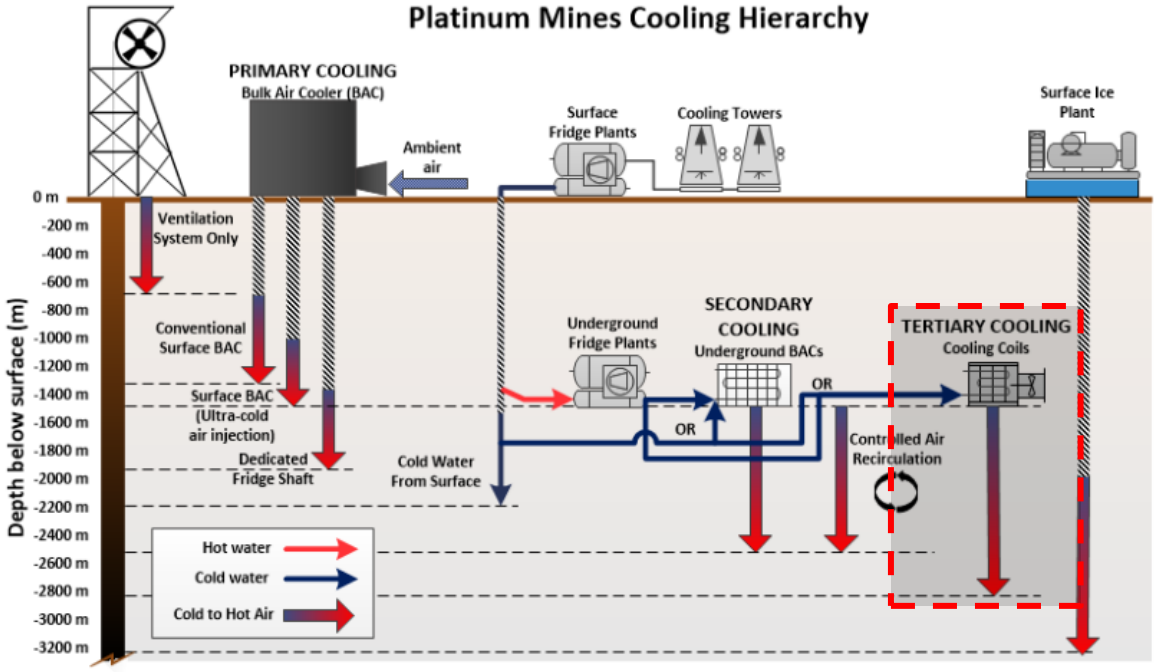

Figure 6: Hierarchy of cooling infrastructure in mines used as a function of depth. (adapted from [18]).

Tertiary spot coolers, such as Finned Tube BACs (FBACs) and cooling coils, provide less cooling in magnitude than large spray chamber BACs, however possess a higher positional efficiency of cooling due to their closer proximity to the working places [5], [10], [14]. Additionally, due to their proximity to the working places, these spot coolers are usually located in remote locations far away from the main station areas [5]. Figure 7 below illustrates examples of tertiary coolers used in deep level mines:

Figure 7: Different tertiary spot coolers used in deep-level mines: (left) Finned tube bulk air cooler (FBAC). (right) cooling coil (adapted from [17])

In deep-level mines, these tertiary spot coolers are essential for maintaining a cool temperature within the working places [5]. The cooling provided by these spot coolers depends on the careful control of various cooling parameters, each influencing the eventual cooling provided. The following sections will firstly provide a deeper understanding of the inner operations of these FBACs and the various effects that these cooling parameters have on cooling performance.

1.3 Finned tube bulk air coolers

In the following section, one is provided with a deeper understanding of the thermodynamic laws and concepts governing the heat exchange process in a typical heat exchanger, such as an underground Finned Tube Bulk Air Cooler (FBAC). The cooling performance of these FBACs is influenced by various cooling parameters, which will be outlined in the next section.

FBACs operate based on the governing principles of thermodynamics such as Fourier's law and the first law of thermodynamics [12], [19]. Fourier's law describes the flow of heat at the interface between two substances or fluids based on the respective temperature gradient, thermal conductivity, and surface area [12]. In the case of FBACs, thermal energy is transferred from the hot ventilation air to the chilled service water, and the rate of heat-flow is dependent on the magnitude of these parameters.

The first law of thermodynamics states that energy is conserved within a closed system [12]. When applied to FBACs, it means that energy is transferred from the hot ventilation air to the cooled service water in equal amounts, resulting in the cooling of the air and the

heating of the water. From the first law, the cooling performance of heat exchangers is often quantified using the heat equation. In conjunction with Fourier's law, these laws emphasise the significance of cooling parameters in the heat transfer process [12].

Therefore, as deduced from these laws, subsequent cooling parameters that affect the cooling performance of FBACs include thermal conductivity, thermal resistance, mass flow rate, temperature gradient, and surface area of heat transfer among others [12], [19]–[25]. Thermal conductivity denotes the rate at which thermal energy flows, while thermal resistance refers to the impedance to heat transfer - usually associated with a low thermal conductivity [26], [27]. Therefore, optimal heat transfer is achieved when the thermal resistance is minimised and thermal conductivity is maximised [23], [27]**.** Tamene *et. al.* portrayed how the thermal conductivity of a system increases in a non-linear manner as the thermal resistance decreases, as well as how the heat transfer coefficient increases with decreases in thermal resistance [27].

The rate of heat transfer is also influenced by the mass flow rates of the working fluids, with increased flow rates resulting in higher heat transfer rates [24]. Mahdi *et. al.* showed that increasing mass flow rates in large cooling towers by 25 l/s would lead to increases in thermal efficiency by 5 % in addition to heat transfer coefficient increases of 400 W/m^2.K [28].

Additionally, the heat transfer rate is also affected by the temperature difference between the hot air and cooled water [25]. Al-Jassani *et. al*. proved that in a finned heat exchanger, increasing the magnitude of the thermal gradient by 90 °C could lead to increases in heat transfer coefficient of up to 100 W/m^2.K for the case investigated [25]. Lastly, the surface area over which heat transfer occurs also impacts the rate of heat flow [22]. Saqr *et. al* displayed that by using different plain and finned pipe configurations, which increases surface area, heat transfer coefficient improvements of up to 50 W/m^2.K was observed [22].

These cooling parameters play a significant role in the cooling performance of FBACs, and their optimal operation ensures efficient cooling. However, over time, inefficiencies start to accumulate and affect the cooling performance of these FBACs [10], [19], [21], [29]–[32]. These inefficiencies typically manifest within the discussed cooling parameters. The impact of these inefficiencies on the cooling performance of FBACs lead to higher outlet

temperatures, resulting in higher working place temperatures which directly impacts mining operations. The following section discusses the impact that inefficiencies have on the cooling performance of heat exchanger infrastructure.

1.4 Impacts of inefficiencies on FBAC cooling performance

FBACs operating underground often experience a degradation in cooling performance due to various inefficiencies affecting the cooling parameters. These inefficiencies result in decreased heat transfer and higher outlet temperatures [23]. Inefficiencies typically manifest in different forms, such as external fouling, internal fouling, leakages and broken infrastructure [23], [29], [32]–[36].

External fouling, where deposits like scaling, precipitation, particulate deposits, and corrosion accumulate on the FBAC's outer surfaces, reduces thermal conductivity and impedes heat transfer [32]**,** [23]. Subsequently, fouling increases the thermal resistance of the cooling infrastructure, affecting cooling performance [29]. Diaz-Bejarano *et. al.* proved that external fouling led to a performance decrease of 24 MW of heat duty over a period of 800 days, which results in a decrease of over 80 % in performance [29]. Markowski *et. al.* showed that external fouling increased the thermal resistance of a heat exchanger 15 fold over a span of 25 months [32]

Internal fouling, which accumulates inside heat transfer surfaces like finned tube piping, further increases thermal resistance and decreases cooling performance [34]**.** Factors such as fluid velocity, flow surface, piping material, pH of service water, salt content, and surface temperature all contribute to fouling [23], [34]–[36]. Shen *et. al.* displayed a 30 % decrease in the heat transfer coefficient over a 36-day period in an industrial heat exchanger, due to the onset of internal fouling [34].

Leakages primarily cause a reduction in coolant mass flow rate to the heat exchanger infrastructure, resulting in decreased cooling performance [33]. Damage to the FBAC's infrastructure, such as broken or inactive banks and faulty service doors, also lead to decreased heat transfer. Pelella *et. al* showed that leakages in refrigeration systems can lead to performance decreases of up to 25 % [33].

These inefficiencies collectively decrease cooling performance, leading to inadequate cooling of ventilation air, and causing higher outlet temperatures. Decreased cooling

performance of these coolers that are close to the working places will lead to higher working place temperatures, potentially compromising safety, sustainability, and profitability of the mining operation. The following section will explore these impacts of high working place temperatures on mining operations.

1.5 Consequences of high temperatures in the working places

Effective mining operations rely on favourable working conditions and efficient cooling [37]. However, inefficiencies in spot coolers like FBACs can lead to decreased cooling performance and higher temperatures in the working areas.

Working in hot conditions raises the core body temperature of mining personnel [5], [7], [11], [15], [37]–[39]. The optimal range for effective bodily function is approximately 36.5 °C to 37.5 °C [40]. Heat stress occurs when the net heat load on a worker exceeds this range, resulting in an increase in body heat storage and core body temperature [7]. This can lead to heat exhaustion, characterised by symptoms such as fatigue, headaches, dizziness, shortness of breath, and syncope [11]. Figure 8 below illustrates the impacts of hot working conditions by showing the cumulative increase in heat cases reported with increases in wet bulb globe temperature (WBGT) and dry bulb temperature:

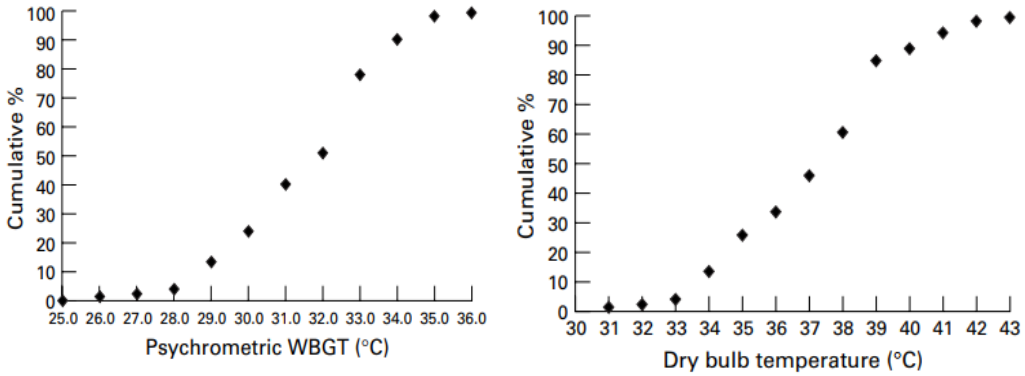

Figure 8: Heat exhaustion cases in a deep underground mine as a function of working place temperature condition. (adapted from [11])

If heat exhaustion is left untreated, it can progress to heat stroke - a severe and potentially fatal condition [11], [38]. Heat stroke is characterised by a core body temperature above 40 °C with symptoms such as dry skin, dizziness, elevated heart rate, nausea, and confusion [15]. Without prompt treatment, heat stroke can lead to loss of consciousness

and even death [11], [38]. Therefore, it is crucial to provide sufficient cooling in the working areas to ensure the safety of mining personnel.

Legal compliance is also a significant concern in mining operations. The Mine Health and Safety Act of 1996 sets specific limits for workplace conditions, including a wet-bulb temperature of 32.5 °C and a dry-bulb temperature of 37 °C [5], [7]. If these limits are exceeded, immediate evacuation of mining personnel is required [7], [11]. Failure to address persistently unfavourable conditions can result in the temporary or indefinite closure of the mine under the instruction of the Department of Mineral Resources (DMRE) [18].

Furthermore, high temperatures in the working places can lead to loss of production. Harmony Gold, a South African mining operation, reported a significant loss of 40,000 ounces of gold in 2014, with thermal safety-related stoppages being one of the largest contributing factors [2]. Additionally, higher temperatures reduce worker productivity and efficiency [37]. Figure 9 below shows how worker efficiency declines with an increase in working place temperatures at different air velocities:

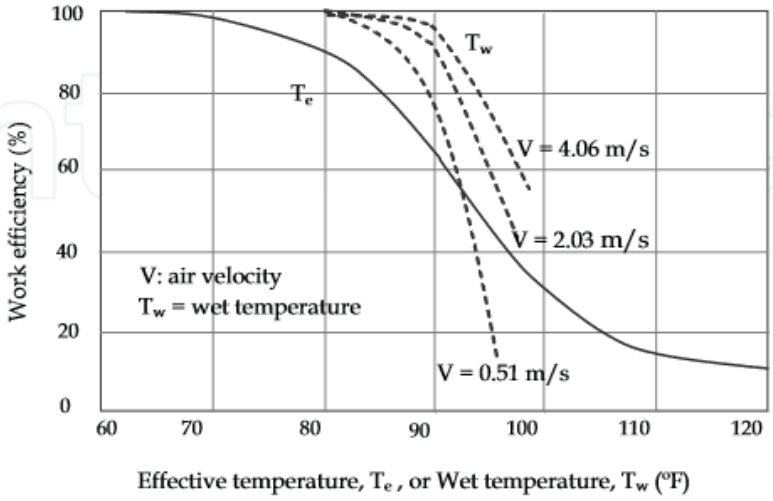

Figure 9: Effects of working place temperatures on work efficiency (adapted from [37])

In conclusion, maintaining favourable working conditions and efficient cooling is crucial for effective mining operations. Inefficiencies in the FBAC infrastructure can lead to elevated temperatures, posing risks to personnel health and safety. Compliance with legal regulations is necessary to ensure the sustainable operation of mines. Furthermore, inadequate cooling can result in production losses.

1.6 Addressing the impacts of inefficiencies

Section 1.3 showed that tertiary spot coolers, specifically underground finned tube bulk air coolers (FBACs), rely on various cooling parameters to ensure that sufficient cooling performance is achieved. However, Section 1.4 revealed that industrial heat exchangers often experience inefficiencies due to issues like fouling, leaks, inadequate water supply, and infrastructure problems. These inefficiencies lead to higher outlet temperatures and (in deep level mines) subsequently higher ambient temperatures at the working places.

Moreover, Section 1.5 highlighted that higher temperatures at the working places have negative effects on mining operations. Inefficiencies in FBACs result in reduced cooling performance, which further impacts the mining operation.

To address these inefficiencies, effective condition monitoring of these coolers is necessary. Condition monitoring enables the identification of inefficiencies at an early stage to determine when maintenance is needed, ensuring consistent cooling performance and favourable working temperatures [18], [23]. Heat exchanger condition monitoring methods are used to achieve these outcomes.

The following section will conduct a comprehensive review of existing literature on condition monitoring methods that are applied to industrial heat exchangers. This review aims to assess the feasibility of implementing these methods in FBACs to promptly address inefficiencies.

1.7 Review of existing condition monitoring methods of industrial heat exchangers

The following few sections provide a holistic review of existing condition monitoring methods found in literature for heat exchangers that are applied to the general industry. However, to be considered for implementation, each method should be evaluated against a set of evaluation criteria, derived from the unique monitoring challenges that would be encountered at these FBACs. Appendix E gives an overview of the relevancy of the literature considered. The following section outlines how the evaluation criteria is established.

1.7.1 Evaluation criteria for the review of existing methods

To effectively determine the feasibility of implementing existing condition monitoring methods to underground FBACs, a set of evaluation criteria is first established. These criteria are constructed from the unique monitoring challenges that underground FBACs would encounter. The unique monitoring challenges expected at these FBACs are outlined and discussed in more detail below, forming the basis for the evaluation criteria to be used in the review:

- Off-Design Monitoring:

Underground cooling infrastructure often operates at off-design conditions as highlighted by Van Rooyen and Pretorius in their respective dissertations [18], [23]. Both authors mention the challenges presented in implementing any form of performance monitoring at these off-design conditions. Therefore, the suitability of condition monitoring methods needs to be assessed before implementing them on FBACs that are operating under off-design conditions.

- Continuous Monitoring:

To detect inefficiencies in cooling performance at an early stage, continuous monitoring is essential. These inefficiencies gradually degrade cooling performance over time, as shown in Section 1.4, which in turn leads to a gradual increase in working place temperature. Therefore, the need for consistent and continuous monitoring to identify and address inefficiencies early-on before they significantly impact cooling performance becomes evident.

- Remote Monitoring:

Considering that spot coolers are typically placed near working areas for increased positional efficiency of cooling (as discussed in Section 1.2), the heat exchanger infrastructure is typically located in remote areas far from the main shaft infrastructure where workshops are situated [5]. Manual monitoring of these FBACs in such scenarios becomes impractical, highlighting the necessity for remote monitoring.

- Detection of Multiple Inefficiencies:

Since inefficiencies affecting cooling performance can manifest in various forms (as shown in Section 1.4) the monitoring method must be capable of detecting multiple types of inefficiencies to effectively assess the overall condition of these FBACs. This is done to determine the holistic impact of inefficiencies on the cooling performance.

- Accuracy and Reliability:

Given the harsh and dynamic operating environment underground, condition monitoring methods must provide reliable and accurate monitoring data to effectively assess the condition of these FBACs. Therefore, the reliability and accuracy of the monitoring methods will need to be evaluated.

Considering the potential challenges condition monitoring methods may have to face as outlined above, a set of evaluation criteria is established:

- Is the method under evaluation applicable to heat exchangers operating at off-design conditions?
- Is the method under evaluation able to monitor in a remote and continuous manner?
- Is the method under evaluation able to monitor and detect the impact of multiple inefficiencies?
- Is the method under evaluation able to conduct condition monitoring accurately and reliably?

These evaluation criteria will serve as a general guideline when conducting the review of existing condition monitoring method literature. Appendix E also gives an overview of the findings from reviewing the literature, where each study and method considered is evaluated for compliance to the evaluation criteria.

The following sections will review different heat exchanger condition monitoring method literature, and then provide an evaluation of these methods for compliance to the criteria defined in this section.

1.7.2 Direct/Destructive monitoring methods

Condition monitoring by direct/destructive inspection consists of physical inspections of the heat exchanger infrastructure [41] . These include inspection policy guidelines that optimise for maintenance scheduling and taking sections of infrastructure for testing and inspection [41]–[43]. Ba *et. al* proposed a dynamic inspection and maintenance policy for a boiler heat exchanger subject to tube thickness losses due to erosion [41].

Prakash *et. al*. mentions that another method of direct monitoring is to take apart the suspected fouled section, and weigh it against the same section when cleaned and inferring the amount of fouling from the difference [43]. The section can then also be tested microscopically for additional defects [43].

Although direct monitoring can assess the condition of heat exchangers even under off-design conditions and with different inefficiency types with good reliability and accuracy to detect the onset or presence of multiple inefficiencies, it still falls short of meeting the other remaining evaluation criteria. These methods involve regular physical inspections, necessitating personnel access to the heat exchanger equipment, and resulting in labour costs and cumbersome efforts. Consequently, direct monitoring methods are not conducive to continuous and remote implementation.

Furthermore, these monitoring methods typically entail destructive procedures, involving the removal of a heat exchanger section, which leads to downtime and additional operational expenses [30], [35], [41]–[44]. Given that downtime of underground FBACs would result in a gradual rise in working place temperatures, such an increase would have adverse consequences, as discussed in Section 1.5. Consequently, implementing these methods underground becomes impractical.

To circumvent the necessity for downtime and address the constraints of continuous and remote monitoring, it is worth exploring non-destructive monitoring methods. The subsequent section will evaluate various non-destructive monitoring methods to assess their viability and compliance to the evaluation criteria.

1.7.3 Non-destructive testing methods

Non-destructive testing (NDT) utilises innovate measuring technology to measure infrastructure without affecting the physical properties of the heat exchanger or causing any downtime for inspection [19], [41], [45]–[47]. The aim thereof is to improve the effectiveness of detecting irregularities and to minimise costs implications of control tests [47], [48]. Non-destructive testing methods include infrared thermography, acoustic emission, and vibration measurement, among other various methods [19], [45]–[48].

Infrared thermography utilises laser radiant heating and infrared (IR) sensors to rapidly monitor surface temperatures, enabling the swift evaluation of heat transfer coefficients of a surface [49]. Berce *et. al.* examined the application of infrared thermography by investigating the formation of calcium carbonate crystallization on heat exchanger surfaces and its effects on performance [46]. Figure 10 below shows the basic operating principle behind the method, and Figure 11 shows typical results obtained by applying the method:

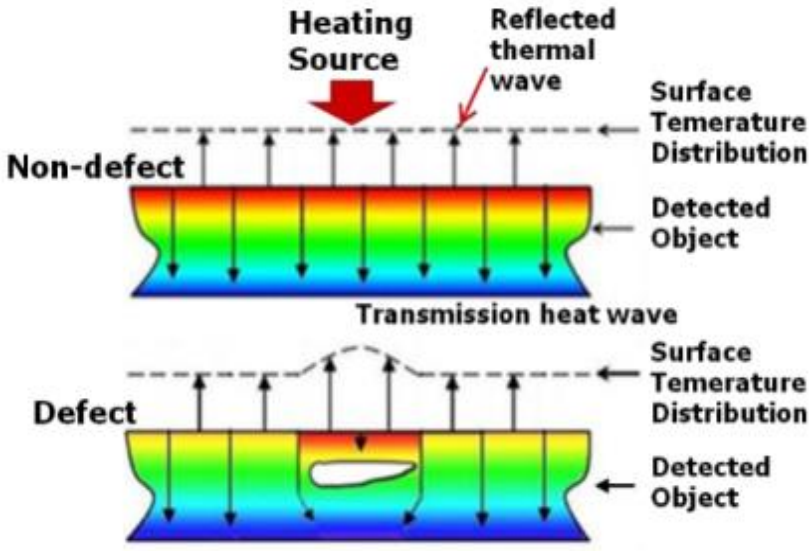

Figure 10: Operating principal behind infrared thermography for the detection of fouling (adapted from [47]).

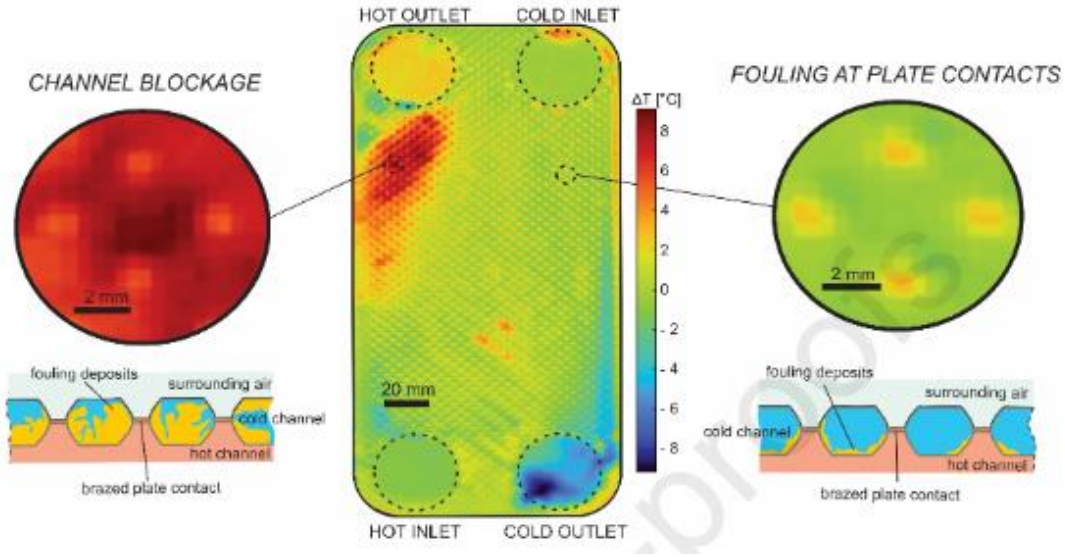

Figure 11: Effect of fouling indicated by infrared thermography as found by Berce *et. al* (adapted from [46])

The acoustic emission monitoring method, a popular NDT method in the industry, utilises acoustic waves propagating through the material and subsequently analysing the power of the return signal to infer fouling growth in heat exchangers [35], [43], [47], [50]–[53]. The method allows for the extent and size of the foulants to be determined by analysing the time of flight (TOF) within the material and comparison against a calculated speed of sound for the same material [23], [35], [43], [51].

Merheb *et. al.* performed acoustic analysis monitoring by using multiple optimised acoustic sensors that were able to detect low frequency acoustic waves propagating through the plates of a heat exchanger [52]. The results he obtained confirmed that low frequency waves were sensitive to fouling as presented in Figure 12 below:

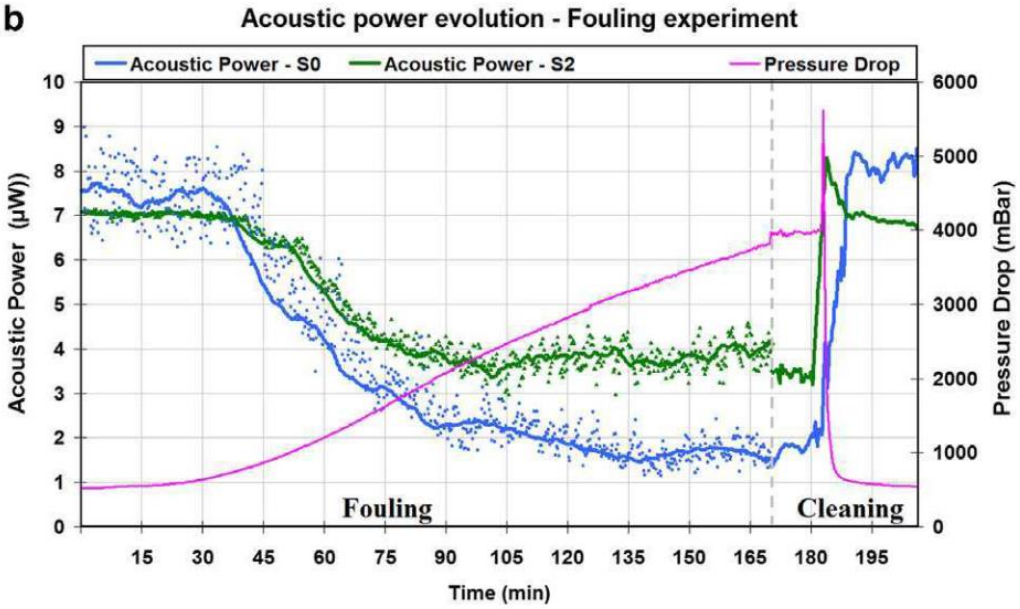

Figure 12: Fouling growth detected by comparing the acoustic emission power to the pressure drop growth (adapted from [52])

Similar to acoustic emission, vibrational analysis utilises the response of heat exchanger infrastructure to an emission pulse [45], [54]. Phenomena such as resonant frequencies and alternating flow regimes due to induced vibrations lead to deuteration and ultimate failure of heat exchanger infrastructure [45], [54].

Huang *et. al* investigated and proposed a method of using vibrational signals to analyse clogging faults in heat exchangers [45]. The method proved that the vibrational differences between normal operating and clogged heat exchangers were greater than 85 %, presented in Figure 13 below:

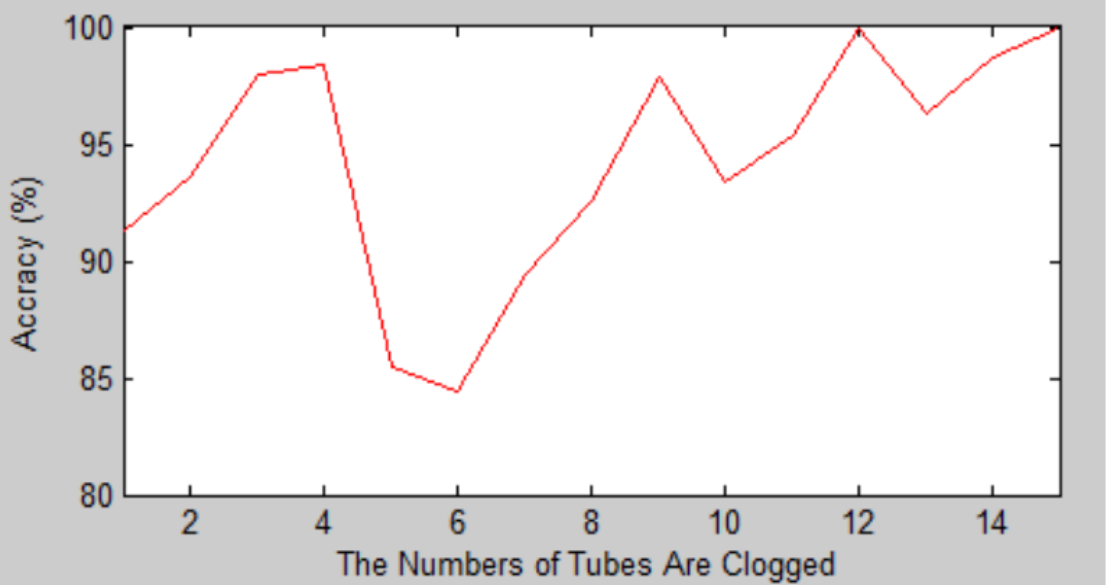

Figure 13: Accuracy of the proposed method of vibrational analysis. (adapted from [45])

While non-destructive monitoring methods offer advantages such as accurate and reliable monitoring, they also have limitations in meeting the evaluation criteria. For instance, infrared thermography is not applicable for monitoring heat exchangers operating under off-design conditions and it is not suitable for continuous and remote monitoring, due to its reliance on single data point measurements and the need for direct access to the heat exchanger [47]. It can only monitor for fouling inefficiencies and no other types of inefficiencies discussed in Section 1.4.

Acoustic emission, another non-destructive method, can only detect the onset of fouling at steady-state operating conditions, and is not feasible for off-design operating conditions. It also relies on the detection of fouling as the primary inefficiency and requires fragile and temperature-dependent ultrasonic sensors, making temperature correction factors complex to determine. Environmental noise, limited frequency ranges, and the inability to test sealed compact heat exchangers further complicate its implementation on FBACs [45], [50], [51], [53].

Vibration monitoring, although capable of continuous and remote monitoring and accounting for multiple inefficiencies impacting flow regimes, presents some limitations. It requires sensitive sensors to detect small vibrations in water tube heat exchangers, making it susceptible to environmental noise and impacting monitoring reliability and accuracy.

Additionally, it relies on steady-state conditions and would not be feasible for off-design condition monitoring [45], [54].

In summary, non-destructive testing methods have shortcomings in terms of monitoring off-design conditions, reliability and accuracy, and the ability to monitor multiple inefficiencies. To address these shortcomings, indirect monitoring methods are considered.

1.7.4 Indirect monitoring methods

To address the lack of remote and continuous monitoring found in direct monitoring methods and the ability of monitoring multiple inefficacies found with NDT methods, a simpler and more cost-effective method is considered - albeit more unreliable and inaccurate.

Indirect monitoring utilises changes in various operating parameters around the heat exchanger over time to infer the condition of the heat exchanger. These monitoring parameters include pressure drop, temperature and the overall heat transfer coefficient of the BAC [34], [43], [44], [50], [51], [55], [56].

The pressure drop over the heat exchanger at constant flow rate can be used to infer the presence of fouling, as build-up of contaminants would result in a drop in pressure in the substance [21], [50]. As fouling decreases the internal flow area of the piping due to deposit build-up, a larger pressure drop over the heat exchanger can be observed [50]. Prakash *et. al.* presents a case where the pressure drop in an industrial heat exchanger in the milk industry was observed to increase over time due to fouling, presented in Figure 14 below. Additionally, Diaz-Bejarano *et. al.* showed how the pressure drop observed correlated with a drop in heat exchange performance, shown in Figure 15 below:

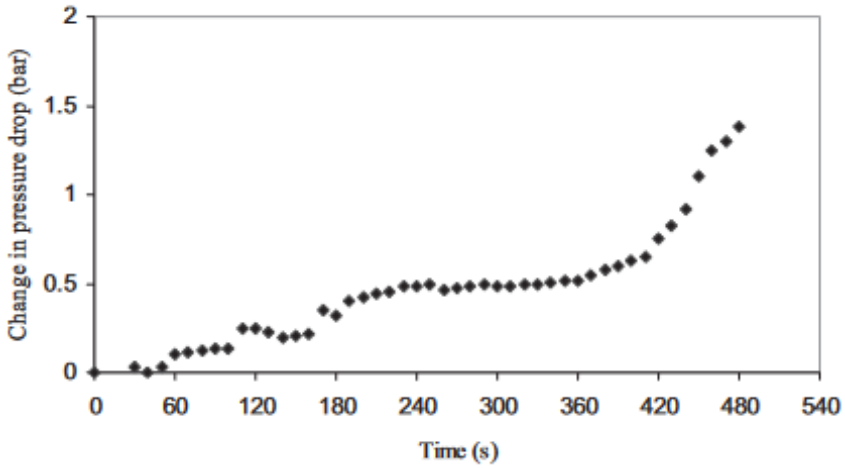

Figure 14: Increase in pressure drop in time over the length of a heat exchanger due to fouling. (adapted from [43])

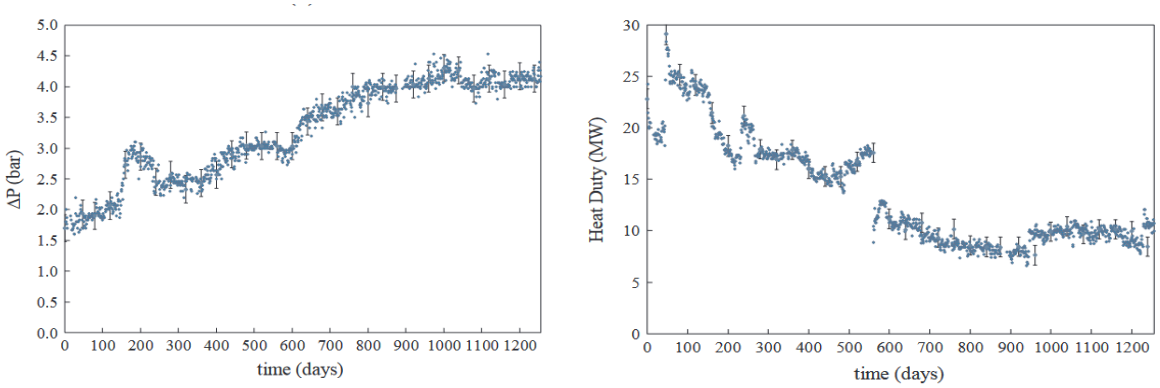

(a) (b)

Figure 15: (a) Pressure drop increases over time due to the onset of inefficiencies in a heat exchanger in the refinery industry, with an (b) associated drop in performance of the heat exchanger seen (adapted from [29])

The onset of fouling decreases the heat exchange efficiency of the heat exchanger, causing a gradual rise in outlet temperature over time at the same conditions [50], [51]. This will be due to the decline in the overall heat transfer coefficient of the heat exchanger [34], [43]–[45], [50], [51], [55], [56]. Therefore, both the temperature and overall heat transfer coefficient can be monitored to indicate fouling formation. Prakash *et. al.* presented a case where both parameters were monitored to infer fouling conditions, shown in Figure 16 below:

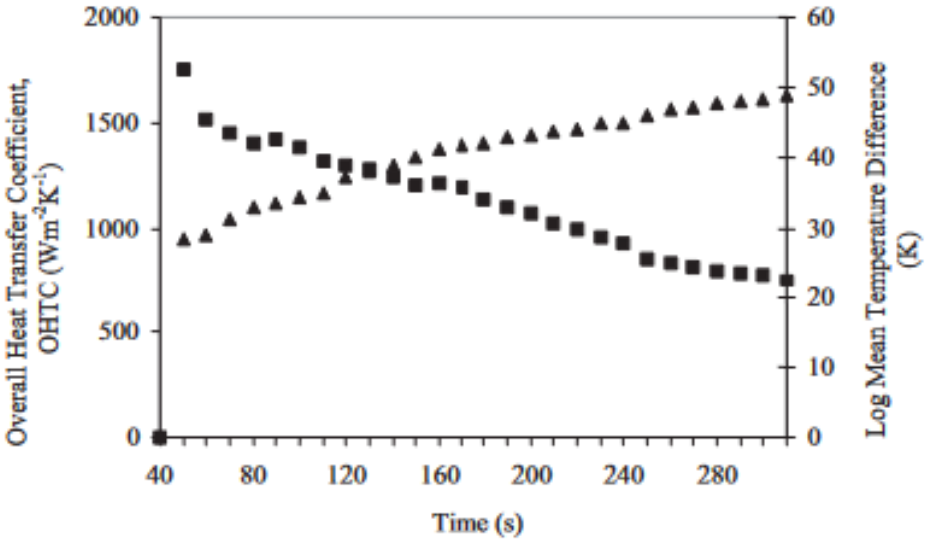

Figure 16: Decline in overall heat transfer coefficient with subsequent rise in temperature over time in a heat exchanger due to fouling (adapted from [43])

Indirect monitoring initially proves to be promising for use as for the purposes of this study, due to its ability to monitor the condition of the FBAC continuously and remotely. In addition, due to evaluating the performance of the FBAC by monitoring various parameters, the impacts of multiple inefficiencies on cooling performance may be considered.

However, the main shortcoming for this condition monitoring method is the effect of non-steady, dynamic inlet conditions on measurement accuracy [43], [44], [50], [56], meaning that the method is only applicable to steady-state design conditions [44], [45], [50]. This would mean that, similarly, the rest of the monitoring methods considered thus far prove that off-design monitoring would not be possible. In addition, and similar to NDT methods, the issue persists that the method is unreliable due to the influences of dynamic inlet parameters and other factors affecting monitoring data [43].

In summary, considering the evaluation criteria, indirect monitoring methods are unable to monitor the condition of the FBAC at off-design conditions in an accurate and reliable manner. To augment the shortcomings of indirect monitoring, a method of monitoring at off-design conditions with a high degree of accuracy would need to be implemented. The following section will evaluate previous work where condition monitoring methods were applied at off-design conditions.

1.7.5 Off-design monitoring methods

When considering the evaluation criteria set forth in Section 1.7.1, all existing condition monitoring methods reviewed proved ineffective for use in monitoring heat exchangers that are operating at dynamic off-design conditions with a high degree of accuracy and reliability. The following section will briefly discuss previous endeavours into off-design condition monitoring on FBACs by use of normalised performance monitoring.

Zhou *et. al* proposed using a wet-dry transformation to model heat exchanger performance [57]. The model considers air-dehumidification, a phenomenon which happens when air outlet temperature drops below the inlet dew-point temperature, leading to condensation and a simultaneous heat and mass transfer [57], [58]. The study used the e-NTU method, which is a mathematical method of modelling heat exchanger performance [59]. This study presents examples where off-design operating conditions are considered to increase modelling accuracy.

In his master's dissertation, Van Rooyen proposed implementing a performance and fouling prediction model for underground finned tube heat exchangers, operating at off-design conditions [23]. The study used an integrated method consisting of three distinct prediction models: performance, fouling and maintenance. The model was derived using first principals, psychometry, Bayesian - and Markov methods, and thermal-to-production relations. The developed model was successfully applied to underground FBACs operating at off-design conditions, where deviations from optimal performance were found.

Sánchez-Escalona *et. al.* and Laskowski *et. al* proposed novel performance monitoring methods of heat exchangers using the Buckingham – Pi Theorem, which is commonly used in dimensional analysis [60], [61]. The method allowed the user to offset the effects of off-design operating conditions by normalizing system parameters. This led to a performance prediction model that was able to predict outlet air temperatures of the case study heat exchanger operating at off-design conditions in a remote and continues manner with extreme accuracy and reliability.

While powerful, Zhou *et. al*. acknowledged limitations in using mathematical models to assess heat exchanger performance in situations involving air de-humidification. He mentions that these limitations stem from the complexity of the process and the scarcity of

available literature [31], [57]. Consequently, such models would grapple to incorporate various inefficiencies that affect cooling performance, thus compromising their accuracy and reliability.

Van Rooyen's model, although effective in accurately and reliably monitoring the condition of the FBAC under off-design operating conditions, only considered the impact of internal and external fouling on cooling performance. The study did not account for other inefficiencies. Furthermore, the method relies on periodic physical audits rather than continuous remote monitoring.

Sánchez-Escalona *et. al.'s* and Laskowski *et.al.'s* novel performance-monitoring methods offers a strong foundation for a monitoring method that meets all the evaluation criteria. However, the method was designed to characterise heat exchanger performance rather than serving as a condition monitoring approach. Although successful in remotely and continuously monitoring off-design performance with high accuracy and reliability, the model does not address the impact of existing inefficiencies on cooling performance. This limitation arises because the model is calibrated using current operating data, thus inherently incorporating the effects of present inefficiencies.

1.8 Problem and need for the study

Section 1.6 emphasises the need for effective condition monitoring of underground finned tube bulk air coolers (FBACs) to identify inefficiencies early on, prioritise maintenance, and maintain cool temperatures in deep-level mines.

To address this need, a comprehensive literature review evaluated various condition monitoring methods applicable to industrial heat exchangers for use in underground FBACs. The evaluation criteria for these methods were derived from expected monitoring challenges specific to underground FBACs, as discussed in Section 1.7.1.

The reviewed monitoring methods included direct/destructive, non-destructive, indirect, and off-design monitoring. Direct/destructive monitoring methods were deemed infeasible due to remote and continuous monitoring complications, required downtime, and infrastructure damage. Non-destructive methods were impractical due to difficulties experienced when implementing them at off-design conditions, sensitivity issues affecting accuracy and reliability, and an inability to detect multiple inefficiencies.

While indirect monitoring initially showed merit for remote and continuous monitoring while considering cooling performance inefficiencies, it was found impractical for off-design conditions and was influenced by dynamic inlet conditions affecting accuracy and reliability. Off-design monitoring methods had some success, but none fully met all evaluation criteria - except for a proposal by A. Sánchez-Escalona *et. al*., which lacked the ability to detect multiple inefficiencies.

In conclusion, the literature review revealed a lack of existing heat exchanger condition monitoring methods capable of accurately and reliably monitoring off-design conditions in a remote and continuous manner to detect multiple inefficiencies that impact cooling performance, as determined by the evaluation criteria. This gap in literature also translates to a lack of monitoring methods applicable to underground FBACs.

To address this problem, this dissertation will present an innovative heat exchanger condition monitoring method that will fulfil all the evaluation criteria from Section 1.7.1. This method will build on the novel performance modelling proposed by A. Sánchez-Escalona *et al*. and Laskowski *et. al*. [60], [61].

The success of this proposed method would enable effective condition monitoring for crucial cooling infrastructure. To ensure its feasibility, a set of study objectives is established, closely resembling the evaluation criteria in Section 1.7.1, which the method must meet for implementation. Only when all these study objectives are achieved, will the method be considered feasible. The following section outlines these objectives.

1.9 Study objectives

To address the problem and subsequent need outlined in Section 1.8, it was stated that this dissertation aims to present an innovative condition monitoring method which is capable of addressing all the evaluation criteria determined in Section 1.7.1. To ensure the method complies to the evaluation criteria, the study objectives will be set as such to ensure that each of these criteria are addressed to provide a comprehensive response to the identified problem and need.

The study objectives encompass presenting a method of a condition monitoring capable of:

1. Continuously and remotely monitoring the
2. Condition of underground finned tube bulk air coolers
3. Operating at off-design conditions in an
4. Accurate and reliable manner, with the ability to
5. Detect the onset and presence of multiple inefficiencies impacting cooling performance.

By focusing on these study objectives, the proposed method will adequately address the identified need and be deemed feasible for implementation on these underground FBACs.

1.10 Research approach

As discussed in Section 1.9, the aim of this dissertation is to present a method capable of meeting the criteria discussed. Therefore, the research approach followed within this dissertation will be the case study methodology.

This is due to the general strength of this approach in evaluating the merits of a particular method being researched. Figure 17 below outlines the general procedure followed:

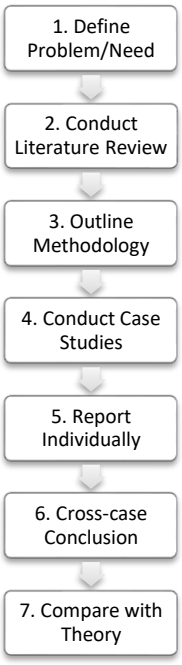

Figure 17: Overview of the case study research methodology

Thus far, the dissertation provided background to define the main problem and subsequent need to be addressed, in addition to providing the study objectives set forth ensure the shortcoming is fulfilled.

The outline of the method will be provided, constructed closely to that of previously similar literature. Careful consideration will be given as to how the method would be verified to ensure sufficient monitoring and prediction accuracy and precision.

Thereafter, the method outlined would be implemented on a set of case study FBACs to assess the effectiveness of the method in achieving condition monitoring as set out in the study objectives. The method would first be validated on a single FBAC to assess the ability of the model to monitor the condition of the FBAC against the set objectives. Thus, the monitoring results would need to be bcross verified against other inspection/monitoring methods such as physical audits. Only after the model is validated, can it be applied to the remaining FBACs in the case study, to assess the condition thereof.

After all results are obtained, it will be discussed how these results then compare to that obtained from previous literature. Insights and conclusions of the data would be given as to assess the effectiveness of the method against the study results.

The following section provides a brief overview of the dissertation.

1.11 Study Chapter Overview

Chapter 1 – Introduction and literature Review

This chapter presented the introduction and literature review relevant to the dissertation. A detailed literature review was conducted and resulted in the need for a method of implementing condition monitoring on underground FBACs compliant to a determined set of criteria. It was highlighted that this dissertation presents an innovative condition monitoring method of heat exchangers capable of complying to all the identified criteria. Study objectives were set to ensure the presented method adheres to the identified need and will serve as guidelines for the remainder of the dissertation.

Chapter 2 – Method outline

This chapter will present the outline of the method presented. A comprehensive overview of each phase and subphases of the innovative method is presented and outlined, and a discussion for how each phase of the method complies with the study objectives is put forth.

Chapter 3 – Method implementation

In this chapter, a case study on seven underground finned tube bulk air coolers (FBACs) is conducted to evaluate the compliance of the method to the study objectives established. The method is implemented in a systematic order following the outline given in Chapter 2. The subsequent result of implementing the method is then shown.

Chapter 4 – Conclusion and recommendations

In this chapter, a summary of the dissertation will be presented. Thereafter, the compliance of the outcomes from implementing the method is evaluated against the established study objectives. Finally, limitations of the study are stated whereafter recommendations for future work is given.

CHAPTER 2 METHOD OUTLINE

2.1 Chapter preamble

In the following chapter, the proposed method will be outlined. The outline of the method is constructed closely to that presented by A. Sánchez-Escalona *et al*. and Laskowski *et. al*. in their respective articles [60], [61]. Therefore, any statements, decisions or strategies presented in this chapter can be closely related back to the general processes followed by these respective authors.

The primary target of the method is to develop a normalised prediction model that enables remote and continuous condition monitoring of underground FBACs operating at off-design conditions. The model obtained aims to detect multiple inefficiencies that are impacting cooling performance with a high degree of accuracy and reliability. The prediction model utilises OEM design data to forecast the expected outlet conditions of the FBACs under off-design inlet conditions. By comparing the predicted design outlet conditions, such as outlet air temperature, with the observed outlet conditions, the method assesses the magnitude of deviation over time. This analysis allows for the inference of the FBACs' condition and the identification of potential inefficiencies.

Overall, the upcoming chapter will provide a cohesive overview of the proposed method, outlining each phase and sub-phase of the method, and shows how each phase aims to address and comply to the study objectives set forth in Section 1.9. This ensures that the method will be able to effectively identify inefficiencies affecting FBAC performance and address the identified problem in Section 1.8.

2.2 Overview of method

The method presented in this study will consist of three distinct phases, each following after the other. These three phases are broken up into various sub-phases. The three main phases presented include:

- Phase 1: Parameter Normalization
- Phase 2: Development of Prediction Model
- Phase 3: Implementation of Prediction Model

Each phase will be described in detail in the following sections. The holistic outline of the method containing each phase in addition to each respective subphase is presented in Figure 18 below:

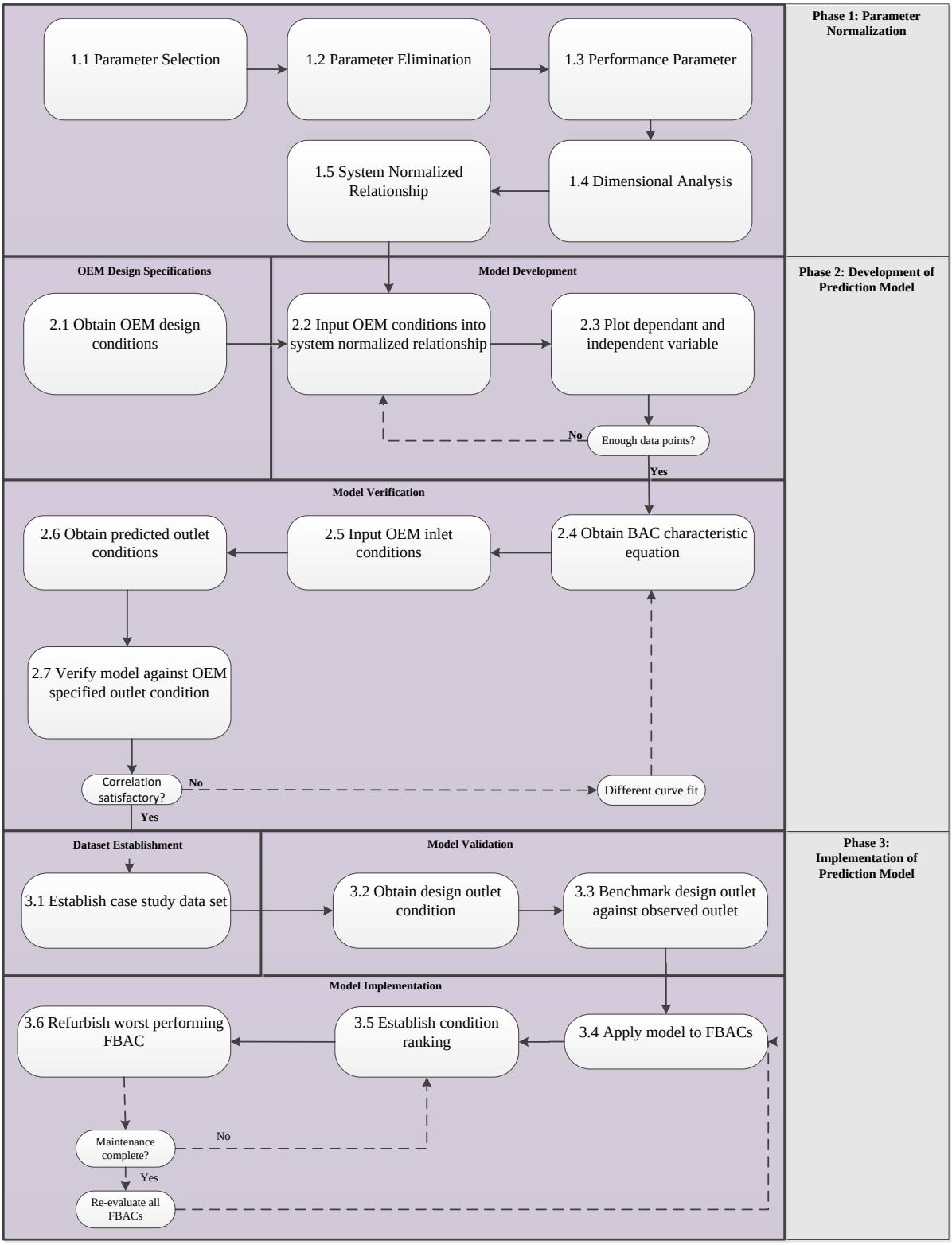

Figure 18: Holistic overview of the condition monitoring method presented (Self illustration).

2.3 Phase 1: Parameter normalization

A brief overview first phase of the method is given below:

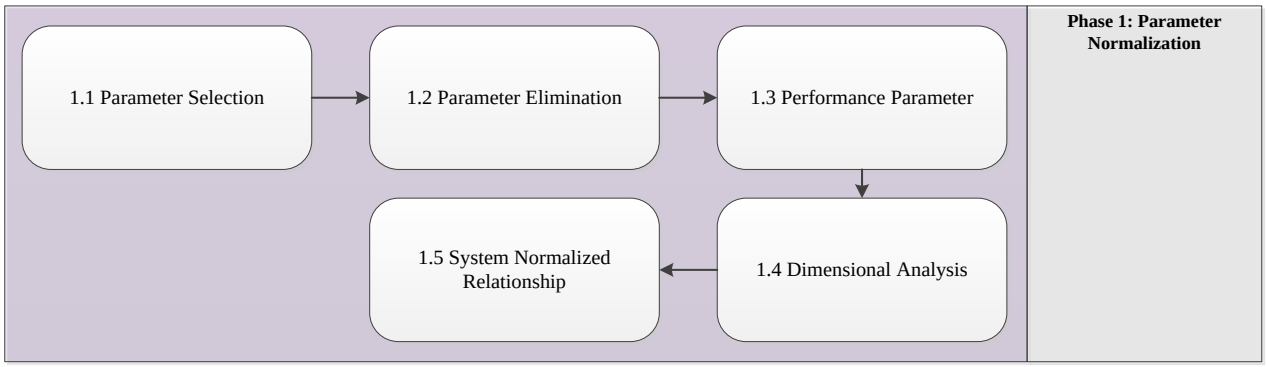

Figure 19: Overview of the first phase of the method (Self-illustration)

The purpose of the first phase is to obtain a normalised relationship between all the operating system parameters that influence the performance of the FBAC. This would allow the method to negate the effects of off-design operation on the condition monitoring data. In addition, this would also ensure the accuracy and reliability of the condition monitoring data obtained. The following sub-sections will outline the first phase of the method in more detail.

2.3.1 Parameter selection

The first step of Phase 1 is to identify all operating parameters that affect the operation and cooling performance of the heat exchanger [60], [61]:

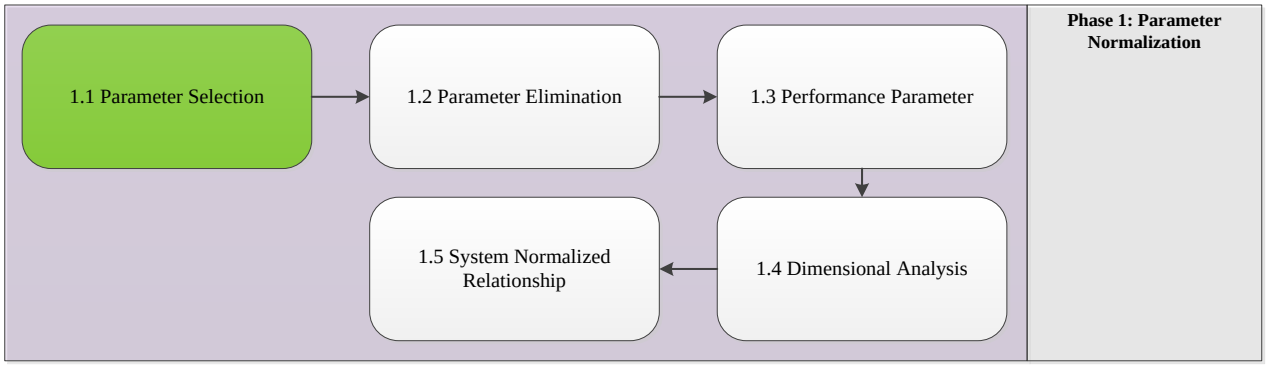

Figure 20: The first step for Phase 1 of the method (Self-illustration)

The three parameters that affect radiator-type heat exchanger performance are the air side (air passing over the BAC coils), the water side (chilled service water flowing through the

tubing) and the geometric side (physical characteristics and material properties of the piping and infrastructure), as shown in Figure 21 below. Table 1 thereafter shows all operating parameters inferred as a result:

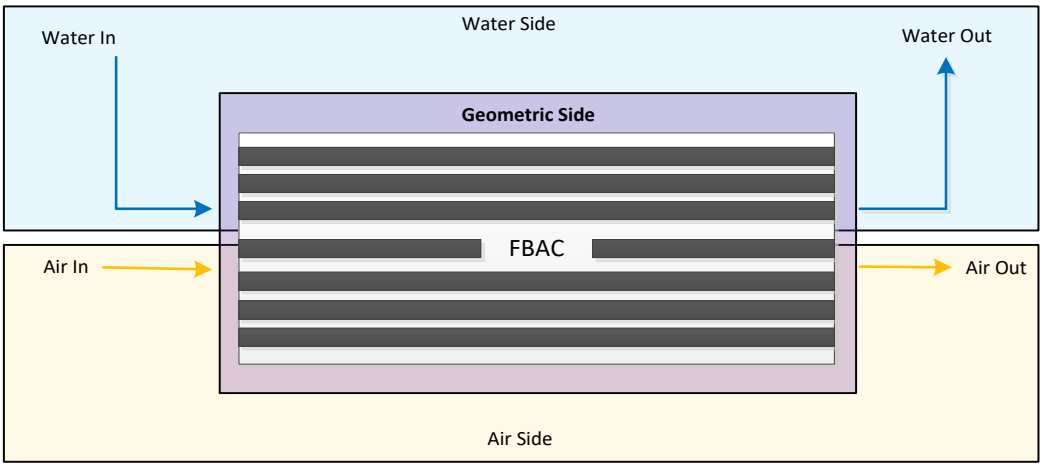

Figure 21: Schematic illustration of the three primary operating sides around a general radiator-type heat exchanger (Self-illustration)

Table 1: Example - System parameters identified that will affect the performance and operation of a FBAC

System	Parameter	Unit
Air Side	Inlet Temperature	°C
	Outlet Temperature	°C
	Mass Flow Rate	kg/s
	Density	kg/m^3
	Viscosity	kg/m.s
	Pressure	$N.s/m^2$
	Thermal Conductivity	W/m.K
	Specific Heat Capacity	J/kg.K
Water Side	Inlet Temperature	°C
	Outlet Temperature	°C
	Mass Flow Rate	kg/s
	Density	kg/m^3

	Viscosity	kg/m.s
	Pressure	N.s/m^2
	Thermal Conductivity	W/m.K
	Specific Heat Capacity	J/kg.K
Geometric Side	Pipe diameter	m
	Pipe wall thickness	m
	Pipe thermal conductivity	W/m.K
	Pipe length	m

The process of identifying parameters around the heat exchanger operation should be thorough and exhaustive as to increase prediction accuracy [62]. Only time-variant parameters should be considered, as constant variables are redundant when arriving at the dimensional analysis subphase of the method [62] presented further on. The next section will outline the elimination of these redundant parameters:

2.3.2 Parameter elimination

After identifying the operating system parameters, all constant operating parameters that do not vary with time is to be eliminated:

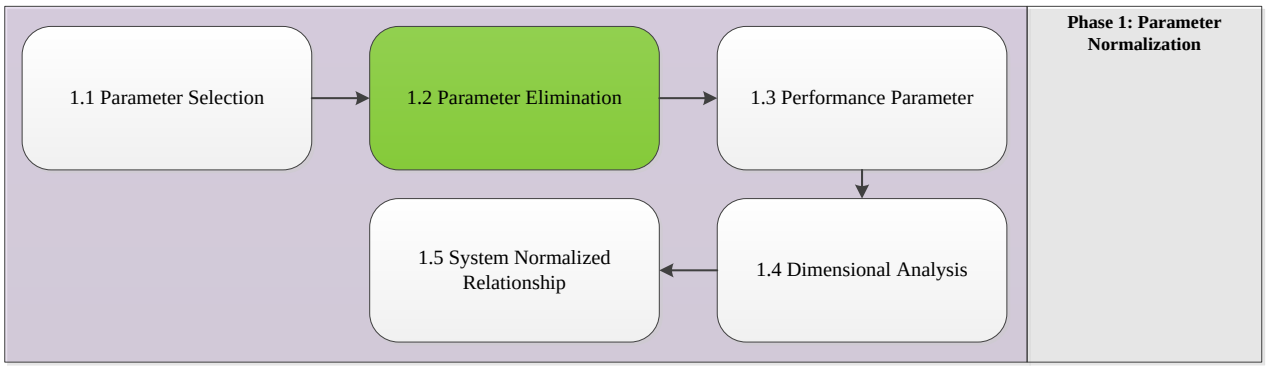

Figure 22: The second step for Phase 1 of the method (Self-illustration)

There are two forms of redundant constant parameters in the typical operation of a radiator-type heat exchanger, namely, inherit properties of the working fluids and the geometric properties [60], [61]. Density, viscosity, thermal conductivity, and specific heat capacity are inherent properties of the working fluids. These parameters are assumed to be constant

as they vary by small amounts at FBAC operating conditions. Geometric properties such as pipe length, diameter, and wall thickness are also assumed constant as they do not vary with time or change in system parameters.

Eliminating constant parameters simplifies the number of system parameters to consider. The remaining time-varying parameters are the mass flows and inlet/outlet temperatures of the working fluids [60], [61], shown in Table 2 below:

Table 2: Remaining system parameters after all non-time variant parameters have been eliminated [60], [61]

System	Parameter	Unit
Air Side	Inlet Temperature	°C
	Outlet Temperature	°C
	Mass Flow Rate	kg/s
Water Side	Inlet Temperature	°C
	Outlet Temperature	°C
	Mass Flow Rate	kg/s

After identifying the relevant system parameters, the next step would be to choose a key performance parameter that reflects the heat exchanger infrastructure instantaneous cooling performance. This will be discussed in the next section.

2.3.3 Performance parameter

The purpose of this step is to identify a key parameter that reflects the current cooling performance of the FBAC. This performance parameter will be based on the remaining operating parameters identified in Section 2.3.2:

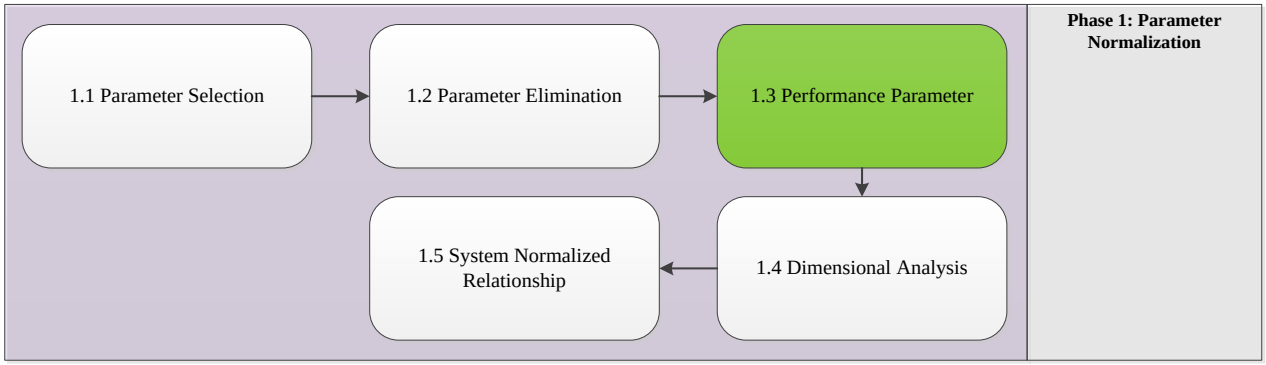

Figure 23: The third step for Phase 1 of the method (Self-illustration).

As coolers serve to reduce or raise the temperature of the respective working fluids, cooling performance of the FBAC would therefore be indicated at the outlet conditions of the cooler. Furthermore, the outlet conditions are dependent on the inlet conditions provided. Therefore, the outlet conditions of the FBAC should be considered when choosing the performance parameter.

The two main outlet parameters of a generic radiator-type heat exchanger are the water outlet temperature and the air outlet temperature. Both can be used to evaluate the cooling performance, however, since the air outlet temperature reflects the amount of cooling power available to mining personnel, it is chosen as the performance parameter. As a result, outlet water temperature is redundant, and negated from the remaining parameters. Table 3 and Equation (2.1) below illustrates the case where the outlet air temperature is chosen as the performance parameter:

Table 3: The air outlet temperature is chosen as the performance parameter.

System	Parameter	Unit
Air Side	Inlet Temperature	°C
	Outlet Temperature	°C
	Mass Flow Rate	kg/s
Water Side	Inlet Temperature	°C
	Mass Flow Rate	kg/s

As stated previously, the outlet temperature of a generic radiator type heat exchanger is dependent on the other independent system inlet parameters, which are referred to as “input parameters” going forward. Therefore, the outlet air temperature is a function of the input parameters [60], [61]:

$$T_{air_{out}} = f\left(T_{water_{in}}, T_{air_{in}}, \dot{m}_{air}, \dot{m}_{water}\right) \quad (2.1)$$

In Equation 2.1, the outlet air temperature ($T_{air_{out}}$) would be some function (f) of the remaining independent system parameters. As stated in Section 2.3.1, the outlet air temperature of the heat exchanger is dependent on the values of the input parameters to the FBAC. Due to the natural variations of input parameters into the heat exchanger over time, this would indicate that the outlet air temperature would vary in accordance. In practice, this would complicate the process of comparing the ideal performance of the heat exchanger to the actual performance, as the input parameters would need to be identical for both cases. Therefore, due to these natural variations, conducting fair comparisons would prove difficult.

To negate any variation in input parameters affecting the comparisons, the parameters would need to be normalised. This is in close adherence to study objective three, stating the need for a monitoring method that is capable of use at off-design operating conditions. In the next section, dimensional analysis is used to obtain a normalised relationship between remaining system operating parameters.

2.3.4 Dimensional analysis

The purpose of this step is to normalise the remaining system operating parameters to offset any variation in input parameters that are impacting the ability to predict outlet air temperature. The process of dimensional analysis is therefore used to normalise operating parameters.

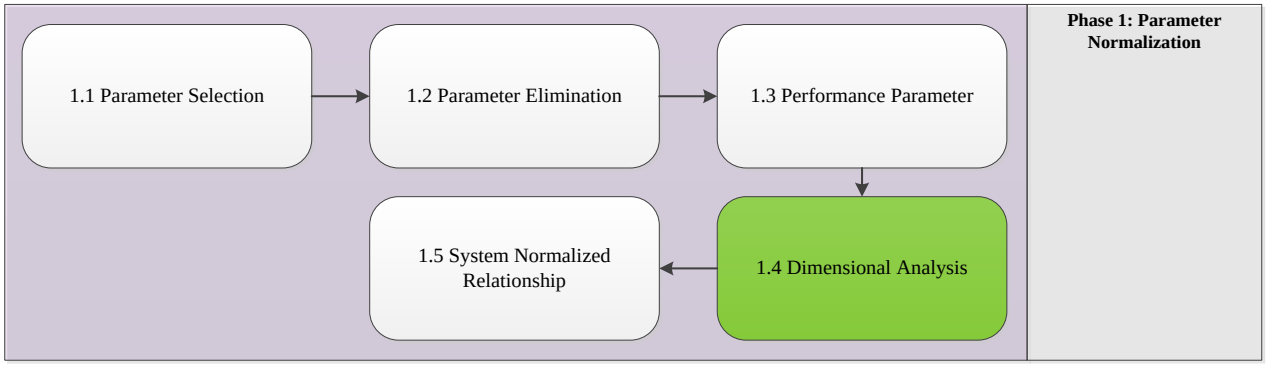

Figure 24: The fourth step for Phase 1 of the method (Self-illustration)

Dimensional analysis is a method for normalizing system parameters by manipulating their base units to create dimensionless groups. These dimensionless groups can then be set equal in a normalised relationship, as their base dimensions are the same [62].

The first step in the process is to convert all remaining system operating parameters to their base units [60], [61], [62]. Base units are the fundamental, mutually independent units for mass (M), length (L), time (T), temperature (θ), mole (n), electric current (A) and luminosity (cd) [62]. The unit of any quantity is made up of a single base unit or combination of these base units. Figure 25 below shows some common quantities, their respective units, and the corresponding base units:

		Dimensions	
Quantity	Symbol	$MLT\Theta$	$FLT\Theta$
Length	L	L	L
Area	A	L^2	L^2
Volume	$\mathcal{V}$	L^3	L^3
Velocity	V	LT^{-1}	LT^{-1}
Acceleration	dV/dt	LT^{-2}	LT^{-2}
Speed of sound	a	LT^{-1}	LT^{-1}
Volume flow	Q	L^3T^{-1}	L^3T^{-1}
Mass flow	$\dot{m}$	MT^{-1}	FTL^{-1}
Pressure, stress	p, σ	$ML^{-1}T^{-2}$	FL^{-2}
Strain rate	$\dot{\epsilon}$	T^{-1}	T^{-1}
Angle	θ	None	None
Angular velocity	ω	T^{-1}	T^{-1}
Viscosity	μ	$ML^{-1}T^{-1}$	FTL^{-2}
Kinematic viscosity	ν	L^2T^{-1}	L^2T^{-1}
Surface tension	Υ	MT^{-2}	FL^{-1}
Force	F	MLT^{-2}	F
Moment, torque	M	ML^2T^{-2}	FL
Power	P	ML^2T^{-3}	FLT^{-1}
Work, energy	W, E	ML^2T^{-2}	FL
Density	ρ	ML^{-3}	FT^2L^{-4}
Temperature	T	Θ	Θ
Specific heat	c_p, c_v	$L^2T^{-2}\Theta^{-1}$	$L^2T^{-2}\Theta^{-1}$
Specific weight	γ	$ML^{-2}T^{-2}$	FL^{-3}
Thermal conductivity	k	$MLT^{-3}\Theta^{-1}$	$FT^{-1}\Theta^{-1}$
Expansion coefficient	β	Θ^{-1}	Θ^{-1}

Figure 25: Common system parameters and their corresponding base units (adapted from [62])

For the generic case of a radiator-type heat exchanger, by using Figure 25, the base units of the remaining system operating parameters presented in Table 2 can be determined. These identified base units are presented in Table 4 below:

Table 4: Remaining system parameters with the performance parameter highlighted.

System	Parameter	Unit	Base Unit
Air Side	Inlet Temperature	°C	θ
	Outlet Temperature	°C	θ
	Mass Flow Rate	kg/s	MT^{-1}
Water Side	Inlet Temperature	°C	θ
	Mass Flow Rate	kg/s	MT^{-1}

Once all base units are established for each remaining system operating parameter, the process of dimensional analysis is used to obtain a set of dimensionless groups. The *Buckingham Pi Theorem* states that the number of dimensionless groups (k) that can be formed from a system with (n) dimensionless variables and (j) base units is given by [62]:

$$k = n - j \tag{2.2}$$

For the generic case of a radiator-type heat exchanger used in this Chapter, there are five dimensionless variables with three base units (mass, time, and temperature). Applying the Buckingham Pi Theorem, this equates to two dimensionless groups being:

$$k_{FBAC} = (5) - (3) = 2 \tag{2.3}$$

And subsequently by applying the process of dimensional analysis[1], the two dimensionless groups that can be formed are:

$$\Pi_1 = \frac{\boldsymbol{T_{air_{out}}} - T_{air_{in}}}{T_{air_{in}} - T_{water_{in}}} \qquad \Pi_2 = \frac{\dot{m}_{water}}{\dot{m}_{air}} \tag{2.4}$$

These dimensionless groups therefore relate the remaining system operating parameters in a normalised, dimensionless manner. This means that the two groups can be set equal, as to obtain a functional and normalised relationship. The next section discusses how the identified dimensionless groups are combined to obtain a normalised relationship between remaining system operating parameters.

2.3.5 System normalised relationship

The steps conducted in the previous section thus far would lead to the formation of a set of dimensionless groups containing all the remaining system operating parameters. These dimensionless groups can be combined into a normalised relationship, related by an unknown function, which is determined empirically further on. The following section will outline the process of using the identified dimensionless groups to obtain a normalised relationship between the system parameters:

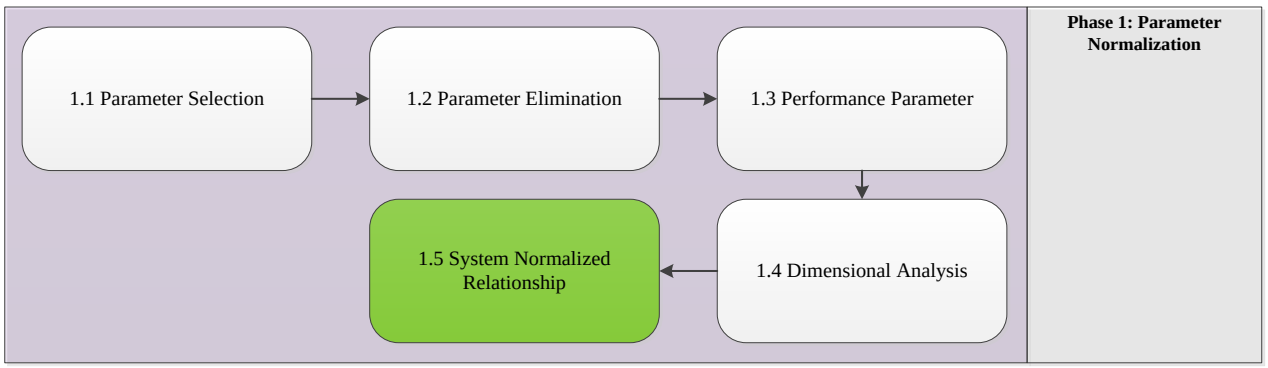

Figure 26: The fifth and final step for Phase 1 of the method (Self-illustration)

[1] The process of obtaining the dimensionless groups through dimensional analysis is shown in Appendix A.

After the set of dimensionless groups are obtained, the chosen performance parameter discussed in Section 2.3.3 would naturally be contained in one of these dimensionless groups. In the case of a generic heat exchanger, the first dimensional group contained the performance parameter, which was the air outlet temperature. The normalised relationship between system parameters can be formed from the dimensionless groups by setting the dependant dimensional group, which is the group containing the performance parameter, equal to the remaining dimensional groups related by an unknown function [60], [61]:

$$\Pi_1 = \mathrm{f}(\Pi_2, \Pi_3, \Pi_4, \Pi_5 \ldots \Pi_\mathrm{k}) \tag{2.5}$$

where: (Π_1) = The dependant dimensionless group containing the performance parameter

(Π_n) = Remaining independent dimensionless group

f = unknown function relating the dependent dimensional group to the remaining independent

The two dimensionless groups identified in the previous section were found to be:

$$\Pi_1 = \frac{T_{air_{out}} - T_{air_{in}}}{T_{air_{in}} - T_{water_{in}}}; \qquad \Pi_2 = \frac{\dot{m}_{water}}{\dot{m}_{air}} \tag{2.6}$$

Substituting these two dimensionless groups above into Equation (2.5), the system normalised relationship is obtained:

$$\frac{T_{air_{out}} - T_{air_{in}}}{T_{air_{in}} - T_{water_{in}}} = f\left(\frac{\dot{m}_{water}}{\dot{m}_{air}}\right) \tag{2.7}$$

Simplifying the system normalised by denoting:

$$\Delta T = T_{air_{out}} - T_{air_{in}} \tag{2.8}$$

and

$$\Delta T_{max} = T_{air_{in}} - T_{water_{in}} \tag{2.9}$$

A simpler form of the normalised relationship is obtained:

$$\frac{\Delta T}{\Delta T_{max}} = f\left(\frac{\dot{m}_{water}}{\dot{m}_{air}}\right) \tag{2.10}$$

The unknown function (f) relating the system operating parameters presented in the system normalised relationship is determined empirically. The process of empirically determining the unknown function (f) will be referred to as “calibration” from this point forward.

Calibrating the normalised relationship would yield a prediction model capable of forecasting the value of the performance parameter in a normalised manner, addressing the third study objective. In addition, this ensures forecasting in an accurate and reliable manner where the effects of varying inlet parameters are negated, providing accurate and reliable data, and addressing the fourth study objective. The process of calibrating the normalised relationship and developing the prediction model is discussed in the next section where the next phase of the method will be outlined.

2.4 Phase 2: Development of prediction model

A brief overview of the second phase of the method is presented below and is discussed further in this section:

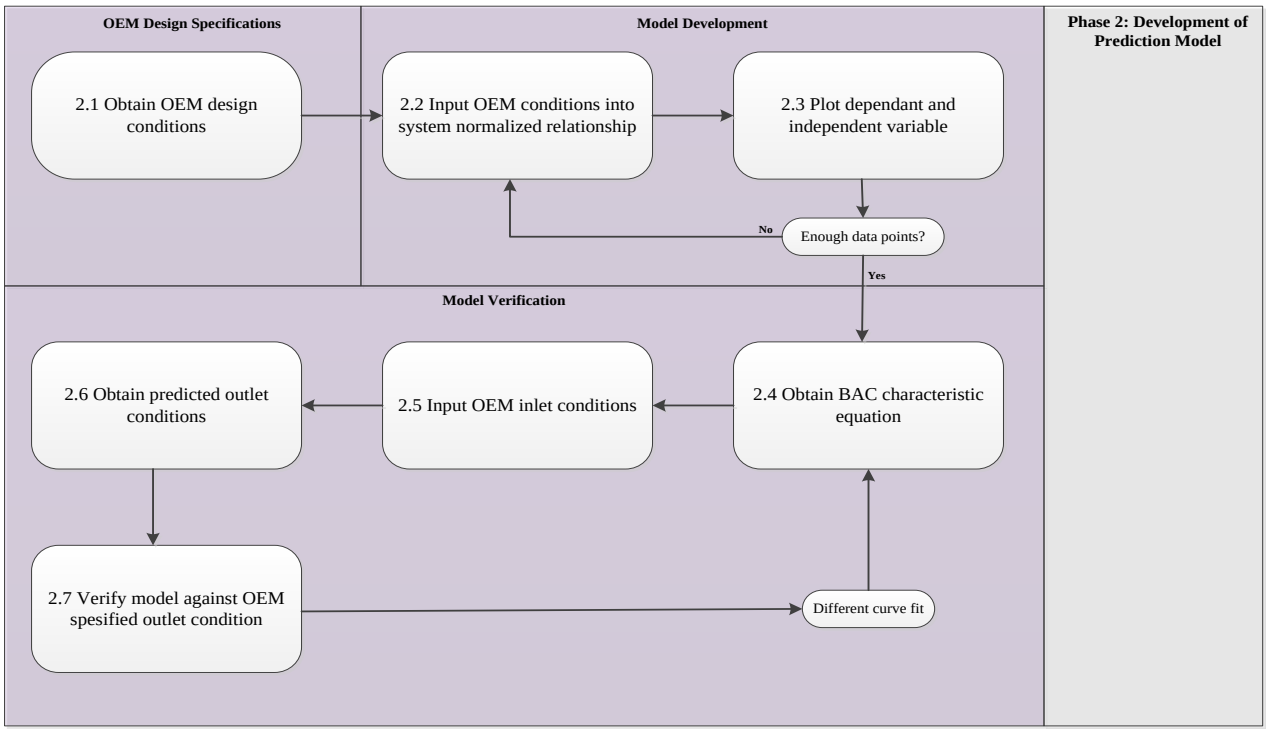

Figure 27: Overview of the second phase of the method, with each of the three respective sub-phases (Self-illustration)

The purpose of the second phase would be to develop a prediction model from the normalised system relationship obtained during the first phase. This is achieved by empirically determining the form of the unknown function in Equation (2.10).

In contradiction to the novel performance model proposed by Sánchez-Escalona *et. al.* [61], the prediction model developed by this method will use original equipment manufacturer (OEM) design specification data for calibration purposes. This would yield a performance monitoring prediction model capable of accurately predicting design outlet conditions at various off-design inlet conditions. Due to the simple nature of the model, this also allows implementation to be done in a continues and remote manner using monitoring systems. The following sub-sections will outline the second phase of the method in more detail.

2.4.1 OEM design specifications

The first step in the second phase of the method is to obtain a comprehensive set of OEM design specifications for the infrastructure under evaluation to be used for calibration:

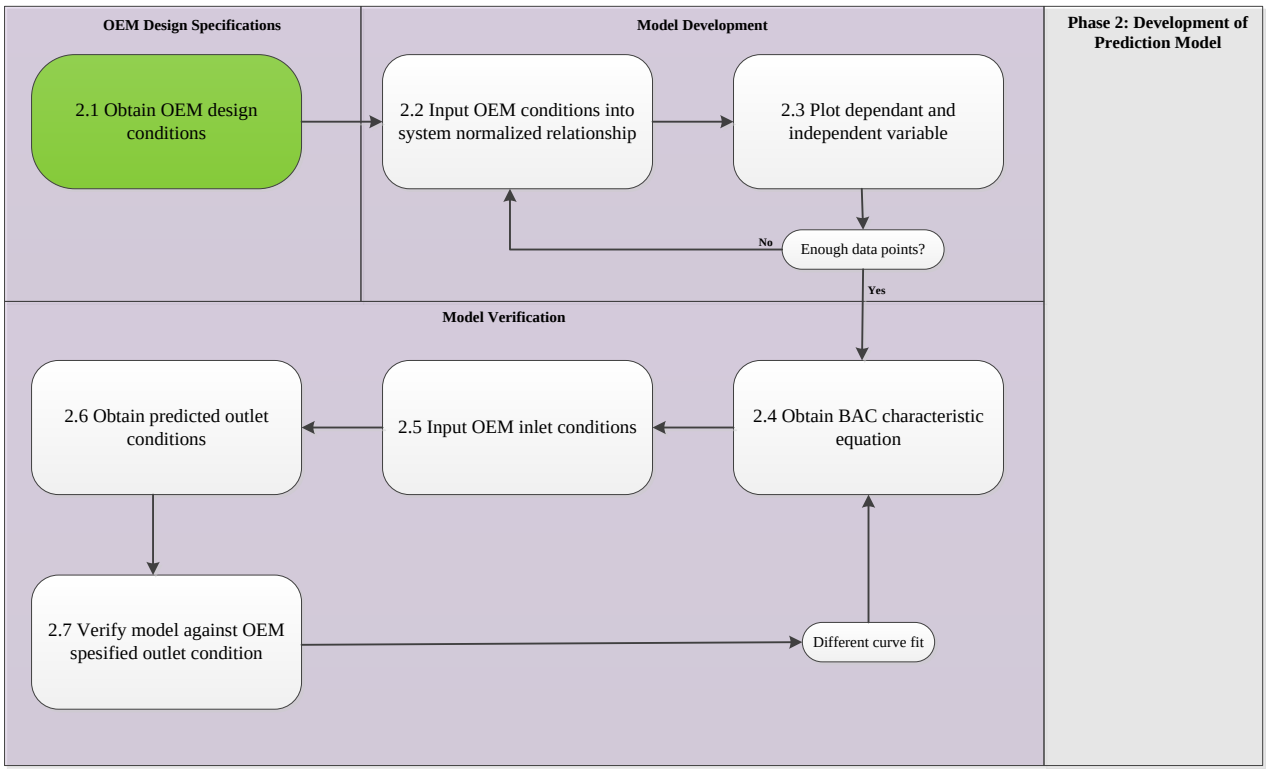

Figure 28: First sub-phase for Phase 2 of the method (Self-illustration)

OEM design specifications are sets of design outlet conditions related to a set of corresponding inlet conditions that are expected when a new piece of infrastructure is commissioned. These conditions will reflect the design performance of the infrastructure. As inefficiencies start to accumulate over time, the observed outlet condition will start to deviate from the design outlet condition due to the degradation in cooling performance.

By utilizing OEM design data for calibration, it allows the user to monitor the difference in the measured outlet condition over time to what the outlet condition would have been should the inefficiencies not have been present (i.e., design conditions). This would ensure that for the same set of inlet conditions, the deviation in observed outlet conditions could be effectively quantified for the detection in onset or presence of inefficiencies.

To ensure sufficient calibration accuracy, sufficiently varying design specification data sets would need to be obtained to cover all operating cases [62]. This will be achieved by

acquiring exhaustive sets of OEM specification data sheets at different inlet conditions, as to ensure that a sufficient and diverse population of data is used for calibration. Different OEM design specification sets are calculated using complex and powerful mathematical models developed by the OEMs, in conjunction with experimental data obtained using expensive testing equipment and infrastructure. This is not ideal, as the procurement for both complex mathematical models and experimental setups are costly and time consuming.

The prediction model developed in this section essentially mimics the OEM design specifications, bypassing the need to compile time-consuming data sheets for each case of inlet condition combinations. The following section will discuss how the OEM design specifications is used to calibrate the prediction model by determining the nature and form of the unknown function in Equation (2.10).

2.4.2 Model development

As briefly discussed, the purpose of this section is to use the OEM design specification data in conjunction with Equation (2.10) to determine the nature and form of the unknown function, giving the characteristic equation of the prediction model:

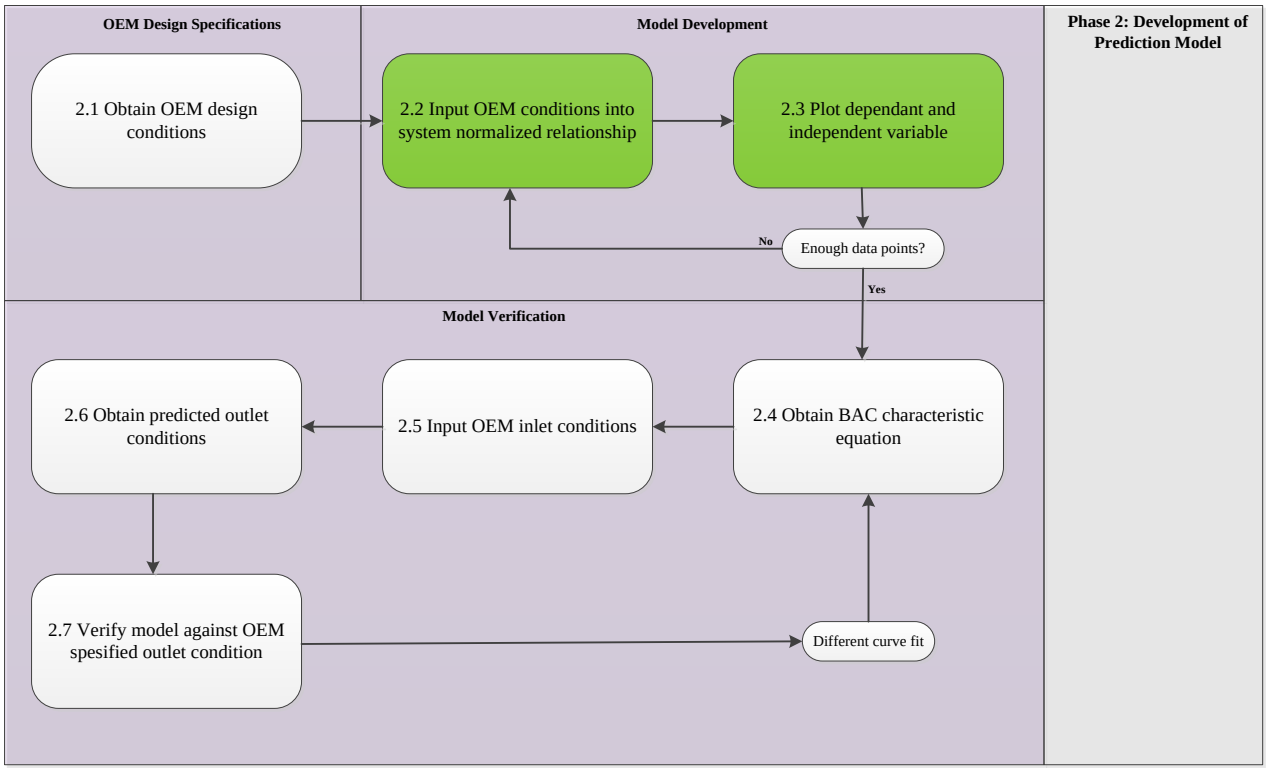

Figure 29: Second sub-phase for Phase 2 of the method (Self-illustration)

Due to both the inlet and corresponding outlet conditions being given in the OEM design specifications, the dependant, and independent groups of Equation (2.10) can be plotted directly against one another. Therefore, one complete set of OEM design conditions would lead to one data point, and the number of data points corresponds with the number of independent sets obtained from the OEM design specifications.

To ensure sufficient calibration accuracy, the available set of OEM design conditions should be as exhaustive as possible. Figure 30 below presents a plot obtained from Laskowski *et.al* when using current operating data sets as the calibration data. A similar plot is expected when using OEM design data for FBACs:

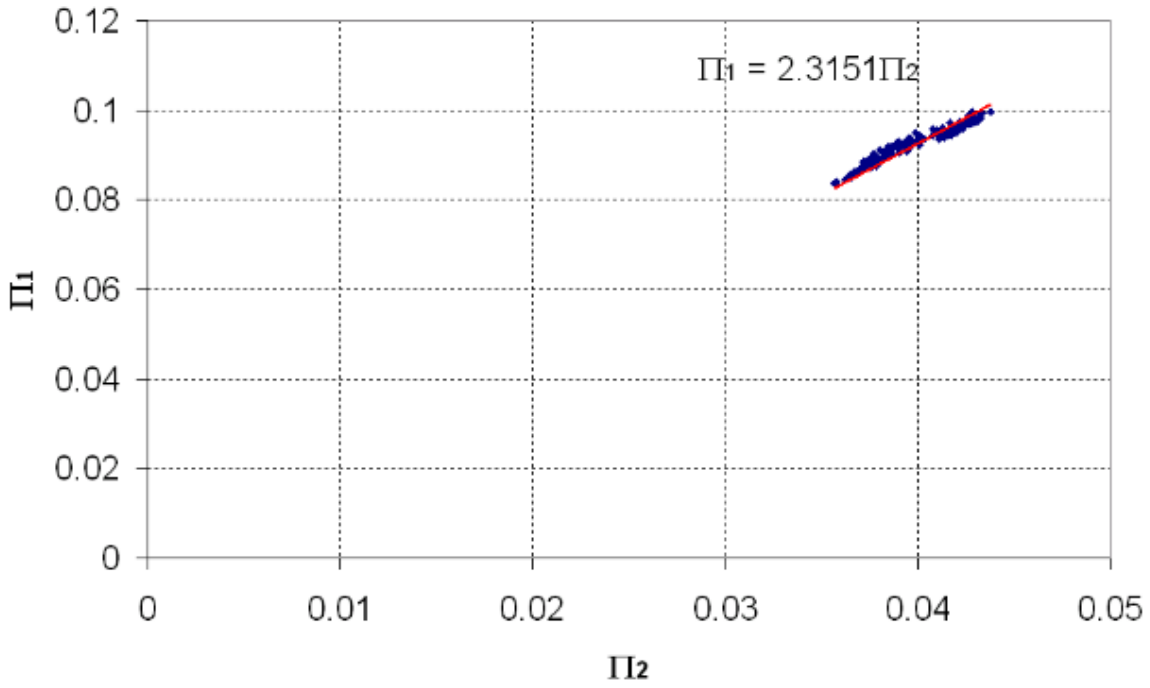

Figure 30: Use of calibration data in both dimensionless groups to obtain the characteristic equation (Adapted from [60])

The function describing the relationship between the normalised system operating parameters in Equation (2.10) is obtained by utilizing curve fitting methods after all data points have been plotted. Curve fitting refers to using a mathematical equation to relate a series of data points by means of a single equation or function. Curve fitting methods are applied to two distinct data regression types, namely linear and non-linear.

Linear regression data are where the dependant variable directly links to the independent variables in a constant and scalable manner. Non-linear regressions have no inherent link between dependant and independent variables and is usually solved by iterative methods. Due to the nature of the output obtained during dimensional analysis, it is reasonable to assume that a linear regression data set may be assumed [60]–[62].

The most common method of linear regression curve fitting is known as the *Least-Squares method*. The least squares method would produce a best fit curve to represent the data set. The best fit curve may have different forms and types, such as linear, polynomial, logarithmic and exponential. The higher the number and accuracy of the OEM data applied in this section, the more accurately the equation from the best fit curve will represent the data set [62].

Applying curve fitting to the calibration data will allow for the unknown function in Equation (2.10) to be solved, yielding the characteristic equation of the prediction model. This characteristic equation would allow the model to predict an OEM design outlet condition for any set of inlet conditions being given. Therefore, the proper choice of best fit curve to represent the characteristic equation of the prediction model is equally as important as using an accurate and large OEM data set. The following section will describe how different best fit curves are evaluated for prediction accuracy, ensuring the best fit type has been used.

2.4.3 Model verification

The previous section describes how during the calibration process, curve fitting methods can be used to describe the data set obtained by inputting OEM design conditions into Equation (2.10), yielding the characteristic equation of the prediction model. The following section discusses how the prediction model is verified against OEM design data by testing the accuracy of different curve fits. This will simultaneously ensure the accuracy and reliability of the prediction model as well as verifying the model in the process:

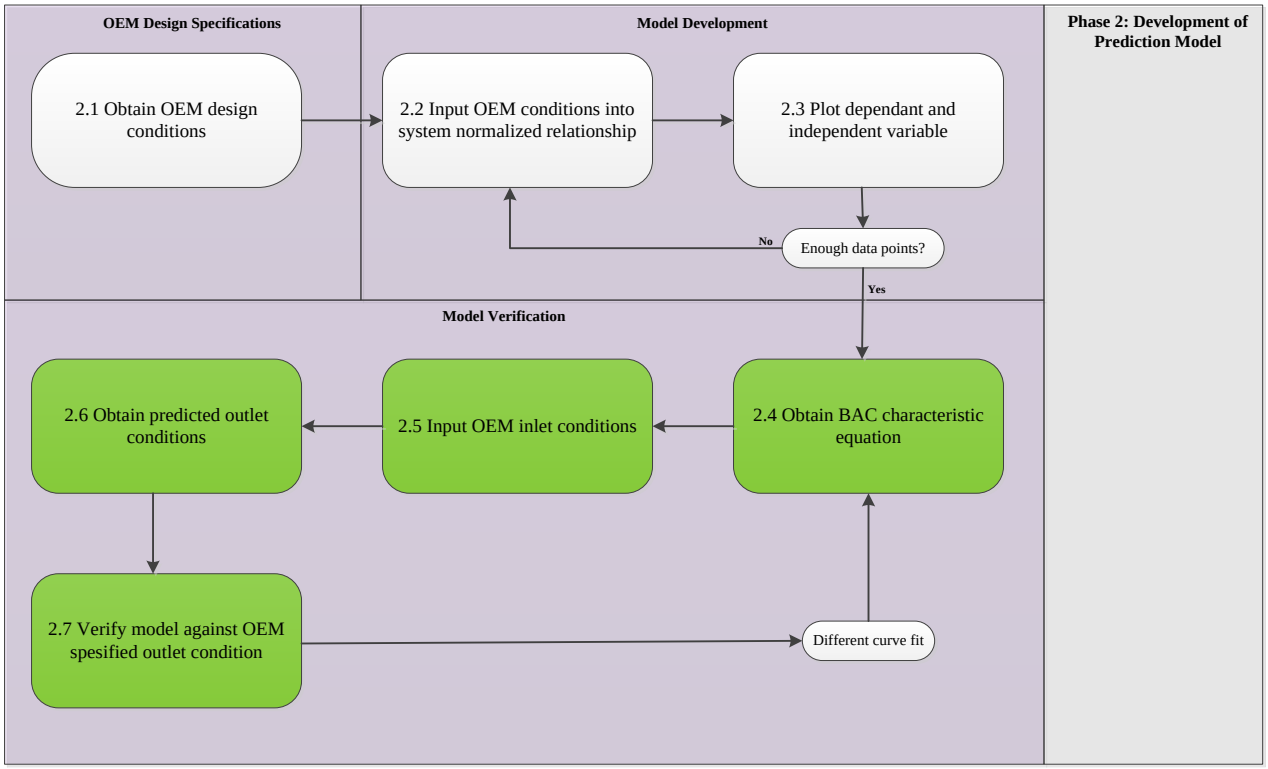

Figure 31 Third and final sub-phase for Phase 2 of the method (Self-illustration)

To verify the prediction model, the design outlet conditions predicted will be compared to the OEM specified outlet condition for the same corresponding set of inlet conditions. For the prediction model to predict design outlet conditions, the equation would need to be rearranged as to have the chosen performance parameter as the subject. Recalling from Section 2.3.3, in the generic case presented in this chapter, the chosen performance parameter would be the outlet air temperature:

$$\frac{T_{air_{out}} - T_{air_{in}}}{T_{air_{in}} - T_{water_{in}}} = f\left(\frac{\dot{m}_{water}}{\dot{m}_{air}}\right) \tag{2.11}$$

$$T_{air_{out}} = T_{air_{in}} + \left(T_{air_{in}} - T_{water_{in}}\right) f\left(\frac{\dot{m}_{water}}{\dot{m}_{air}}\right) \tag{2.12}$$

Equation (2.12) above forms the equation that enables the prediction model to predict a design outlet air condition for a set of corresponding inlet conditions specified in Section 2.3.3. The predicted design outlet air temperature for the chosen curve fit will then be compared to the OEM specified design outlet air temperature for the same set of inlet conditions used. An acceptable deviation between predicted outlet and OEM specified outlet would have to be obtained as to effectively consider the prediction model verified.

Figure 32 below illustrates the results obtained from Sánchez-Escalona *et. al.* and Lazowski *et. al.* when using current operating data as input for calibration. Subsequently, the predicted outlet conditions given by their respective performance models were compared with the observed outlet conditions for the same set of corresponding inlet conditions:

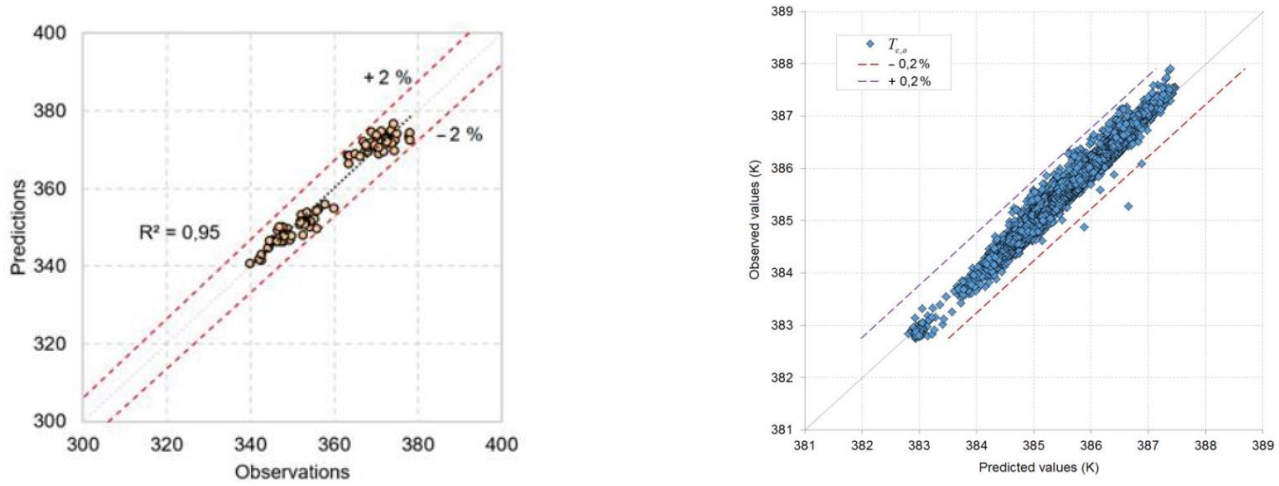

(a) (b)

Figure 32: (a) Correlation between predicted vs observed outlet temperature for the jacketed shell-and-tube heat exchanger (adapted from [64]). (b) Correlation between predicted vs observed rich amine exit temperatures (adapted from [60]).

Sánchez-Escalona *et. al.* and Lazowski *et. al.* obtained relative prediction errors of ~2% and less, respectively [60], [61] during their “calibration” process. Therefore, the prediction model obtained using the method presented in this dissertation aims to have the same range of prediction error.

To ensure the optimal best fit curve has been chosen, the process described thus far would have to be repeated for every best fit curve type considered. The resultant correlation and prediction error between predicted outlet temperature and the OEM specified design outlet condition for each case would then have to be compared. The curve fit that yields the lowest relative error in prediction and highest correlation between the predicted and OEM specified design outlet, while keeping in range of that shown previously, will be used as the best choice to use for the characteristic equation. Once sufficient prediction accuracy is obtained, this would consider the model verified.

Model verification would ensure that the method is able to implement continuous and remote monitoring at off-design conditions in an accurate and remote manner, ensuring adherence to study objectives one, three and four. Once the model has been verified and the best fit curve has been chosen, the model is ready to be validated in the effectiveness of implementing condition monitoring, adhering to the study objectives outlined in Section

1.9. The following section will describe the third phase of the method, where the prediction model is implemented and validated for the remaining study objectives.

2.5 Phase 3: Implementation of prediction model

A brief overview of the third phase in the presented method is given below:

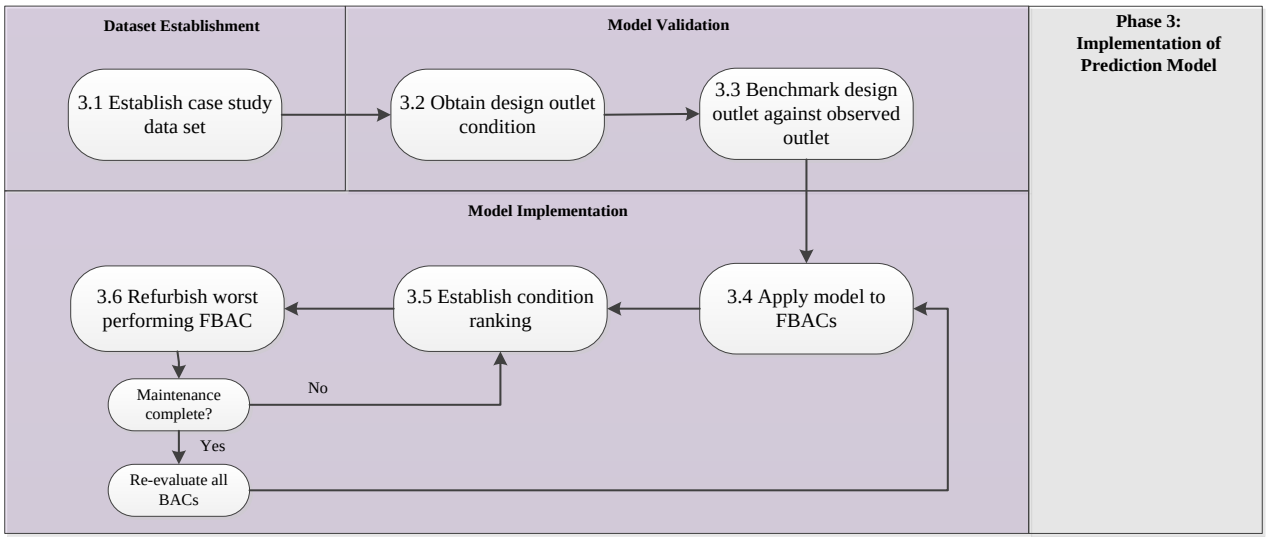

Figure 33: Overview of the third phase for the method (Self-illustration)

The purpose of the third phase in the method is to implement the prediction model on a set of case study FBACs to validate the model's ability to monitor the condition of the FBAC by effectively detecting the onset and presence of multiple inefficiencies impacting cooling performance. The following sections will outline the third phase of the method in more detail:

2.5.1 Dataset establishment

Before the method can be implemented on a set of case study FBACs, a comprehensive data set of case study operating conditions would first need to be established. Therefore, the first step in the third phase of the method is to establish an exhaustive set of operating conditions around the FBAC infrastructure being monitored:

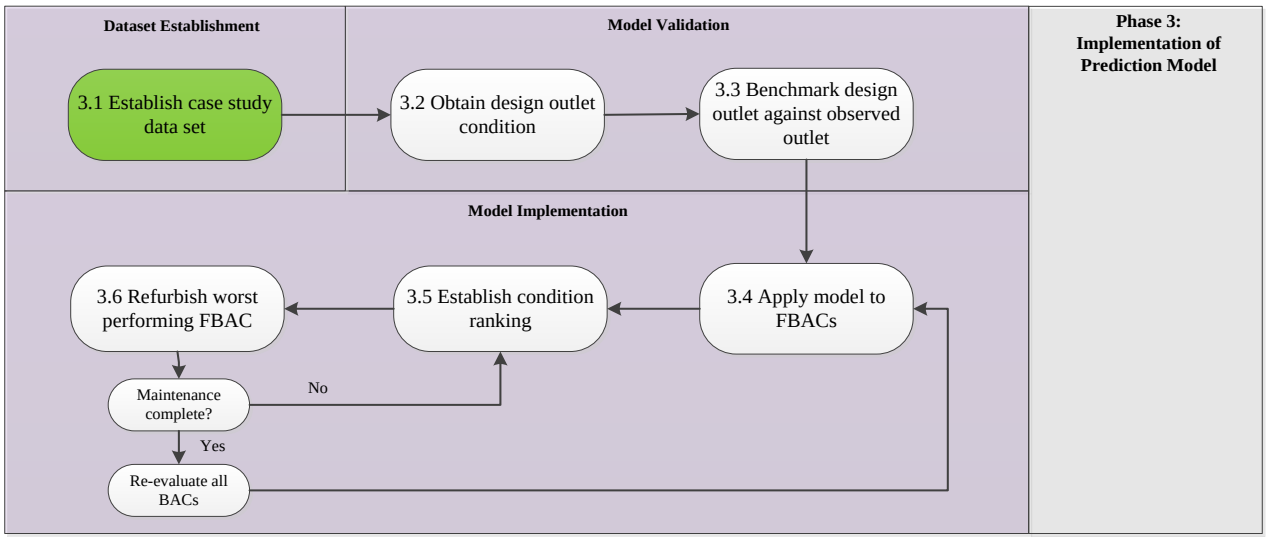

Figure 34: First sub-phase for Phase 3 of the method (Self-illustration)

As one of the objectives of this dissertation is to present a method able to conduct condition monitoring in a remote and continuous manner, the method of data collection around the FBAC should be done using environmental and hydraulic sensors, able to provide continuous and remote data to monitoring systems such as SCADA systems.

Environmental sensors are digital measurement instrumentation that measures various environmental conditions such as temperature, pressure, relative humidity, and velocity[2]. Environmental sensors can be placed strategically in places around the heat exchanger infrastructure, measuring key operating parameters outlined in Section 2.3.1.

Environmental sensors are mechanical devices that transpose mechanical motion/displacement into digital signals when exposed to environmental conditions. These digital signals can then be converted into measurements that present the value of different environmental factors, as stated previously. The environmental data is logged by using an integrated monitoring system, such as a supervisory control and data acquisition (SCADA) systems. Due to the digital nature of the measurements, the biggest advantage offered by using environmental sensors is that the data can be logged over large periods of time [65]. This leads to large volumes of measurement data being available for analysis, providing ample scope to address study objective one.

[2] "Environmental Sensors.". Internet: https://www.sunbirddcim.com/glossary/environmental-sensors, June 2023

SCADA systems are integrated monitoring software that provides an overview of a system. SCADA systems are used in various industries to monitor pumps, turbines, electric systems, plants, and mines. In the mining industry, the SCADA system monitors the refrigeration, compressed air, electrical, and ventilation systems [16], [18], [23] . Environmental sensors feed data directly into the SCADA system where it is stored and available for analysis. Figure 35 below presents the data acquisition and handling process:

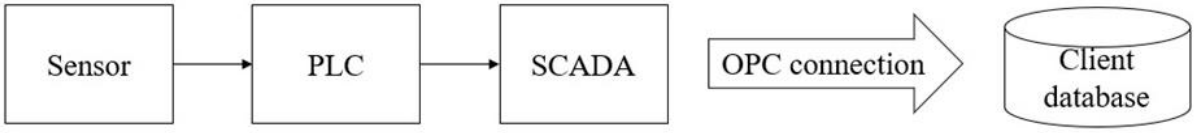

Figure 35: Data acquisition process (adapted from [65])

However, the biggest disadvantage of environmental sensors in the mining industry are their susceptibility to breakdowns [23]. Power failures and environmental contamination can cause sensors to experience various faults such as shutdowns, data loss or data flatlining [66], [67] . This hinders the subsequent reliability of monitoring data. To negate these effects and ensure compliance to study objectives, it is important to filter out faulty measurements during the analysis process to ensure that the most accurate representation of the FBAC cooling performance is given.

Once a sufficiently large set of conditions have been obtained, observed outlet temperatures can be benchmarked against predicted design outlet air temperature, obtained from the prediction model. The process of using the measured conditions and the prediction model to predict a design outlet air temperature is outlined in the next section.

2.5.2 Model validation

Once an exhaustive set of relevant case study operating conditions have been established during the previous section, the prediction model is used to benchmark observed outlet conditions against the predicted outlet conditions:

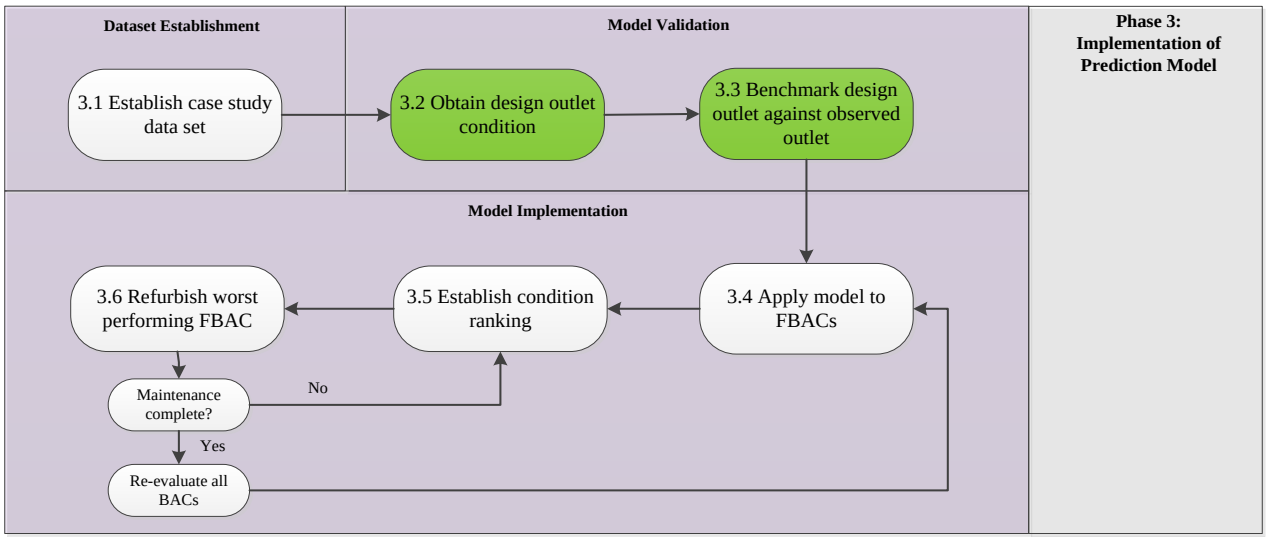

Figure 36: Second sub-phase for Phase 3 of the method (Self-illustration)

The previous section outlined how case study operating conditions are obtained. These include inlet conditions/parameters such as air temperature, air mass flow, water temperature and water flowrates, and observed outlet conditions such as outlet air temperature. These operating conditions should correspond to the conditions related in the characteristic Equation (2.12) of the prediction model. In this section, the prediction model will be used to predict a design outlet air temperature for the set of obtained operating conditions.

The results from Sánchez-Escalona *et. Al.* and Laskowski *et. Al* of predicted outlet vs observed outlet condition over time, obtained by their respective performance models, are shown below in Figure 37. The respective performance models attempted to mimic the operation of the heat exchanger infrastructure, and was applied with great accuracy and effectiveness:

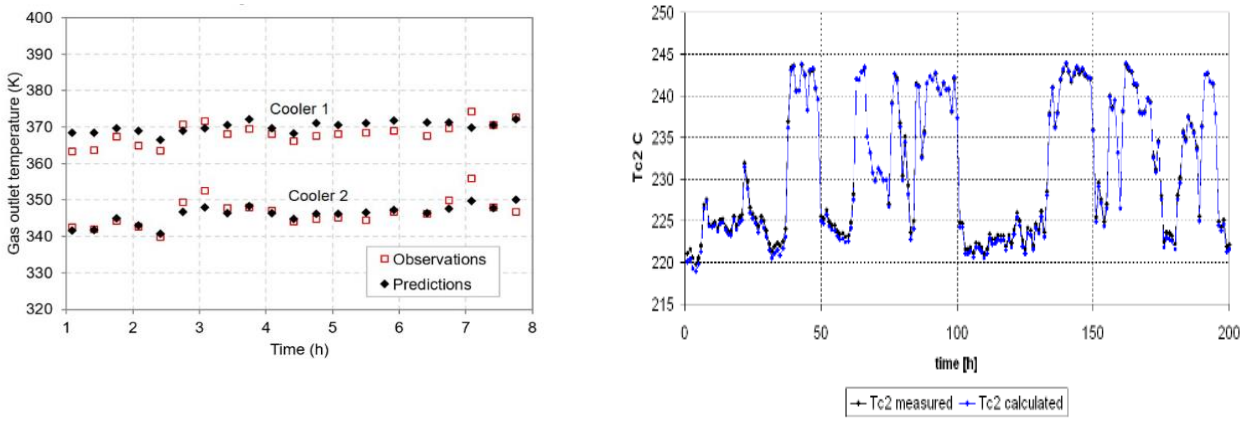

(a) (b)

Figure 37: (a) Gas outlet temperatures of the HX obtained by the prediction model compared to the observed gas outlet temperatures (adapted from [64]). (b) Water outlet temperatures of the HX obtained by the prediction model compared to the observed water outlet temperatures (adapted from [60])

The prediction model derived from the method proposed in this dissertation will be applied in a similar manner. However, since the prediction model is calibrated based on OEM design specifications, a gradual deviation between the predicted outlet condition and the observed outlet condition is expected over time as inefficiencies develop. If inefficiencies are already present, it is anticipated that the predicted outlet condition will exhibit a similar trend as that obtained by Sánchez-Escalona *et. al.* and Laskowski *et. al*, but with an offset due to the impact of existing inefficiencies on cooling performance.

The magnitude of deviation over time will provide an indication of the deteriorating condition of the FBAC. This validation process confirms the suitability of the model for condition monitoring of underground FBACs, enabling the detection of multiple inefficiencies affecting cooling performance. As a result, the second and fifth study objectives are effectively addressed.

To ensure comprehensive compliance with the study objectives, the benchmarking process will be repeated for each FBAC in the case study mine. The resulting deviations will be compared to determine the FBAC with the most severe condition. The subsequent section outlines the implementation process of the prediction model on various FBACs in the case study mine.

2.5.3 Model implementation

In the following section, the steps of the method outlined in Section 2.5.1 and 2.5.2 is to be applied at each FBAC present in the case study mine under evaluation. The magnitudes in deviation for each respective FBAC will then be determined and compared to establish a condition ranking.

From the condition ranking, the FBAC in the worst operating condition can be identified and prioritised maintenance and refurbishment efforts can be conducted. The process can be subsequently repeated till all FBAC infrastructure is within acceptable condition:

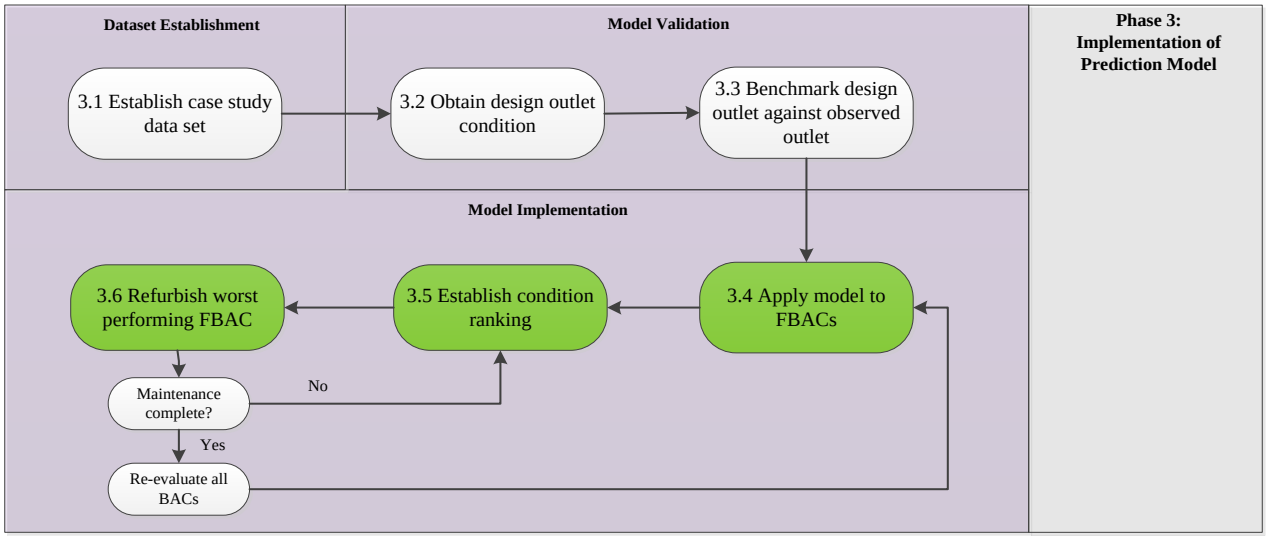

Figure 38: Third and final sub-phase for Phase 3 of the method (Self-illustration)

Figure 39 below illustrates an example of an expected comprehensive comparison between the average magnitude of deviation in outlet air temperatures for each respective FBAC in a case study mine:

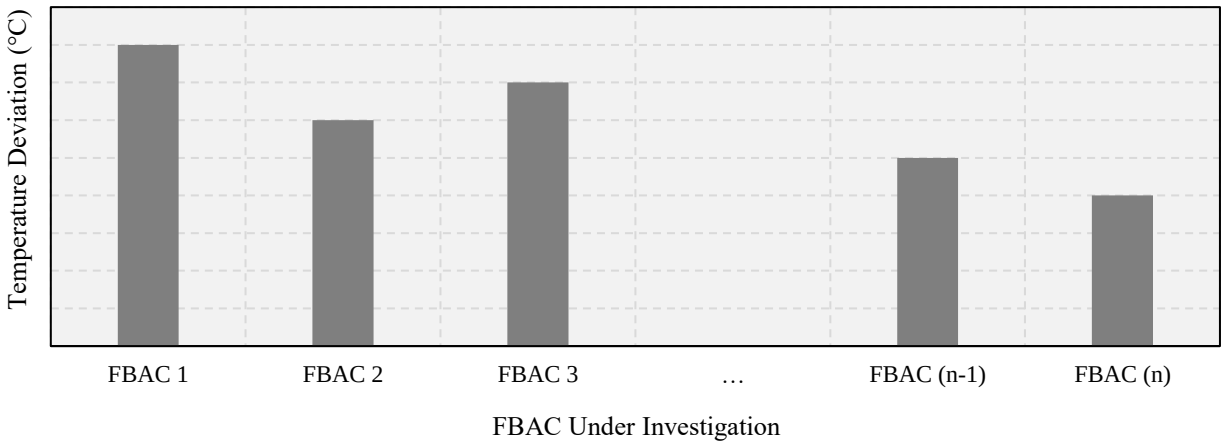

Figure 39: Example comparison of (n) amounts of FBAC outlet temperature deviations from the predicted outlet air temperature, showing a clear hierarchy of FBAC condition, ranging from highest deviation to lowest deviation (Self illustration).

From the comparison of the respective deviations for each respective FBAC, a clear condition ranking will emerge. Figure 40 below illustrates an example in the case where the deviation comparison of Figure 39 is rearranged to show the condition ranking of FBAC condition:

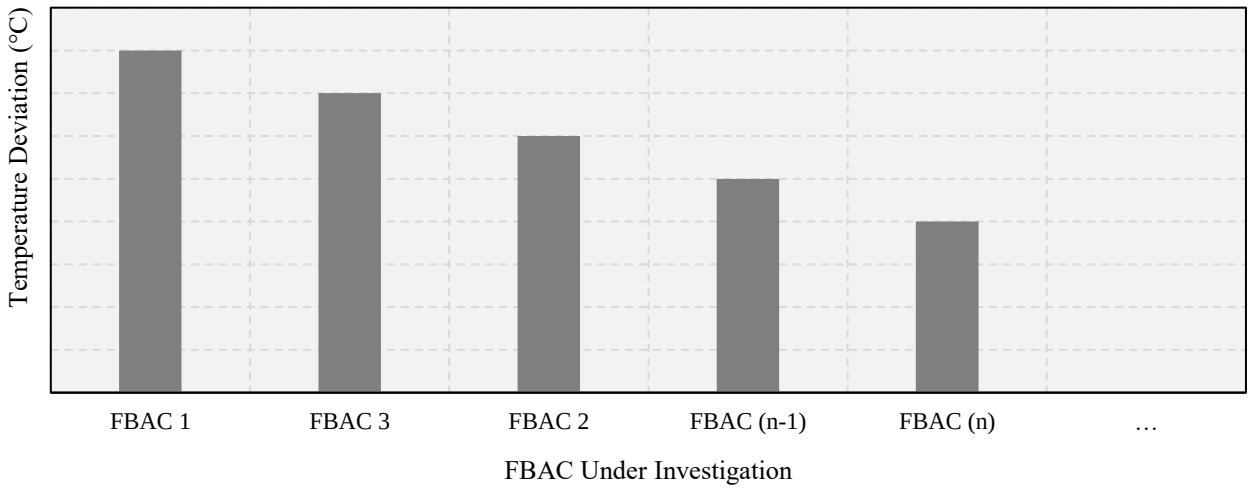

Figure 40: Example of FBAC condition ranking based on the deviation of outlet air temperature from the predicted outlet temperature. Adapted from Figure 39 (Self-illustration)

From the condition ranking, the FBAC with the highest temperature deviation and subsequently the most severe condition degradation, can be identified. An illustrative example is provided in Figure 41 below:

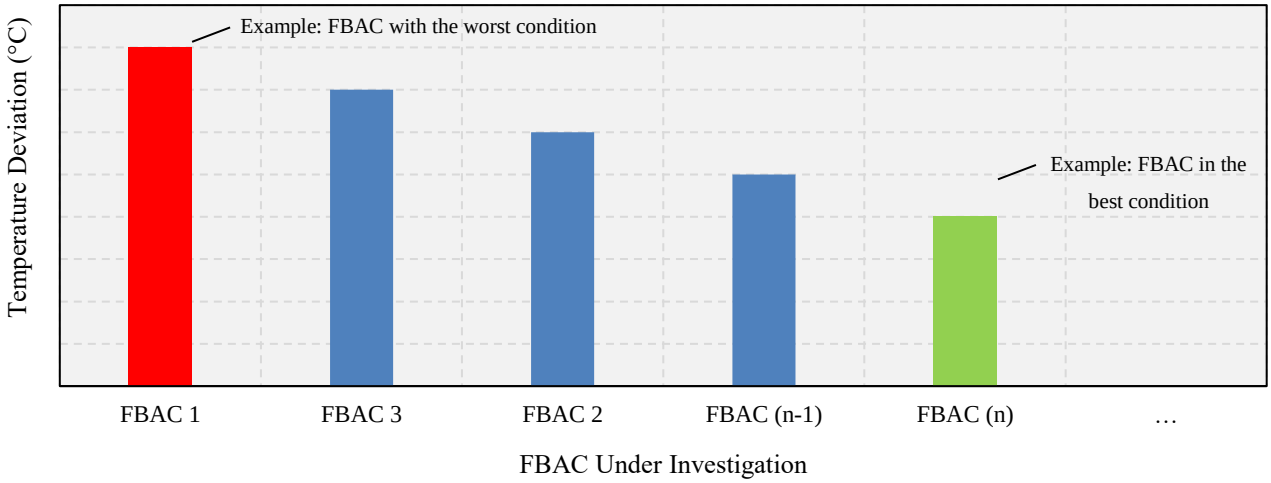

Figure 41: FBAC with the most severe condition of degradation identified from the condition ranking shown in the example in Figure 40 (Self-illustration)

Once the worst performing FBAC is identified, inspections can be conducted to assess the nature and severity of the inefficiencies. Van Rooyen estimates that every 1 °C loss in cooling performance would result in a monthly production revenue loss of R 2 086 783 due to declines in worker efficiency [23]. This relates closely to the worker efficiency correlations shown in Figure 9 of Section 1.5, although the author had used another correlation, albeit similar.

Based on the findings, restorative measures such as maintenance, refurbishment, or replacement can be considered and implemented [23]. Maintenance involves regular cleaning of heat transfer surfaces using chemical compounds. However, it may be expensive and challenging for FBACs located far from workshops. Refurbishment is considered for severe inefficiencies, involving the removal and rigorous refurbishment of FBAC banks. Replacement is the final option for highly degraded components. It is the costliest option but yields significant improvements [23].

Once corrective maintenance efforts had been conducted, a re-evaluation of all FBAC may be done to assess the next worse performing cooler. Corrective maintenance measures can then be redone, and the cycle can be repeated till all FBAC cooling performance falls within acceptable ranges.

2.6 Summary review of method compliance to study objectives

In this section, a summary review of the compliance of each phase of the method to the study objectives is given. Recalling the objectives of the study outlined in Section 1.9, the study aims to present a method of condition monitoring capable of:

1. Continuously and remotely monitoring the
2. Condition of underground finned tube bulk air coolers
3. Operating at off-design conditions in an
4. Accurate and reliable manner, with the ability to
5. Detect the onset and presence of multiple inefficiencies impacting cooling performance.

In this chapter, the three distinct phases were putt forth, each of which respectively aim to address the established study objectives. Table 5 below presents a summary of each phase's compliance to the study objectives:

Table 5: Summary of the compliance of each phase in the method to the study objectives put forth in section 1.9

	Phase 1: Parameter Normalization	**Phase 2:** Development of Prediction Model	**Phase 3:** Implementation of Prediction Model
Study Objective 1: Continues and remote monitoring.		×	
Study Objective 2: Condition monitoring of underground FBACs.			×
Study Objective 3: Monitoring at off-design conditions	×	×	
Study Objective 4: Accurate and reliable	×	×	
Study Objective 5: Detect the onset or presence of inefficiencies			×

The first phase of the method outlined in Section 2.3 ensures that various operating parameters around the FBAC infrastructure are normalised to allow for monitoring at off - design conditions in a reliable and accurate manner. This ensures that study objectives three and four are met.

The second phase of the method outlined in Section 2.4 uses the normalised relationship between various operating parameters obtained during the first phase to develop a normalised prediction model capable of predicting OEM design outlet conditions for any set of inlet conditions. The prediction model is then verified against OEM design specifications to ensure prediction accuracy, further ensuring the ability to perform monitoring at off-design conditions in a reliable and accurate manner. Additionally, due to the simplistic nature of the characteristic equation of the prediction model, the ability of the model to be implemented in a remote and continuous manner by use of monitoring systems is outlined. To this point, this ensures that the method addresses study objectives one, three and four.

Finally, the third phase of the method outlined in Section 2.5 uses the verified prediction model for implementation on case study FBAC infrastructure to evaluate the ability of the method to implement condition monitoring on underground FBACs to detect the onset or presence of multiple inefficiencies affecting cooling performance. Once successful, this ensures that the remaining objectives of the study are addressed, namely study objective two and study objective five.

In the following chapter, the method is implemented on a case study mine to assess the compliance of the method presented to the set study objectives outlined in Section 1.9.

CHAPTER 3 METHOD IMPLEMENTATION

3.1 Chapter preamble

In the previous chapter, an outline of the method presented in this dissertation was given in systematic order to ensure compliance to all the study objectives set in Section 1.9. The following chapter presents the results of applying the proposed method to a case study deep-level mine to evaluate the compliance of the method to the study objectives.

The results are presented as a holistic collective, where the method is applied in a systematic order following the outlined phases and sub-phases presented in Chapter 2 of this dissertation. The following section will give details of the case study mine used to evaluate the method, and the subsequent sections will outline the systematic application of the method to the case study mine.

3.2 Case study background

The method presented in this dissertation was applied to seven case study FBACs at Mine A in South Africa. Mine A is a deep-level mine which includes four current production levels. Each production level contains two FBACs except for one, as shown in Figure 42 below:

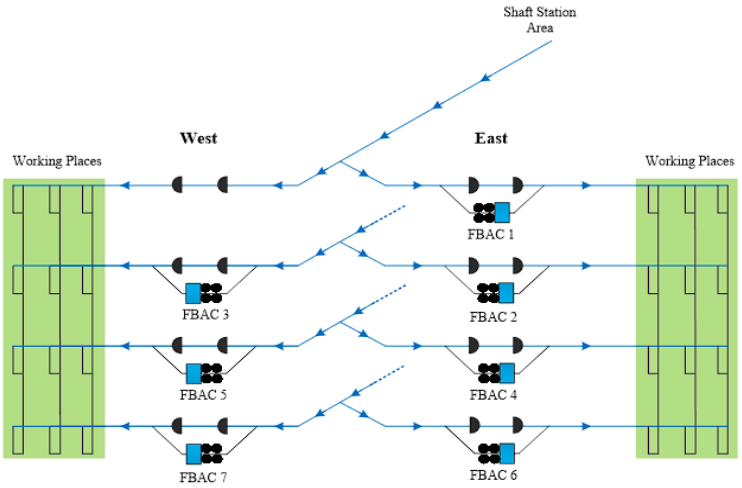

Figure 42: Schematic layout of the four production levels with their respective FBACs located on Mine A. The production levels consist of an eastern and western side, each supplied by a FBAC. The working place areas are denoted in green (Self illustration)

The FBACs cool down the ventilation air before reaching the working places. Each production level is divided into an eastern and western side, forming a Y shape. Each FBAC is of the same type and manufacturer and is rated for a design cooling duty of 1 500 kW. Additionally, each FBAC on Mine A has two 90 kW fans that supply 60-100 kg/s of ventilation air to the half-level on average.

Each FBAC is supplied by a service water pipe carrying chilled water as cool as 11 °C at 60 l/s on average to ten parallel FBAC banks with smaller parallel finned pipes. A diagram of the configuration for a single FBAC on Mine A is illustrated in Figure 43 below:

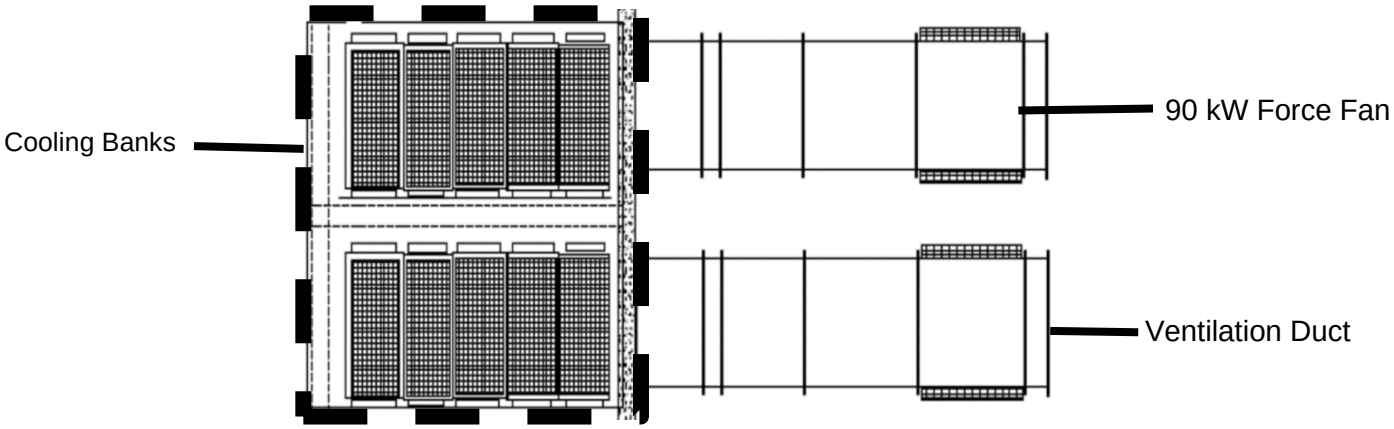

Figure 43: Schematic layout of a FBAC found on Mine A (adapted from [23])

The ten cooling banks on each FBAC serves as the main interface for heat transfer. After cool service water has passed through the FBAC banks, the water is routed back to the level station by means of a return line. The water is then routed up through various hot dams to surface and other levels, which contain fridge plants to then cool the service water down again and complete the cycle.

These FBACs are designed for 21-24 °C wet-bulb air inlet temperatures and 5-10 °C service water inlet temperatures. However, each half-level FBAC is located 2 km away from the shaft station area on average, complicating regular access. As a result, physical measurements showed 24-28 °C wet-bulb air inlet temperatures and 11-13 °C service water inlet temperatures, indicating off-design operating conditions and the potential presence of inefficiencies. This is due to changing ambient conditions, sub-optimal cooling of upper BACs supplying air to the production block, sub-optimal fridge plant performance, and insufficient pipe cladding on main service lines raising intake water temperatures [5], [23].

FBAC performance on Mine A is monitored by environmental sensors at the inlet and outlet that log ambient temperature, pressure, and humidity in 30-minute intervals. However, these sensors are prone to malfunction due to harsh operating conditions underground, resulting in periodic data loss or inaccurate readings.

Moreover, Mine A has no scheduled maintenance plan for their FBACs, and replacements are infrequent [23]. However, maintenance and restorative efforts were conducted on FBAC 3 in early 2021. The fact that maintenance efforts were conducted on one of the FBACs allows an opportunity for the prediction model to evaluate the expected steady deterioration in condition of the FBAC over the evaluation period. This will ideally serve to validate the prediction model, which can then be used to evaluate the remaining FBACs on Mine A.

Therefore, from the summary of the chosen case study, opportunity for ample testing and evaluation of the proposed method's compliance to the study objectives put forth is available. The following sections will apply the method to these case study FBACs in a systematic manner, closely following the phases and sub-phases outlined in Chapter 2 of this dissertation. The fact that the FBACs found on Mine A are radiator-type heat exchangers simplifies the application of the method.

3.3 Results - Phase 1: Parameter normalization

The following section will follow the process outlined in Section 2.3 to construct a normalised relationship between operating parameters of an FBAC. Table 1 in Section 2.3.1 presented typical cooling parameters around a generic radiator-type heat exchanger, and the same cooling parameters were used for analysis in this chapter.

As per Section 2.3.2, all geometric parameters were assumed to be constant - as well as density, viscosity, pressure, thermal conductivity, and specific heat capacity of both working fluids. Therefore, the remaining variable system parameters were the respective mass flows and inlet/outlet temperatures of both working fluids, i.e., ventilation air and service water. Following Section 2.3.2, all identified parameters that remain constant with time were eliminated. Table 6 below presents the remaining system operating parameters:

Table 6: Remaining time-variant operating parameters around at the FBAC obtained.

System	Parameter	Unit
Air Side	Inlet Temperature	°C
	Outlet Temperature	°C
	Mass Flow Rate	kg/s
Water Side	Inlet Temperature	°C
	Outlet Temperature	°C
	Mass Flow Rate	kg/s

Following Section 2.3.3, the outlet air temperature of the FBACs were chosen as the performance parameter from the remaining set of operating parameters to ultimately represent the cooling performance of the FBACs in this case study. As in Section 2.3.3, water outlet temperature is removed as a result. Table 7 below presents the chosen performance parameter from the remaining operating parameters:

Table 7: Remaining time variant operating parameters obtained with chosen "performance parameter".

System	Parameter	Unit
Air Side	Inlet Temperature	°C
	Outlet Temperature	°C
	Mass Flow Rate	kg/s
Water Side	Inlet Temperature	°C
	Mass Flow Rate	kg/s

To normalise the remaining system parameters, dimensional analysis was used as outlined in Section 2.3.4 and shown in Appendix A. The resulting dimensionless groups obtained were:

$$\Pi_1 = \frac{T_{air_{out}} - T_{air_{in}}}{T_{air_{in}} - T_{water_{in}}} \qquad \Pi_2 = \frac{\dot{m}_{water}}{\dot{m}_{air}} \tag{3.10}$$

Following Section 2.3.5, and the dimensionless groups shown in Equation (3.10) above, the obtained normalised relationship is presented below in Equation (3.11)

$$\frac{\Delta T}{\Delta T_{max}} = f\left(\frac{\dot{m}_{water}}{\dot{m}_{air}}\right) \tag{3.11}$$

After the simplified normalised relationship shown by Equation (3.11) above was obtained, the second phase of the method was applied, outlined in Section 2.4.

3.4 Results – Phase 2: Development of prediction model

Section 2.4 was followed to obtain a normalised prediction model, calibrated using OEM design specifications. Following section 2.4.1, a comprehensive set of OEM design specifications containing OEM design conditions were obtained and is discussed in the following section.

3.4.1 OEM design specifications

The OEM's proprietary software was used to calculate design outlet conditions for their FBACs, and a comprehensive set of design tables were obtained thereafter directly from the OEM. These tables show the outlet wet-bulb air temperature at various inlet conditions, such as inlet wet-bulb air temperature, inlet service water temperature, inlet air flow rate, and inlet water flow rate among others. Appendix C presents the bulk of the OEM design tables obtained.

3.4.2 Model development and verification

Using the obtained OEM design conditions, Section 2.4.2 was followed to calibrate the system normalised relationship. The resulting calibration data sets obtained are shown in Figure 44 below:

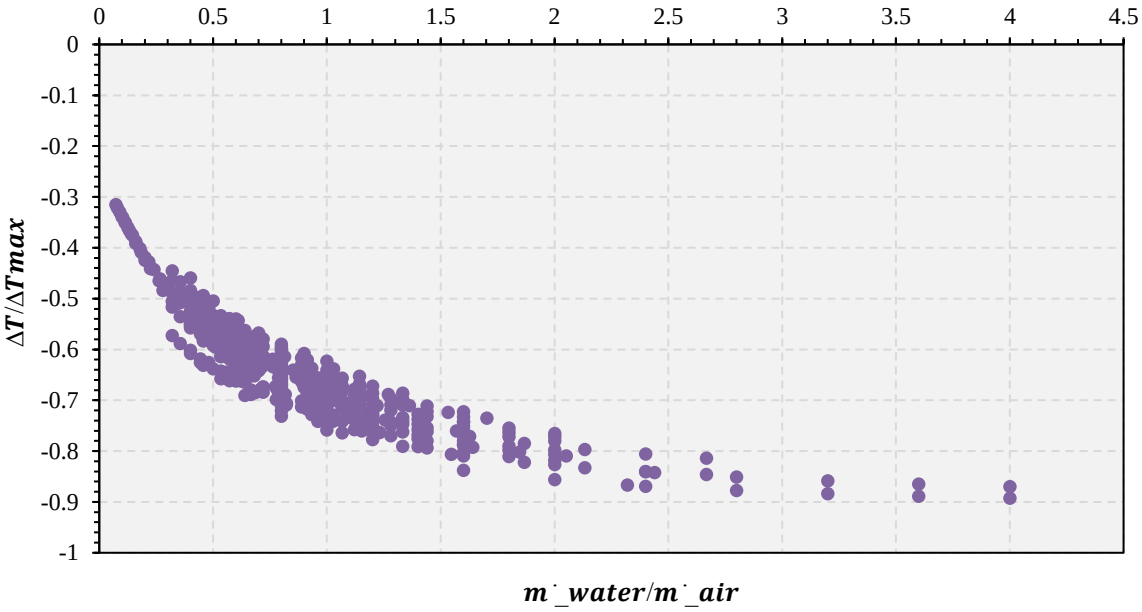

Figure 44: Characteristic curve from the data sets obtained when applying OEM design conditions (n=448) to the respective parameters in the obtained normalised system relationship outlined in Section 2.4.2.

Section 2.4.2 and 2.4.3 were subsequently followed to choose a suitable curve fit for the obtained data set. Microsoft Excel was used to evaluate three curve fits: linear, polynomial, and logarithmic. An exponential curve fit was not possible, as the calibration dataset obtained contains negative values. The equation for each curve fit was re-arranged and used to predict the outlet temperature in adherence to Section 2.4.3. Table 8 below shows the correlations and predicted errors for each curve fit investigated:

Table 8: Correlation and prediction errors of each respective curve fit investigated when compared to the OEM specified outlet temperature at the same inlet conditions:

Best Fit Curve Type	Model Prediction Error %	Model Prediction Correlation
Linear	3.24	0.856
Polynomial (5th order)	1.98	0.9678
Logarithmic	2.03	0.9503

Although the logarithmic curve fit had a strong correlation and minimal prediction errors, the 5th order polynomial curve fit proved to be the best option for the strongest correlation and least amount of prediction error.

To ensure complete verification of the best curve fit used, different orders of polynomial curve fits were subsequently investigated and compared to ensure the highest prediction accuracy is achieved. Table 9 below shows the correlation and prediction accuracy of different orders of polynomial fits investigated:

Table 9: Comparison of different order polynomials used as curve fits investigated with their respective correlations and prediction errors when compared to the OEM design specified outlet air temperature.

Best Fit Curve Type	Model Prediction Error %	Model Prediction Correlation
Polynomial (3rd order)	2.15	0.9628
Polynomial (4th order)	2.03	0.9676
Polynomial (5th order)	1.98	0.9678
Polynomial (6th order)	2.08	0.9664

From Table 9, it was determined that the 5th order polynomial curve fit was still found to best represent the data and provided the most accurate prediction of design outlet temperatures. Therefore, a 5th order polynomial curve fit was chosen to represent the characteristic equation of the prediction model.

The characteristic equation of the prediction model obtained and used for verification is presented in Equation (3.12) below[3]:

$$T_{air_{out}} = T_{air_{in}} + T_{max}\left[-0.0081\left(\frac{\dot{m}_w}{\dot{m}_a}\right)^5 + 0.0915\left(\frac{\dot{m}_w}{\dot{m}_a}\right)^4 - 0.3907\left(\frac{\dot{m}_w}{\dot{m}_a}\right)^3 + 0.8119\left(\frac{\dot{m}_w}{\dot{m}_a}\right)^2 - 0.936\left(\frac{\dot{m}_w}{\dot{m}_a}\right) - 0.2618\right] \quad (3.12)$$

[3] The outline of how the characteristic equation was obtained is given in Appendix D

Figure 45 below presents the correlation obtained when using the characteristic equation shown in Equation (3.12) and OEM design tables to evaluate the degree of correlation between the respective predicted and OEM specified outlet temperatures:

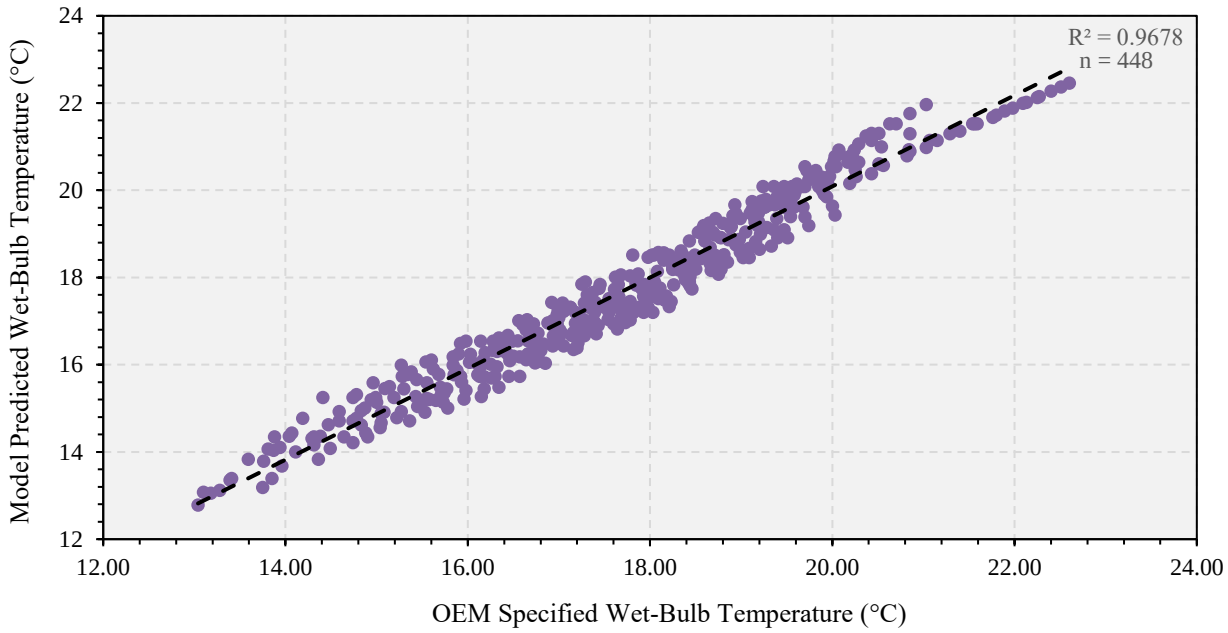

Figure 45: Correlation between the predicted outlet air temperature of the FBAC characteristic equation and the OEM specified outlet air temperature for the same set of inlet conditions (n=448).

From Figure 45 comparison above, a correlation of $R^2 = 0.9678$ was obtained with an average prediction error of 1.98 %. This meant that the prediction model was able to accurately predict the OEM's design outlet temperature for any given set of inlet conditions within 0.35 °C on average. These obtained correlations and prediction errors fell within the set range of allowable prediction variations stated in Section 2.4.3. Therefore, the prediction model was assumed verified from this point forward[4]. The following section will discuss the results obtained from implementing the verified prediction model on the case study mine and FBACs, as per Section 2.5.

[4] The development of the characteristic equation of the prediction model is shown in Appendix D

3.5 Results – Phase 3: Implementation of prediction model

Section 2.5 was followed to implement the prediction model to validate the outcomes of the method against the study objectives set forth in Section 1.9. The verified prediction model is first applied to a single FBAC - to validate the model - whereafter the model is applied to the remaining set of case study FBACs. However, per Section 2.5.1, a comprehensive data set was first to be established. The following section describes the acquisition and processing of the data set obtained for all FBACs.

3.5.1 Dataset establishment

The data sets obtained for all FBACs included inlet and outlet temperatures of both air and service water, as well as the corresponding mass flow rates of each. Hydraulic sensors on the supply side water line provided sufficient readings for water temperature and water mass flow rate.

Environmental sensors placed at the inlet and outlet of the FBAC were used to obtain air conditions such as air inlet and outlet wet-bulb temperature over the evaluation period. Figure 46 below illustrates the sensor placements around the FBAC cooling loops, and Figure 47 presents a photo of the environmental sensor at the inlet of the cooling loop:

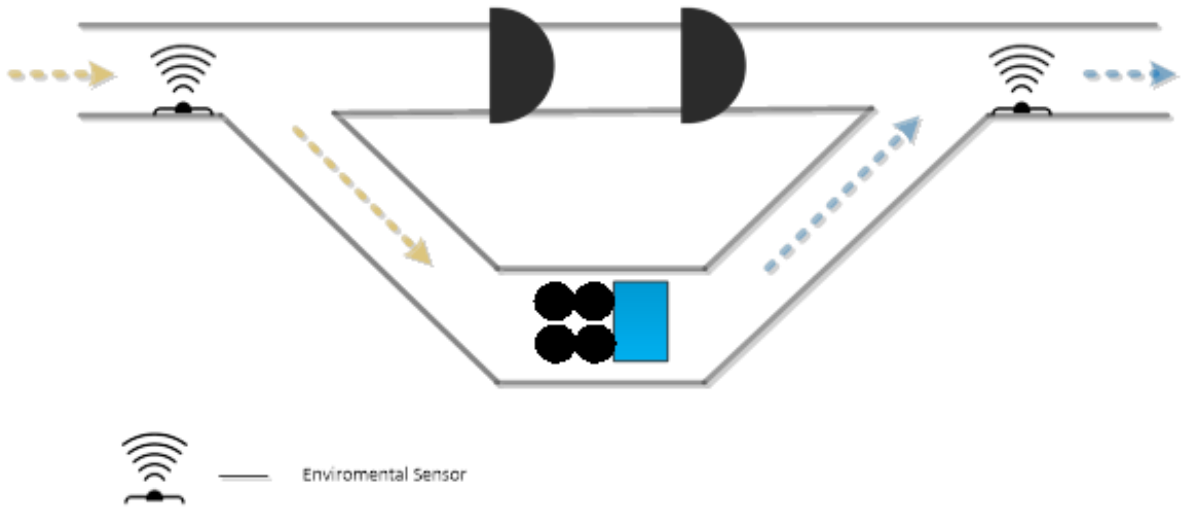

Figure 46: Schematic of a FBAC cooling loop with associated sensor placements, located on Mine A (Self-illustration)

Figure 47: Environmental sensor located at the inlet of the FBAC loops at Mine A. (Photo taken by author)

As briefly outlined in Section 3.2, the environmental sensors can measure inlet and outlet temperature, pressure, and humidity every 30 minutes. However, the mass flow rate of the air is usually determined using a supplementary velocity sensor connected to the environmental sensor, shown below in Figure 48:

Figure 48: Vane measuring wind speed of air at the entrance of the FBAC. (Photo taken by author)

In this case study, velocity sensors were initially used to measure air mass flow rate at the FBAC but were found to be unreliable due to harsh conditions that contaminated the rotary bearings, subsequently contaminating measurement data.

To ensure data availability and improve accuracy, the average air flow rate was physically measured using a vane anemometer and a laser distance meter to measure air flow velocity and flow area respectively. Using the relevant conditions to calculate the local air density, Equation (3.13) below was then used to calculate the respective mass flow rate:

$$\dot{m} = \rho V A \tag{3.13}$$

where $\dot{m} = mass\ flow\ rate\ of\ ventilation\ air$

$\rho = local\ air\ density\ (calculated\ from\ conditions)$

$V = measured\ velocity\ of\ air\ (using\ vane\ anometer)$

$A = measured\ flow\ area\ (using\ laser\ distance)$

To mimic the varying conditions at the FBAC, the mass flow rate was randomly varied within reasonable range using an Excel function (=RANDBETWEEN) to account for natural variations and provide a more accurate estimate for the air flow at each data point.

As outlined in Section 2.5.1 to ensure monitoring reliability and accuracy, data points with faulty measurements were filtered out manually. The chosen filter criteria for the obtained operating data sets included filtering out:

- Any water flow rates below 15 kg/s
- Any outlet water temperatures exceeding 16 °C.
- Any data sets where the outlet air temperature exceeds that of the inlet (zero cooling)
- Any data sets where the difference between inlet and outlet water temperature varied by more than that possible considering the design duty of the FBAC (1 500 kW)
- Any zero or null data sets
- Any “flatlining” data set

Considering the various applied filters to the datasets obtained, each FBAC would have a unique amount of usable data remaining. Table 10 below outlines the remaining sets of usable data for each respective FBAC on the case study mine to use for evaluation:

Table 10: Sample size of remaining data sets used for analysis after filtering.

FBAC Identifier	Number of Data Points (n)
FBAC 1	4920
FBAC 2	5856
FBAC 3	10556
FBAC 4	10479
FBAC 5	3652
FBAC 6	7488
FBAC 7	11634

In addition, after data filtering, each FBAC would have an upper and lower bound to which the value of each parameter varies.

Table 11 below presents the maximum (95th percentile) and minimum (5th percentile) values for each respective parameter of each respective FBAC, as this gives an indication of the operating ranges of each parameter evaluated:

Table 11: Operating ranges (5th to 95th percentile) obtained after data filtering was applied to the original data set for each respective FBAC's cooling parameters obtained.

	Air Side			Water Side	
	Inlet Temperature (°C Wet-bulb)	Outlet Temperature	Mass Flow (kg/s)	Inlet Temperature (°C)	Mass Flow (°C)
FBAC 1	24.41 – 28.39	19.43 – 24.31	51 - 69	11.22 – 15.38	20.05 – 69.53
FBAC 2	24.19 – 28.21	20.57 – 24.37	71 - 89	11.59 – 15.53	38.14 – 80.20
FBAC 3	19.13 – 24.53	17.73 - 23.02	51 - 69	14.62 – 17.66	28.20 – 70.07

FBAC 4	24.38 – 27.86	20.17 – 25.22	41 - 59	11.54 – 14.49	26.92 – 62.78
FBAC 5	25.43 – 30.34	22.39 – 25.48	51-69	12.02 – 15.70	23.2 – 72.36
FBAC 6	24.5 – 28.56	22.84 – 26.3	91 – 109	11.67 – 14.76	38.75 – 102.5
FBAC 7	24.59 – 28.75	22.72 – 27.35	71 - 89	12.13 – 15.83	16.15 – 79.64

The following section will discuss the results when applying the prediction model to FBAC 3 using the filtered case study datasets obtained and outlined in this section.

3.5.2 Model validation

As per Section 2.5.2, the prediction model was applied to an initial FBAC for validation Mine A. FBAC 3 was chosen as the initial FBAC for implementation, as the FBAC had been recently refurbished in early 2021, as stated in Section 3.2. This allowed for ample opportunity to validate the model, as it is expected that inefficiencies would emerge over time as shown in Section 1.4.

The evaluation period used was from 03 January 2021 to 21 May 2022 and measurements were obtained in 30-minute intervals. The resulting comparison of the design outlet prediction versus the measured outlet temperature obtained is presented below in Figure 49:

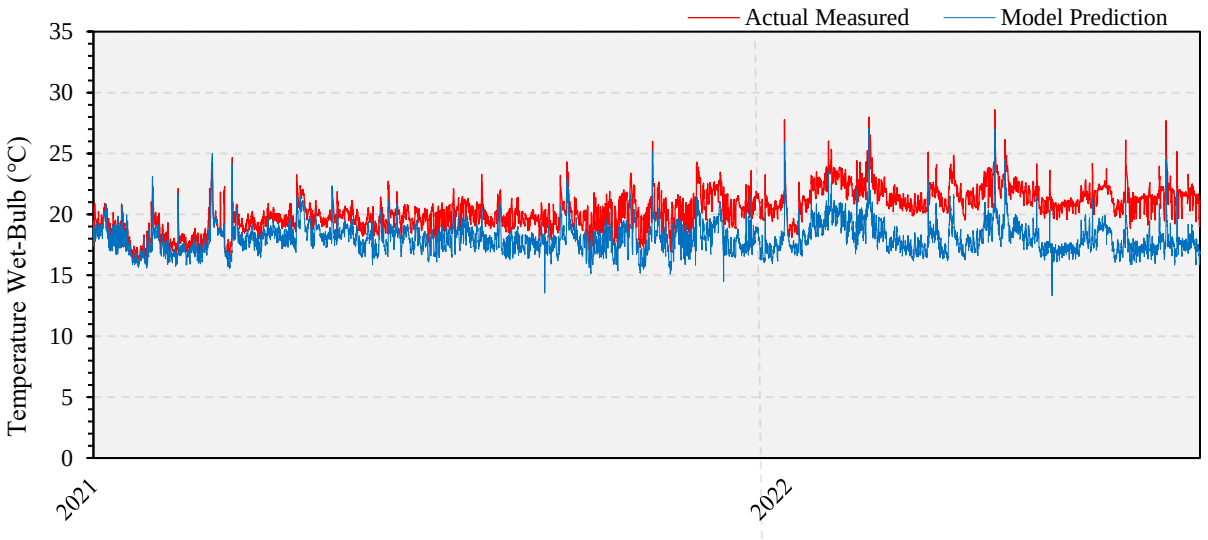

Figure 49: Comparison obtained of the model predicted outlet temperature versus the measured outlet temperature over the initial evaluation period for FBAC 3.

The initial comparison appears erratic due to variations in underground inlet conditions, in addition to the resolution of data used in relation to the evaluation period. To present the data in a more intuitive manner, a moving average trendline was applied to the results obtained with an interval of n = 255 using Excel functionality. The resulting graph obtained is presented in Figure 50 below:

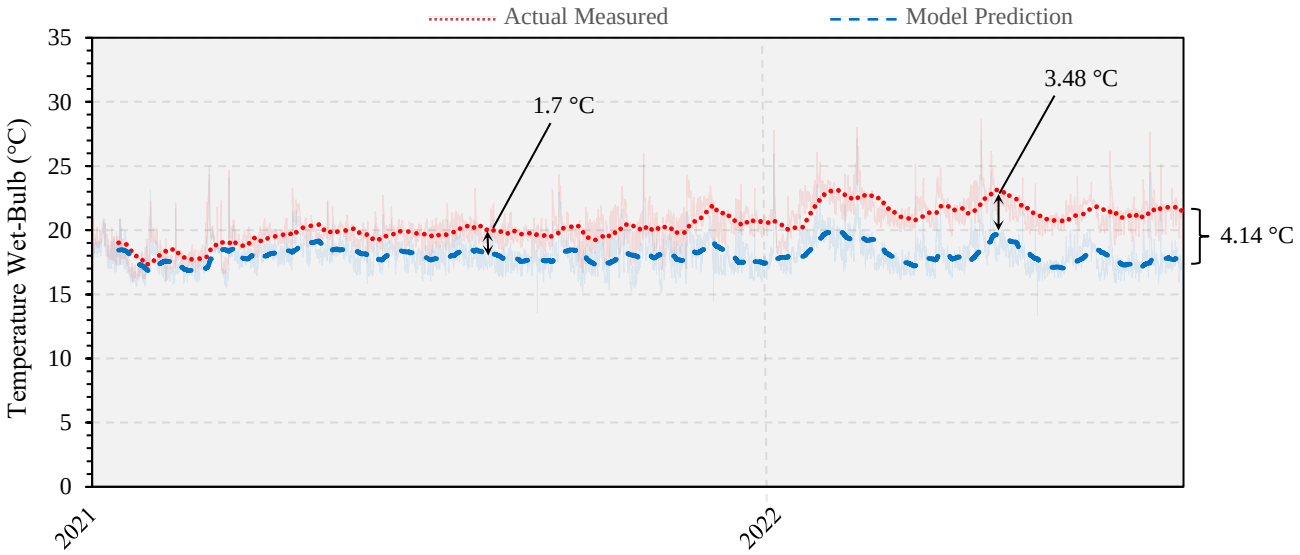

Figure 50: Moving average trendline applied to the raw data from Figure 49.

The prediction model had shown that FBAC 3 had deviated from its design outlet temperature over the evaluation period, as predicted in Section 2.5.2. The deviation had started in mid 2021 and increased in magnitude up until late May 2022. By the end of the first year (2021), the average deviation was found to be 1.7 °C on average for that period. By the end of May in the second year (2022), it had increased to 3.48 °C on average for that period. The maximum deviation at the end of the evaluation period was determined to be 4.14 °C.

This suggests that inefficiencies gradually emerged at FBAC 3 over the evaluation period, which aligns with the data from literature presented in Section 1.4. The obtained monitoring outcomes and results warranted further investigation into the condition of the FBAC. Subsequently, an underground investigative audit was conducted at the end of the evaluation period in June of 2022. Figure 51 and Figure 52 below presents the initial results of the investigation, and a discussion into the various findings is put forth in the following passages:

Figure 51: Corrosion as well as external fouling is visible on the heat transfer surfaces. Unaffected refurbished cooling banks can be seen at the bottom left (Photo taken by author)

Initial inspection of the FBAC showed no broken infrastructure, and the newly replaced banks briefly discussed in the case study background can be seen in the three lower left rows of the first column of cooling banks. Due to requirements that FBACs operate continuously, physical inspection of the internal condition of the piping for internal fouling at FBAC 3 could not be determined.

Additionally, external fouling was found on the heat transfer surfaces of the cooling banks. This was due to wet dust accumulating on the cooling bank, forming a mud-like substance on the surface. Slight corrosion was also found on the newly replaced banks, however not so pronounced as to warrant a concern. Figure 52 below shows a closer look at the FBAC investigated:

Figure 52: External fouling and corrosion observed on the heat transfer surfaces (Photo taken by author)

An inspection of the intake side of the FBAC was also conducted. A prominant hole was found in the wall seperating the FBAC force fans and cooling banks, allowing warm ventilation air to bypass the cooling banks and raising the FBAC outlet temperature. This is shown in Figure 53 below:

Figure 53: Gaping hole in wall identified above the mainline supply piping (Photo taken by author)

In summary, the prediction model showed that FBAC 3 had deviated from its design outlet temperature, starting in mid 2021 and continuing to degrade throughout 2022. An

underground investigation/audit of the FBAC revealed that FBAC 3 had ineffiencies resulting from the type of replacement piping used, fouling of the cooling banks, and a hole in the wall seperating the force fans and cooling banks.

Following the initial results of implementation, the method showed the ability to accurately and reliably monitor the condition of the FBAC operating at off-design conditions in a remote, continuous manner as to detect the onset or presence of multipleinefficiencies. This proves as a strong case for validation of the method for implementing condition monitoring, satisfactory to the study objectives set forth in Section 1.9. The following section will present the results of implementing the prediction model on the remaining FBACs on Mine A, as per Section 2.5.3.

3.5.3 Model implementation

Following initial implementation, the prediction model was then applied to the remaining FBACs on Mine A using the data sets obtained to determine the average approximate deviation of each respective FBAC from its design outlet conditions in an attempt to identify the worst performing cooler. A two year case study dataset (January 2021 – Desember 2022) was obtained and filtered as discussed in Section 3.5.1. The comprehensive filtered dataset was then used for all FBACs to evaluate the degree of deviation for each.

As per Section 2.5.3, comparing the degree of deviation of each resepctive FBAC would allow for a condition ranking. The condition ranking obtained by applying the prediction model to the remaining FBACs on Mine A using the filtered case study dataset is presented in Figure 54 below:

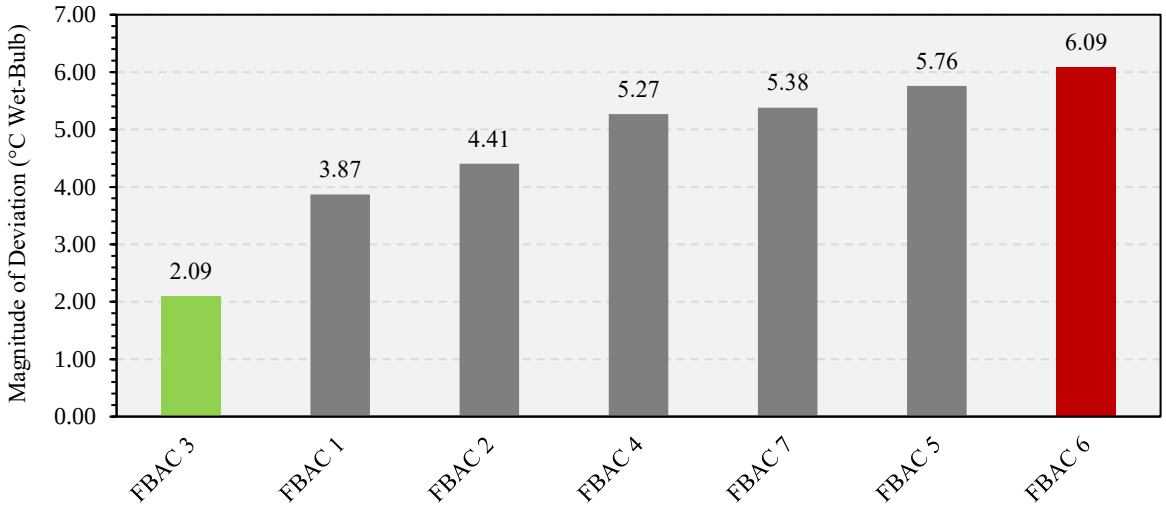

Figure 54: Condition ranking of the average wet- bulb air temperature deviations obtained by implementing the prediction model over the evaluation period.

Using the estimate of production losses discussed in Section 2.5.3, and the results presented in Figure 54, an estimate for the expected revenue loss at Mine A was given:

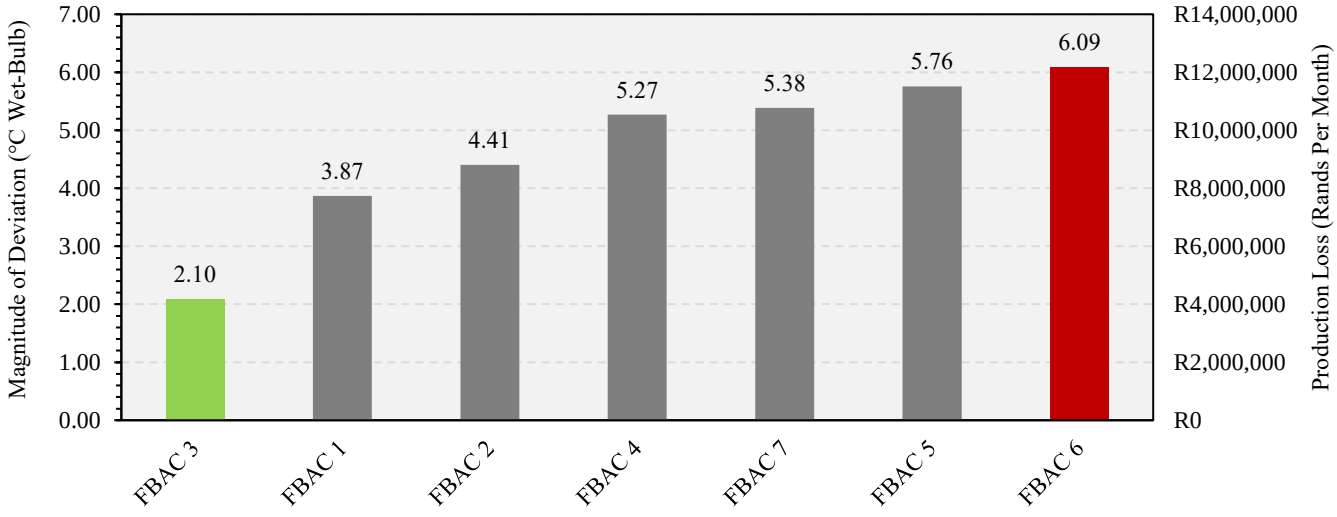

Figure 55: Average monthly production loss estimates due to temperature deviations from design at the respective FBACs evaluated (continued from Figure 54)

When adding up all the estimates for the average production losses due to each respective FBAC evaluated, total monthly production losses of R68 570 505 may be expected due to drops in worker efficiency, which is related to the increased working place temperatures. This alone highlights the importance of mitigating inefficiencies at these coolers, as to

ensure profitable mining – an aspect discussed in Section 1.4. However, confirming this estimate would serve to be impossible due to other influencing factors, and should therefore only be considered for assessing the potential impact of inefficiencies present.

Figure 55 above indicates that FBAC 3 had the lowest overall magnitude of deviation and subsequently the best average cooling performance among all FBACs at Mine A for the evaluation period. This is expected as it aligns with the effects of the maintenance and restorative efforts conducted in early 2021, as outlined in the Section 3.2.

Additionally, the performance ranking showed that FBAC 6 had the highest degree of degradation with an average temperature deviation of 6.09 °C from design over the two-year evaluation period. Figure 56 below shows the monitoring profile for FBAC 6 obtained for the evaluation period:

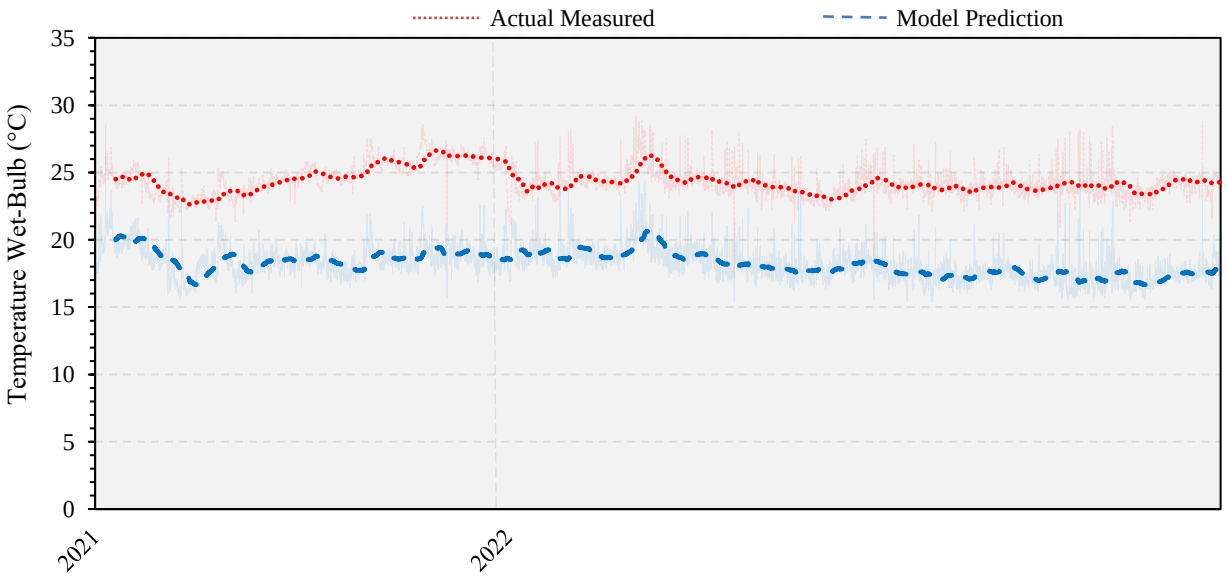

Figure 56: Two-year monitoring comparison of the outlet temperatures for FBAC 6 obtained, showcasing the impact of inefficiencies present on the cooling performance.

The results obtained did not exhibit a gradual deviation from the design, as observed in FBAC 3. Instead, a consistent offset was observed in the measured outlet temperature compared to the design. As stated in Section 2.5.2, this might be attributed to pre-existing inefficiencies that impacted cooling performance from the beginning of the evaluation period. It is also possible that a constant level of inefficiencies persisted throughout, without any additional onset.

An investigative audit of FBAC 6 was conducted in June of 2022 to evaluate the extent of inefficiencies present. It was found that significant damage to cooling infrastructure was present as well as significant fouling of the cooling banks, the details of which are outlined below:

Broken infrastructure included damaged and broken cooling banks, damaged ventilation doors, and inactive piping. Additionally, extreme fouling was present on the outer surfaces of the cooling banks. The magnitude of internal fouling could not be established, as that would require the FBAC to be turned off and the banks to be transported to the surface, leading to operational downtime - a disadvantage discussed in Section 1.7.2. Figure 57 below presents these various inefficiencies identified:

(a)

(b)

(c)

(d)

Figure 57 : (a) Inactive piping (b) Damage ,fouling and calcification on the heat transfer surface (c) Broken ventilation door leaking air past the cooling banks (d) Corrosion and external fouling present on the heat transfer surface (Photos taken by author)

Figure 58 below presents a closer look at one of the many fouled cooling banks inspected during the investigation. Calcification, characterised by the faint sparkle seen, was found on this particular cooling bank:

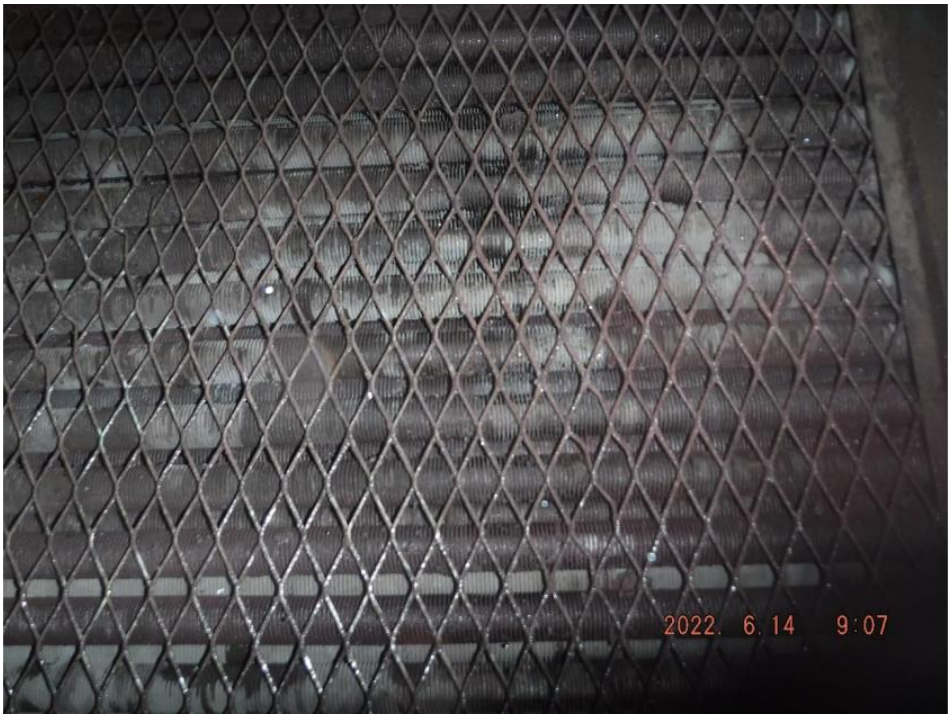

Figure 58: Calcification seen on the heat transfer surface of the cooling bank (Photo taken by author)

As shown in Figure 55, these inefficiencies have profound impacts on the production output of the half-level. It was estimated that FBAC 6 alone contributes to a monthly production loss of R12 708 508 for the case study mine. Furthermore, due to FBAC 6 being located on the deepest production half-level, the impacts of these inefficiencies were compounded due to the particular half-level having the most working places.

Therefore, comprehensive maintenance and refurbishment efforts would have significant impacts on the rate of production, as well as the safety of mining personnel and the sustainability of the mining operation. Following the investigative audit, the condition of FBAC 6 was reported to the responsible persons on Mine A and maintenance efforts are currently underway. It was recommended that the damaged cooling banks be replaced, and the banks that contained extreme fouling be removed from the cooler and transported to surface for restorative measures, as outlined in Section 2.5.3. The completion date of the maintenance efforts is currently unknown as of the time of writing this dissertation.

3.6 Summary overview of results

In this chapter, the method was applied to seven case study FBACs to evaluate the compliance of the method to the study objectives put forth. The method was initially applied to FBAC 3, which had been recently refurbished, to validate the prediction model obtained by following the method.

The prediction model successfully detected temperature deviations from the design outlet temperature, indicating the presence of inefficiencies affecting the cooling performance. The investigation conducted into the condition of FBAC 3 revealed external foulants on the cooling bank infrastructure, in addition to an air-leakage in the wall separating the FBAC from the force fans. This resulted in hot ventilation air bypassing the cooling banks, resulting in higher outlet temperatures. These findings provided evidence for the method's ability to monitor the condition of the FBAC operating at off-design conditions to detect the onset and presence of multiple inefficiencies.

Applying the prediction model to the remaining FBACs on Mine A allowed for a comprehensive comparison of the cooling performance of each, inferred from the respective average temperature deviations from design. Using worker efficiency relations, it was estimated that the case study mine had a monthly production loss of R68 570 505 due to the downstream impacts of these inefficiencies. This would have significant impacts on the profitability and sustainability of the case study mine and highlights the importance of condition monitoring.

FBAC 3 exhibited the lowest magnitude of deviation, which was attributed to the refurbishment efforts conducted previously. FBAC 6 showed the largest magnitude of deviation, indicating significant damage to cooling infrastructure and fouling present, among others. A comprehensive investigation into the condition of FBAC 6 revealed significant inefficiencies present affecting the cooling performance of the cooler. The impact of inefficiencies on this particular cooler alone accounted for a monthly production loss of R12 708 508. The condition of the FBAC was reported to the relevant responsible personnel, and restorative measures are currently underway.

Considering the holistic condition monitoring results obtained for all the FBACs (presented in Appendix B), each FBAC except FBAC 3 had shown to have a constant deviation from design, rather than a gradual deviation caused by the slow onset of inefficiencies over time. This would suggest that inefficiencies accumulated over the operating lifetime of these FBACs and had tapered off over a certain timeframe to reach a maximum point of impact. This is substantiated by the constant offset seen between predicted and design outlet temperatures, indicating sparse maintenance had been conducted on these FBACs. Therefore, it is suggested that a certain “cut off” point is reached where, short of complete system failure, no further impacts on performance is made by further onset of inefficiencies (such as fouling for instance). This may be studied more in the future.

The implications of these findings not only highlight the importance of regular maintenance efforts to negate the impacts of inefficiencies, but also shows the power of the condition monitoring method presented in this dissertation to detect the onset and presence thereof. All the technical findings presented were obtained in a completely remote and continuous manner, without the need for regular inspection. Due to the connection of these monitoring sensors to PLC systems, which feed monitoring data directly to SCADA systems, data analysis methods through the use of software could automate data procurement and processing. Trends, patterns, time of onset and many other insights into inefficiencies at these FBACs could be extracted from the monitoring data as a result. This would provide any operator with valuable insight into the condition of the cooling infrastructure in a far more efficient manner, aiding informed decision making.

The next chapter will provide a comprehensive overview of the dissertation, evaluate the degree of compliance of the obtained results to the set study objectives, provide limitations of the method, and provide recommendations for future work.

CHAPTER 4 CONCLUSION, LIMITATIONS AND RECOMENDATIONS

4.1 Overview of the study

This dissertation successfully presented an innovative condition monitoring method for underground finned tube bulk air coolers (FBACs) operating at off-design conditions. The method complied closely with the established study objectives, aiming to detect the onset or presence of inefficiencies impacting cooling performance.

Chapter 1 provided an overview of the heating challenges faced in deep-level mining and highlighted the importance of FBACs in cooling ventilation air. It emphasised the need for condition monitoring to address inefficiencies to ensure safety, sustainability, and profitability in mining operations. From a comprehensive literature review, it was established that current condition monitoring methods would not be sufficient for implementation. It was then stated that an innovative condition monitoring method would be presented in this dissertation, with the goal to meet set study objectives to ensure successful implementation.

Chapter 2 systematically outlined the proposed method in three distinct phases. The first phase focused on normalizing system operating parameters using dimensional analysis. The second phase involved developing a prediction model from the normalised system parameters to forecast design outlet conditions. The third phase then shows how the model is to be implemented to evaluate its compliance with the study objectives. Finally, it was shown how each phase of the method is to comply to the study objectives put forth.

Chapter 3 applied the method to a case study mine to evaluate compliance with the study objectives. The prediction model that was developed accurately forecasted design outlet conditions within 0.35 °C, verifying its reliability. Data filtering was applied to ensure accuracy and reliability in monitoring. Implementation of the model on FBAC 3 revealed deviations from design outlet conditions, confirmed through an investigative audit.

The method was then applied to the remaining FBACs on Mine A, identifying FBAC 6 as the worst performing cooler with a significant deviation of up to 6.09 °C from design conditions. An investigative audit revealed various inefficiencies affecting cooling performance, emphasizing the need for maintenance and refurbishment efforts. Using

conservative estimates from previous authors, production losses of R12 708 508 per month due to declines in worker efficiency at FBAC 6 alone were expected.

Overall, the results obtained from the implementation of the method on the case study mine demonstrated its effectiveness in monitoring FBACs and detecting inefficiencies. The method successfully provided strong evidence for meeting study objectives by providing accurate, reliable, remote, and continuous condition monitoring of these FBACs running at off-design conditions. The outcomes highlighted the importance of addressing inefficiencies for improved safety, production efficiency, and sustainability in mining operations. Additionally, the results obtained proved the effectiveness of the method to implement condition monitoring on these bulk air coolers. The following section will conduct a comprehensive review to analyse the degree of compliance of the obtained results to the study objectives set forth in Section 1.9.

4.2 Review of compliance to study objectives

Section 1.9 outlined the study objectives of this dissertation, constructed from the problem statement outlined in Section 1.8 and the subsequent need for the study outlined in Section 1.8. The established study objectives included proposing a condition monitoring method able to:

1. Continuously and remotely monitor the
2. Condition of industrial finned tube bulk air coolers
3. Operating at off-design conditions in an
4. Accurate and reliable manner, with the ability to
5. Detect the onset and presence of multiple inefficiencies impacting cooling performance.

Before the outline was given for each phase in Chapter 2, a brief overview of how each respective phase would comply with the study objectives was given. Additionally, Section 2.6 provided a summary overview of how the method presented has planned to meet all the study objectives put forth. Subsequently, a thorough assessment of the extent to which the obtained results align with the study objectives is provided in the following passages:

Chapter 2 presented the outline of the proposed method, and presented how each subsequent phase of the method addresses certain study objectives. In Section 2.3, it was shown how the third and fourth study objectives would be addressed by normalizing

various system operating parameters to allow for monitoring at off-design conditions in a reliable and accurate manner.

In Section 2.4, it was shown how the first study objectives would be addressed by developing a simple prediction model from the normalised system operating parameters able to implement continuous and remote monitoring using monitoring systems. In Section 2.5, it was shown how the final two study objectives, study objective two and study objective five, would be addressed.

This was to be done by implementing the simple prediction model on case study FBACs to monitor the condition of the FBACs for the presence or onset of multiple inefficiencies impacting cooling performance by comparing the obtained forecasted design outlet temperatures against the observed outlet temperatures and inferring the condition of the FBAC from the magnitude of differences between the two.

Chapter 3 presented the outcomes of implementing the method on seven case study FBACs on Mine A for evaluation to a degree of compliance that the method posed to the established study objectives. A summary evaluation of the results obtained from implementation and the degree to which they comply to the study objectives is given below:

4.2.1 Study objectives one, three and four

In Section 3.3 and 3.4, in accordance with Section 2.3 and 2.4, the prediction model for the case study was initially developed by first normalizing the system operating parameters around the FBACs and calibrating the relationship between the normalised parameters using OEM design specifications obtained.

This resulted in a prediction model able to predict various OEM design outlet conditions for any corresponding set of inlet conditions. The prediction model presented a prediction accuracy of 0.35 °C to the OEM specification. Adhering to accuracy targets set in Section 2.4.3, the prediction model was deemed accurate and verified. This ensured that the prediction model resulting from applying the method contained the ability to apply continuous and remote monitoring at off-design conditions in an accurate and reliable manner, satisfying study objectives one, three and four.

4.2.2 Study objectives two and five

In Section 3.4, and in accordance with Section 2.5, the verified prediction model was applied to seven FBACs on Mine A. Initial implementation of the prediction model was done on a single FBAC (FBAC 3), where corrective maintenance and refurbishment efforts had been conducted at the start of the evaluation period.

The validity of the prediction model was presented when it was shown that FBAC 3 had deviated from its design operating conditions over the evaluation period. Results showed a gradual deviation, indicating the gradual onset of inefficiencies at the FBAC. Physical investigations confirmed the presence of these inferred inefficiencies.

The initial results obtained proved the ability of the method to implement condition monitoring on FBACs to detect the presence or onset of inefficiencies impacting the cooling performance of the FBAC. This was further confirmed after applying the prediction model to the remainder of the FBACs on Mine A, where the worst performing FBAC on the most production-intense half-level was identified from the results. Physical inspection showed several inefficiencies present severely impacting cooling performance.

In conclusion, the results obtained by implementing the l method on seven case study FBACs proved the ability of the method to address and comply with the remaining study objectives - study objective two and study objective five.

4.2.3 Summary overview of study objective compliance

Table 12 below provides a holistic overview of the compliance of the method outcomes to the set study objectives, as discussed in this section:

Table 12: Summary of compliance for method outcomes with the set study objectives (Table re-used from Section 2.6)

	Phase 1: Parameter Normalization	**Phase 2:** Development of Prediction Model	**Phase 3:** Implementation of Prediction Model
Study Objective 1		×	
Study Objective 2			×
Study Objective 3	×	×	
Study Objective 4	×	×	
Study Objective 5			×

As per Table 12 above, all study objectives put forth in this dissertation are deemed to be met. It is therefore concluded that the method is deemed feasible for condition monitoring implementation on underground finned tube bulk air coolers (FBACs) operating at off-design conditions in a remote and continuous manner as to accurately and reliably detect the onset or presence of multiple inefficiencies, impacting cooling performance.

However, as the method presented in this dissertation is still in its infancy, limitations of the method is put forth accompanied by recommendations for future work. The following section will outline these limitations and recommendations.

4.3 Study limitations and future recommendations

The following section will outline the limitations of the study, and subsequently discuss the recommendations for future work to further the effectiveness of the method presented in this study.

- Availability of OEM design specification data

The method presented in this study fundamentally hinges on the availability of a large set of OEM design data that characterises the performance of the infrastructure at various

operating conditions. This study utilised OEM design specifications of a single type of cooling bank infrastructure, specifically found on Mine A.

Therefore, the study was only conducted on one version of cooling coil design. Generally, in the mining industry, due to the aging infrastructure, OEM design data may not always be readily available to use for calibrating the prediction model. Therefore, if OEM data is available, it is recommended to apply the method to other types of cooling bank infrastructure to evaluate the accuracy and effectiveness of the method.

- Dataset size of OEM design specification data

To ensure the absolute accuracy of the prediction model, a sufficiently large sample of calibration data should be used. The prediction model developed in this study utilised an OEM design specification sample size of n = 448 resulting in a prediction error of 0.35 °C.

This would normally be deemed sufficiently accurate for monitoring, however the sample size needed would be dependent on the type of infrastructure being monitored and the number of operating parameters used. It is recommended that the relationship between OEM design data size used for calibration and the corresponding accuracy be determined for each type of application.

- Choice of curve fit.

The choice of curve fit would affect the accuracy of the prediction model and would not necessarily be the same for each case. In this study, a 5^{th} order polynomial curve fit was sufficient in providing an accurate prediction result, however, it may not necessarily be applicable to every case. For example, A. Sanchez Escalona and Laskowski both utilised linear curve fits [60], [61]. It is recommended that, like this study, studies into the effect of different type of curve fits should be used on other applications to determine the prediction accuracy of the model and method that should be conducted.

- Inlet sensor data quality

The quality of any inlet condition data supplied to the prediction model by the environmental and mechanical sensors through the SCADA systems will impact the accuracy and subsequent usability of the method. Data quality may be influenced by factors such as clogged sensor ports, air recirculation, null data values, data “flatlining” (where subsequent

data values are equal to the previous due to an error), sensor calibration errors, and power cuts leading to sensor failure.

This will lead to subsequent prediction errors from the model, resulting in misrepresentations of the condition of the FBAC. Additionally, an issue encountered throughout this study is the inability to continuously determine air mass flow rate. Therefore, it is recommended that the study be conducted in a more controlled setting where off-design measurements can be effectively and accurately represented by reliable measuring sensors.

- Identification of types of inefficiencies

The condition monitoring method presented is not able to detect the types of inefficiencies present at the FBACs, but only the combined magnitude of impact they have on cooling performance. It is therefore recommended that future work focuses on combining the method proposed in this study with other means of determining the nature of the inefficiencies causing degradations in cooling performance.

- Evaluating the efficiency of maintenance efforts conducted

The evaluation conducted in this dissertation was unable to re-evaluate the cooling performance of the FBAC after maintenance and restorative efforts were conducted. Future studies could look at re-evaluating heat exchanger infrastructure post-maintenance and additionally look at restorative efforts to evaluate the efficiency and impact of the undertaking.

- Assumption of constant inherit and geometric operating parameters.

For the purposes of this dissertation, it was assumed that the inherit properties of the working fluids and the geometric properties of the heat exchange infrastructure did not vary with time or changes in operating conditions. Although an accurate assumption, future studies should focus on applying the method in more drastic operating environments where the magnitude of operation conditions would affect inherit properties of the working fluids. Additionally, scenarios where the geometric properties of the heat exchanger do vary with time could be considered.

- Choice of performance parameter

Given that this dissertation was mainly applied to underground FBACs, air outlet temperature was naturally chosen as the performance parameter indicating the cooling performance. However, future work should focus on using other outlet conditions to potentially monitor the cooling performance of the heat exchanger, and the subsequent degradation thereof.

- Choice of application industry

The method presented in this dissertation was implemented on finned tube bulk air coolers (FBACs) and on underground bulk air coolers. However, the universality of the presented method proves viable in implementing the method on other heat exchangers or operating infrastructure in the industry as a condition monitoring method. Therefore, future work should focus on implementing the method on other types of heat exchangers in the industry. Furthermore, future work should entail further developing the method to be implemented on other industrial equipment such as compressors, fans, etc. as a condition monitoring method.

4.4 Study closure

This chapter concluded the study by providing a general overview of the study, the compliance of obtained outcomes to study objectives set forth, and the limitations of the study with subsequent recommendations for future work.

Overall, this research contributes to the field of condition monitoring for underground FBACs, where the developed method has the potential to enhance the performance and longevity of FBACs in deep-level mining environments. The study conducted proved the strengths of the proposed method put forth for implementing condition monitoring on challenging infrastructure.

The method developed in this study was applied to heat exchanger infrastructure in the mining industry, however, the method may have implications for condition monitoring on other industrial infrastructure, and more research is needed to evaluate the feasibility thereof.

REFERENCE LIST

[1] US Department of Interior U.S Geological Survey, 'Mineral Commodity Summaries', 2018.

[2] P. N. Neingo and T. Tholana, 'Trends in productivity in the South African gold mining industry', *J. S. Afr. Inst. Min. Metall.*, vol. 116, no. 2, 2016, doi: 10.17159/2411-9717/2016/v116n3a10.

[3] C. Musingwini."Introduction of specialization in Mine Planning and Optimisation within the Master's degree (MSc) programme at the University of Witwatersrand." The 6th International Platinum Conference, 'Platinum–Metal for the Future', The Southern African Institute of Mining and Metallurgy, 2014.

[4] G. M. Mudd, 'Global trends in gold mining: Towards quantifying environmental and resource sustainability', *Resources Policy*, vol. 32, no. 1–2, pp. 42–56, Mar. 2007, doi: 10.1016/j.resourpol.2007.05.002.

[5] M. Van Eldyk, 'An investigation into the dsm and energy efficiency pqtential of a modular underground air cooling unit applied in the south african mining industry', Philosophiae Doctor, North-West University, 2006.

[6] D. H. Diering, 'Ultra-deep level mining—future requirements', Journal of the Southern African Institute of Mining and Metallurgy, 97(6), 249-255., 1997.

[7] R. C. W. Webber, R. M. Franz, W. M. Marx, and P. C. Schutte, 'A review of local and international heat stress indices, standards and limits with reference to ultra-deep mining'Journal of the Southern African Institute of Mining and Metallurgy, 103(5), pp.313-323, 2003.

[8] A. Ali, A. Kuyuk, S. Ghoreishi-Madiseh, and A. Sasmito, 'Numerical Study of Heat Transfer and Fluid Flow in Large-Scale Spray Cooling Systems; Example of Mine-Bulk-Air Cooler', Volume 5: Innovative Solutions for Energy Transitions: Part IV, preprint, Mar. 2020. doi: 10.46855/energy-proceedings-4247.

[9] M. Hooman, R. Webber-Youngman, J. du Plessis, and W. Marx, 'A decision analysis guideline for underground bulk air heat exchanger design specifications', *J. S. Afr. Inst. Min. Metall.*, vol. 115, no. 2, pp. 125–129, 2015, doi: 10.17159/2411-9717/2015/v115n2a6.

[10] C. F. Viljoen and K. Ranasinghe, 'Chilled water reduction on an underground bulk air cooler system by applying engineering principles'. 2013 Proceedings of the 10th Industrial and Commercial Use of Energy Conference (pp. 1-5). 2013

[11] A. M. Donoghue, 'Heat exhaustion in a deep underground metalliferous mine', *Occupational and Environmental Medicine*, vol. 57, no. 3, pp. 165–174, Mar. 2000, doi: 10.1136/oem.57.3.165.

[12] M. J. McPherson, *Subsurface Ventilation and Environmental Engineering*. Dordrecht: Springer Netherlands, 1993. doi: 10.1007/978-94-011-1550-6.

[13] H. G. Brand, M. Kleingeld, P. Mare, and A. J. Schutte, 'The effect of surface Bulk Air Cooler water flow on deep-level mine temperatures', in *2017 International Conference on the Industrial and Commercial Use of Energy (ICUE)*, Cape Town, South Africa: IEEE, Aug. 2017, pp. 1–6. doi: 10.23919/ICUE.2017.8067995.

[14] S. J. Bluhm, B. Se, and A. WHILLIER, 'The design of spray chambers for bulk cooling of the air in mines', Journal of the Southern African Institute of Mining and Metallurgy, 79(1), pp.1-9. 1978

[15] P. Lazaro and M. Momayez, 'Heat Stress in Hot Underground Mines: a Brief Literature Review', *Mining, Metallurgy & Exploration*, vol. 38, no. 1, pp. 497–508, Feb. 2021, doi: 10.1007/s42461-020-00324-4.

[16] M. R. Mulder, 'Improving air distribution in deep-level mine ventilation systems', Masters Degree, North-West University, 2019.

[17] L. Mackay, S. Bluhm, and J. V. Rensburg, 'Refrigeration and cooling concepts for ultra-deep platinum mining'.The 4th International Platinum Conference, Platinum in transition «Boom or Bust», The Southern African Institute of Mining and Metallurgy (pp. 285-292). 2010

[18] J. G. Pretorius, M. J. Mathews, P. Maré, M. Kleingeld, and J. Van Rensburg, 'Implementing a DIKW model on a deep mine cooling system', *International Journal of Mining Science and Technology*, vol. 29, no. 2, pp. 319–326, Mar. 2019, doi: 10.1016/j.ijmst.2018.07.004.

[19] S. Addepalli *et al.*, 'Degradation Study of Heat Exchangers', *Procedia CIRP*, vol. 38, pp. 137–142, 2015, doi: 10.1016/j.procir.2015.07.057.

[20] S. Łopata and P. Ocłoń, 'Numerical study of the effect of fouling on local heat transfer conditions in a high-temperature fin-and-tube heat exchanger', *Energy*, vol. 92, pp. 100–116, Dec. 2015, doi: 10.1016/j.energy.2015.03.048.

[21] S.-Z. Tang, Y.-L. He, F.-L. Wang, and Y.-B. Tao, 'Parametric study on fouling mechanism and heat transfer characteristics of tube bundle heat exchangers for reducing fouling considering the deposition and removal mechanisms', *Fuel*, vol. 211, pp. 301–311, Jan. 2018, doi: 10.1016/j.fuel.2017.09.015.

[22] K. M. Saqr and N. Musa, 'Numerical study of the heat transfer augmentation in pipes with internal discontinous longetudinal fins'.International journal of Mechanical and Materials Engineering, 4(1), pp.62-69. 2009

[23] B. Van Rooyen, 'Performance and fouling prediction model for finned-tube heat exchangers.pdf', Masters Degree, North West University, 2020.

[24] Z. Li, X. Liu, F. Wang, C. Zhu, H. Zhang, and S. Wang, 'Numerical analysis of the flow parameters on the heat transfer performance of a two-stage spiral casing heat exchanger', *TSE*, vol. 5, no. 1, p. 12, Mar. 2022, doi: 10.24294/tse.v5i1.1525.

[25] A. J. J. Al-Jassani, 'Experimental study for optimum fin spacing of rectangular fin arrangements under the influences of free convection.' J Eng Sci Technol, 15, pp.4075-4090. 2020

[26] University of South Florida and G. Zambrano, 'Measuring the Rate of Heat Loss Across Selected Building Materials', *UJMM*, vol. 11, no. 1, Oct. 2020, doi: 10.5038/2326-3652.11.1.4928.

[27] Y. Tamene, C. Bougriou, and R. Bessaïh, 'Thermal behaviour of a multilayer media in transient regime.' Revue des Energies Renouvelables, 10(3), pp.397-405. 2007

[28] Q. S. Mahdi and H. M. Jaffal, 'Experimental Investigation for the Thermal performance of Modified Closed Wet Cooling Tower.' Al-Nahrain Journal for Engineering Sciences, 19(2), pp.310-326, 2016

[29] E. Diaz-Bejarano, E. Behranvand, F. Coletti, M. R. Mozdianfard, and S. Macchietto, 'Organic and inorganic fouling in heat exchangers – Industrial case study: Analysis of fouling state', *Applied Energy*, vol. 206, pp. 1250–1266, Nov. 2017, doi: 10.1016/j.apenergy.2017.10.018.

[30] B. A. Qureshi and S. M. Zubair, 'Predicting the impact of heat exchanger fouling in refrigeration systems', *International Journal of Refrigeration*, vol. 44, pp. 116–124, Aug. 2014, doi: 10.1016/j.ijrefrig.2014.05.002.

[31] H. V. Inamdar, E. A. Groll, J. A. Weibel, and S. V. Garimella, 'Prediction of air-side particulate fouling of HVAC&R heat exchangers', *Applied Thermal Engineering*, vol. 104, pp. 720–733, Jul. 2016, doi: 10.1016/j.applthermaleng.2016.05.082.

[32] M. Markowski, M. Trafczynski, and K. Urbaniec, 'Validation of the method for determination of the thermal resistance of fouling in shell and tube heat exchangers', *Energy Conversion and Management*, vol. 76, pp. 307–313, Dec. 2013, doi: 10.1016/j.enconman.2013.07.052.

[33] F. Pelella, L. Viscito, and A. W. Mauro, 'Combined effects of refrigerant leakages and fouling on air-source heat pump performances in cooling mode', *Applied Thermal Engineering*, vol. 204, p. 117965, Mar. 2022, doi: 10.1016/j.applthermaleng.2021.117965.

[34] C. Shen, C. Cirone, L. Yang, Y. Jiang, and X. Wang, 'Characteristics of fouling development in shell-and-tube heat exchanger: Effects of velocity and installation location', *International Journal of Heat and Mass Transfer*, vol. 77, pp. 439–448, Oct. 2014, doi: 10.1016/j.ijheatmasstransfer.2014.05.031.

[35] S. K. Ogbonnaya and O. O. Ajayi, 'FOULING PHENOMENON AND ITS EFFECT ON HEAT EXCHANGER: A REVIEW', *Frontiers in Heat and Mass Transfer*, vol. 9, Dec. 2017, doi: 10.5098/hmt.9.31.

[36] E. Wallhäußer, W. B. Hussein, M. A. Hussein, J. Hinrichs, and T. M. Becker, 'On the usage of acoustic properties combined with an artificial neural network – A new approach of determining presence of dairy fouling', *Journal of Food Engineering*, vol. 103, no. 4, pp. 449–456, Apr. 2011, doi: 10.1016/j.jfoodeng.2010.11.015.

[37] V. F. Navarro Torres and R. N., ‘Thermal State and Human Comfort in Underground Mining’, in *Developments in Heat Transfer*, M. A. Dos Santos Bernardes, Ed., InTech, 2011. doi: 10.5772/19944.

[38] J. L. Glazer, ‘Management of Heatstroke and Heat Exhaustion’, vol. 71, no. 11, 2005.

[39] B. You, C. Wu, J. Li, and H. Liao, ‘Physiological responses of people in working faces of deep underground mines’, *International Journal of Mining Science and Technology*, vol. 24, no. 5, pp. 683–688, Sep. 2014, doi: 10.1016/j.ijmst.2014.03.024.

[40] H. Mäkinen and K. Jussila, ‘Cold-protective clothing: types, design and standards’, in *Protective Clothing*, Elsevier, 2014, pp. 3–38. doi: 10.1533/9781782420408.1.3.

[41] H. Truong-Ba, M. E. Cholette, P. Borghesani, L. Ma, and G. Kent, ‘Condition-based inspection policies for boiler heat exchangers’, *European Journal of Operational Research*, vol. 291, no. 1, pp. 232–243, May 2021, doi: 10.1016/j.ejor.2020.09.030.

[42] H. Truong Ba, M. E. Cholette, L. Ma, and G. Kent, ‘Condition-Based Inspection Grouping Policy for Boiler Heat Exchanger Tubes’, in *15th WCEAM Proceedings*, J. O. P. Pinto, M. L. M. Kimpara, R. R. Reis, T. Seecharan, B. R. Upadhyaya, and J. Amadi-Echendu, Eds., in Lecture Notes in Mechanical Engineering. Cham: Springer International Publishing, 2022, pp. 400–410. doi: 10.1007/978-3-030-96794-9_37.

[43] S. Prakash, N. Datta, and H. C. Deeth, ‘Methods of Detecting Fouling Caused by Heating of Milk’, *Food Reviews International*, vol. 21, no. 3, pp. 267–293, Jul. 2005, doi: 10.1080/FRI-200061609.

[44] O. Gudmundsson, O. P. Palsson, H. Palsson, and S. Lalot, ‘FOULI G DETECTIO I A CROSS-FLOW HEAT EXCHA GER BASED O PHYSICAL MODELI G’, 2009.

[45] J. Huang, G. Chen, L. Shu, S. Wang, and Y. Zhang, ‘An Experimental Study of Clogging Fault Diagnosis in Heat Exchangers Based on Vibration Signals’, *IEEE Access*, vol. 4, pp. 1800–1809, 2016, doi: 10.1109/ACCESS.2016.2555902.

[46] J. Berce, M. Zupančič, M. Može, and I. Golobič, ‘Infrared thermography observations of crystallization fouling in a plate heat exchanger’, *Applied Thermal Engineering*, p. 120116, Jan. 2023, doi: 10.1016/j.applthermaleng.2023.120116.

[47] Z. Qu, P. Jiang, and W. Zhang, ‘Development and Application of Infrared Thermography Non-Destructive Testing Techniques’, *Sensors*, vol. 20, no. 14, p. 3851, Jul. 2020, doi: 10.3390/s20143851.

[48] K. Peta, J. Żurek, and A. Patalas, ‘Non-destructive testing of automotive heat exchangers’, *MATEC Web Conf.*, vol. 244, p. 03007, 2018, doi: 10.1051/matecconf/201824403007.

[49] S. Freund and S. Kabelac, ‘Investigation of local heat transfer coefficients in plate heat exchangers with temperature oscillation IR thermography and CFD’,

International Journal of Heat and Mass Transfer, vol. 53, no. 19–20, pp. 3764–3781, Sep. 2010, doi: 10.1016/j.ijheatmasstransfer.2010.04.027.

[50] E. Wallhäußer, M. A. Hussein, and T. Becker, 'Detection methods of fouling in heat exchangers in the food industry', *Food Control*, vol. 27, no. 1, pp. 1–10, Sep. 2012, doi: 10.1016/j.foodcont.2012.02.033.

[51] E. Wallhäußer, A. Sayed, S. Nöbel, M. A. Hussein, J. Hinrichs, and T. Becker, 'Determination of cleaning end of dairy protein fouling using an online system combining ultrasonic and classification methods', *Food Bioprocess Technol*, vol. 7, no. 2, pp. 506–515, Feb. 2014, doi: 10.1007/s11947-012-1041-0.

[52] B. Merheb, G. Nassar, B. Nongaillard, G. Delaplace, and J. C. Leuliet, 'Design and performance of a low-frequency non-intrusive acoustic technique for monitoring fouling in plate heat exchangers', *Journal of Food Engineering*, vol. 82, no. 4, pp. 518–527, Oct. 2007, doi: 10.1016/j.jfoodeng.2007.03.022.

[53] I. V. Shvetsov, E. V. Garnyshova, E. V. Izmaylova, Y. V. Vankov, and A. R. Zagretdinov, 'Reducing labor input of monitoring condition of heat exchange equipment surfaces', *IOP Conf. Ser.: Mater. Sci. Eng.*, vol. 939, no. 1, p. 012072, Sep. 2020, doi: 10.1088/1757-899X/939/1/012072.

[54] M. Pang, L. Shu, J. Lu, X. Zhu, and J. Rodrigues, 'A case study: Monitoring heat exchanger based on vibration sensors and nondestructive testing technique', in *2013 8th International Conference on Communications and Networking in China (CHINACOM)*, Guilin, China: IEEE, Aug. 2013, pp. 511–516. doi: 10.1109/ChinaCom.2013.6694649.

[55] C.-M. Astorga-Zaragoza, A. Zavala-Río, V. M. Alvarado, R.-M. Méndez, and J. Reyes-Reyes, 'Performance monitoring of heat exchangers via adaptive observers', *Measurement*, vol. 40, no. 4, pp. 392–405, May 2007, doi: 10.1016/j.measurement.2006.06.009.

[56] C.-M. Astorga-Zaragoza, V.-M. Alvarado-Martínez, A. Zavala-Río, R.-M. Méndez-Ocaña, and G.-V. Guerrero-Ramírez, 'Observer-based monitoring of heat exchangers', *ISA Transactions*, vol. 47, no. 1, pp. 15–24, Jan. 2008, doi: 10.1016/j.isatra.2007.05.003.

[57] G. Zhou, Y. Ye, W. Zuo, X. Zhou, and X. Wu, 'Fast and efficient prediction of finned-tube heat exchanger performance using wet-dry transformation method with nominal data', *Applied Thermal Engineering*, vol. 145, pp. 133–146, Dec. 2018, doi: 10.1016/j.applthermaleng.2018.09.020.

[58] W. Pirompugd, S. Wongwises, and C.-C. Wang, 'A tube-by-tube reduction method for simultaneous heat and mass transfer characteristics for plain fin-and-tube heat exchangers in dehumidifying conditions', *Heat Mass Transfer*, vol. 41, no. 8, pp. 756–765, Jun. 2005, doi: 10.1007/s00231-004-0581-x.

[59] M. A. S. Jerónimo, L. F. Melo, A. Sousa Braga, P. J. B. F. Ferreira, and C. Martins, 'Monitoring the thermal efficiency of fouled heat exchangers: A simplified method',

Experimental Thermal and Fluid Science, vol. 14, no. 4, pp. 455–463, May 1997, doi: 10.1016/S0894-1777(96)00146-X.

[60] R. M. Laskowski, 'The application of the Buckingham theorem to modeling high-pressure regenerative heat exchangers in changed conditions.' Journal of Power Technologies, 91(4), p.198. 2011

[61] A. Sánchez-Escalona, E. Góngora-Leyva, and Y. Camaraza-Medina, 'Monoethanolamine Heat Exchangers Modeling Using the Buckingham Pi Theorem', *MMEP*, vol. 6, no. 2, pp. 197–202, Jun. 2019, doi: 10.18280/mmep.060207.

[62] J. C. Gibbings, *Dimensional Analysis*. London: Springer London, 2011. doi: 10.1007/978-1-84996-317-6.

[63] Frank M. White, *'Fluid Mechanics'*, Fourth. in McGraw - Hill Series in Mechanical Engineering. University of Rhode Island.

[64] A. A. Sánchez-Escalona, Y. Camaraza-Medina, Y. Retirado-Mediaceja, E. Góngora-Leyva, and M. Vega-Almaguer, 'Dimensional analysis applied to jacketed shell and tube heat exchangers modeling', *Enfoque UTE*, vol. 12, no. 3, pp. 36–50, Jul. 2021, doi: 10.29019/enfoqueute.745.

[65] R. A. P. Fockema, 'A customisable data analysis interface for an online electrical energy information system', Masters Degree, North West University, 2014.

[66] A.E Goosen, '"A system to quantify industrial data quality"', Masters Degree, North-West University, 2019.

[67] P.J.J Van Wyk, '"Evaluation of communication systems for deep level mining monitoring applications"', Masters Degree, University of Stellenbosch, 2011.

APPENDIX A – PROCESS OF DIMENSIONAL ANALYSIS

In this section, the process of using dimensional analysis is outlined to obtain a set of dimensionless groups. Table 2 shows the remaining system parameter and their respective base units. In Section 2.3.3, it was determined that the outlet air temperature was to be chosen as the performance parameter.

For simplification purposes, temperature differences of the remaining operating parameters were used instead of each temperature as a standalone variable. This was determined using the heat transfer equation and a version of Fourier's law, described in Section 1.3. This will not, however, affect the primary dimensions obtained, as noted by Sanches Escalona *et. al.* and Lazowski *et. al.* [60], [61].

Equation (3.1) presents the performance parameter as a function of the remaining system parameters:

$$T_{air_{out}} - T_{air_{in}} = f\left(T_{air_{in}} - T_{water_{in}}, \dot{m}_{air}, \dot{m}_{water}\right) \tag{3.1}$$

To obtain dimensional unity, the units of the left side should correspond to the units on the right side, therefore a comparison of dimensions was done. Equation (3.1) was rewritten in another form in preparation for comparing dimensional units:

$$[T_{air_{out}} - T_{air_{in}}] = [T_{air_{in}} - T_{water_{in}}][\dot{m}_{water}][\dot{m}_{air}] \tag{3.2}$$

Each system operating parameter is re-written to their base unit described in Table 2, and is assigned a constant exponent:

$$[\theta]^1 = [\theta]^a\,[MT^{-1}]^b[MT^{-1}]^c \tag{3.3}$$

By inspection, the exponents were determined by:

$$[\theta]: \quad 1 = a \tag{3.4}$$

$$[M]: \quad 0 = b + c$$

$$[T]: \quad 0 = -b - c$$

Therefore, giving the values of the exponents as:

$$a = 1$$

$$c = -b$$

And by Equation (3.3), giving:

$$[\theta]^1 = [\theta]^1 \, [MT^{-1}]^b [MT^{-1}]^{-b} \tag{3.5}$$

Re-arranging the base units back to the operating parameters:

$$[T_{air_{out}} - T_{air_{in}}] = \left[T_{air_{in}} - T_{water_{in}}\right]^1 [\dot{m}_{water}]^b [\dot{m}_{air}]^{-b} \tag{3.6}$$

Re-arranging for the temperature and mass flow terms on either side:

$$\frac{[T_{air_{out}} - T_{air_{in}}]}{\left[T_{air_{in}} - T_{water_{in}}\right]} = \frac{[\dot{m}_{water}]^b}{[\dot{m}_{aim}]^b} \tag{3.7}$$

$$\left[\frac{T_{air_{out}} - T_{air_{in}}}{T_{air_{in}} - T_{water_{in}}}\right] = \left[\frac{\dot{m}_{water}}{\dot{m}_{aim}}\right]^b \tag{3.8}$$

From Equation (3.8), two dimensionless groups had been obtained:

$$\Pi_1 = \left[\frac{T_{air_{out}} - T_{air_{in}}}{T_{air_{in}} - T_{water_{in}}}\right] \quad (3.9)$$

$$\Pi_2 = \left[\frac{\dot{m}_{water}}{\dot{m}_{aim}}\right]$$

This corresponds with the dimensionless groups obtained by both Sanchez Escalona *et. al.* and Laskowski *et. al.* [60], [61].

APPENDIX B – FBAC MONITORING GRAPHS

The following section provides the results of implementing the prediction model on the remaining FBACs on Mine A not specifically presented in the main body:

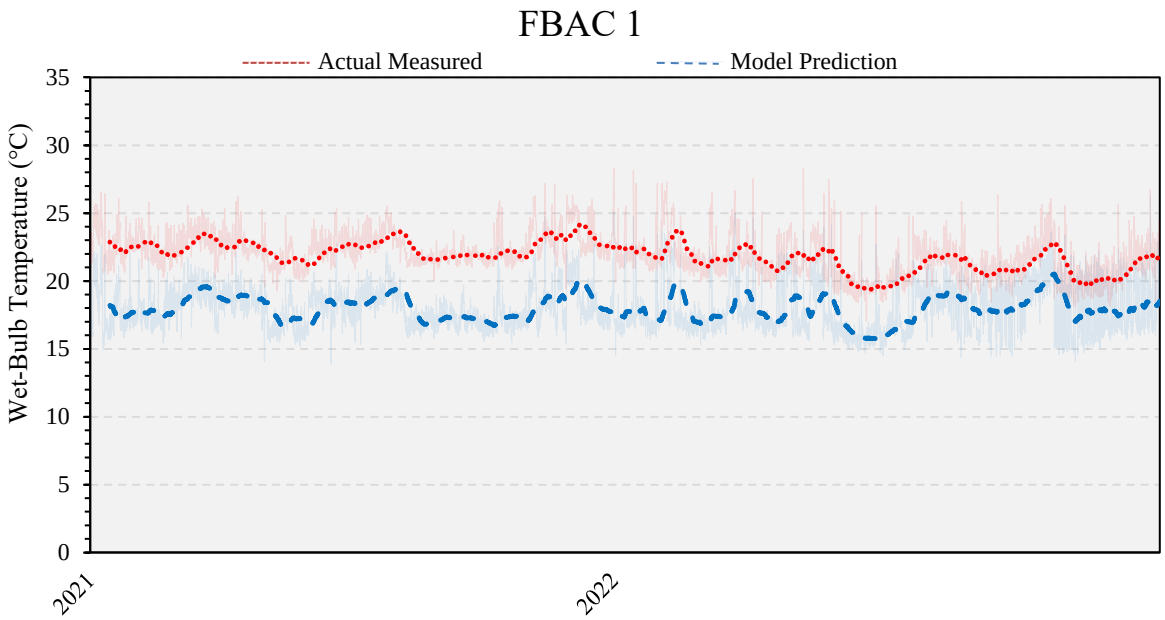

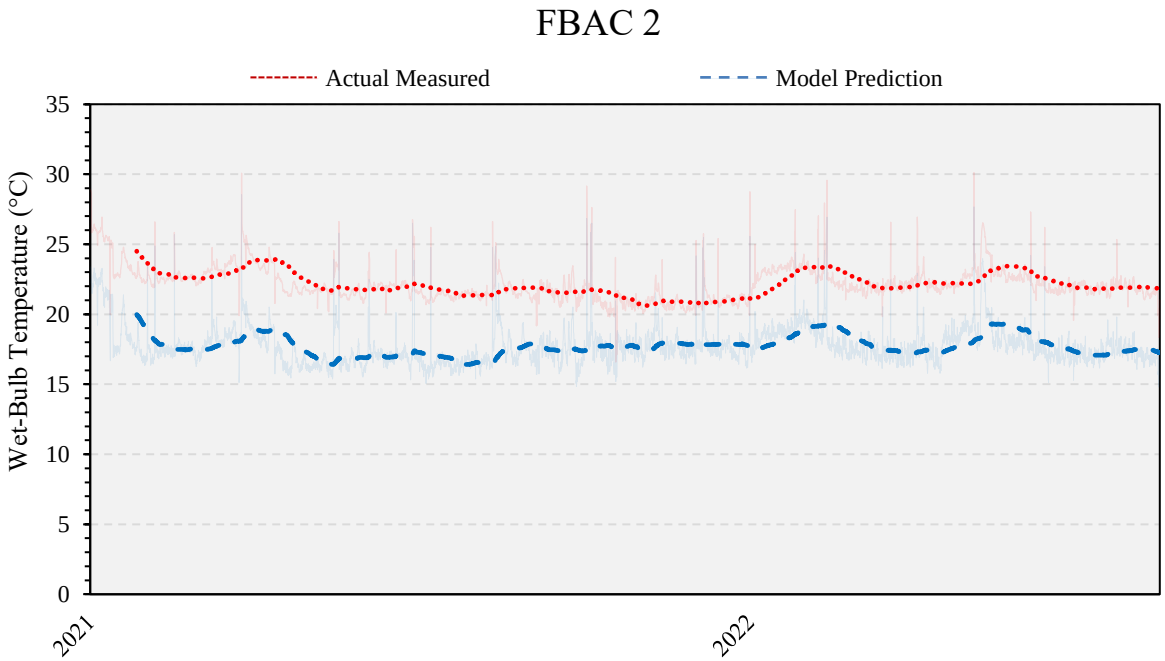

FBAC 3

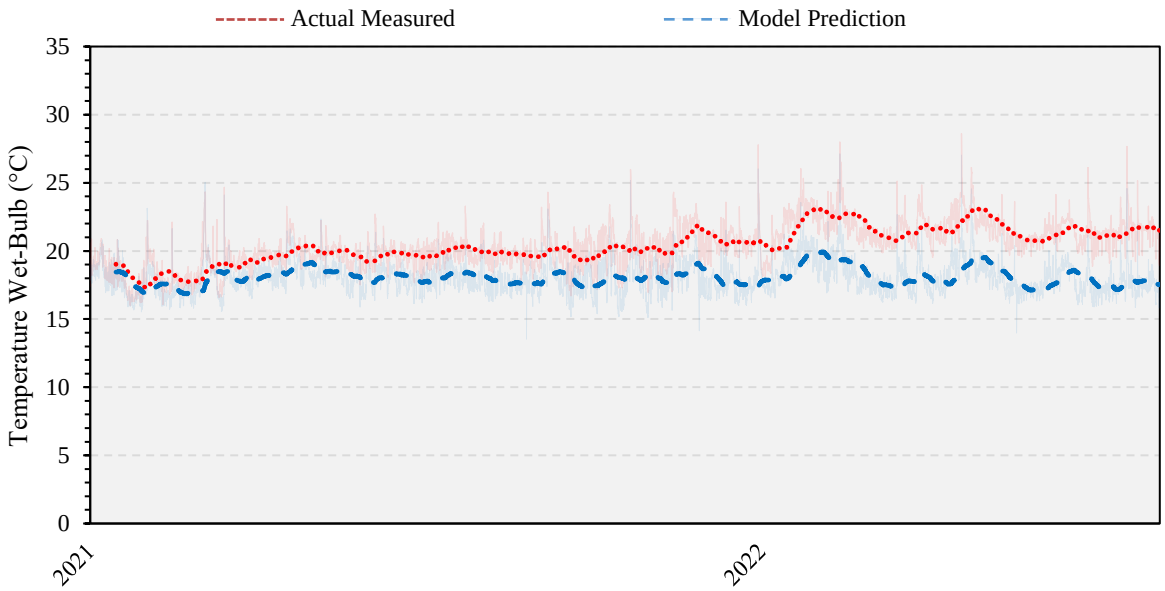
Actual Measured
Model Prediction
Temperature Wet-Bulb (°C)
35
30
25
20
15
10
5
0
2021
2022

FBAC 4

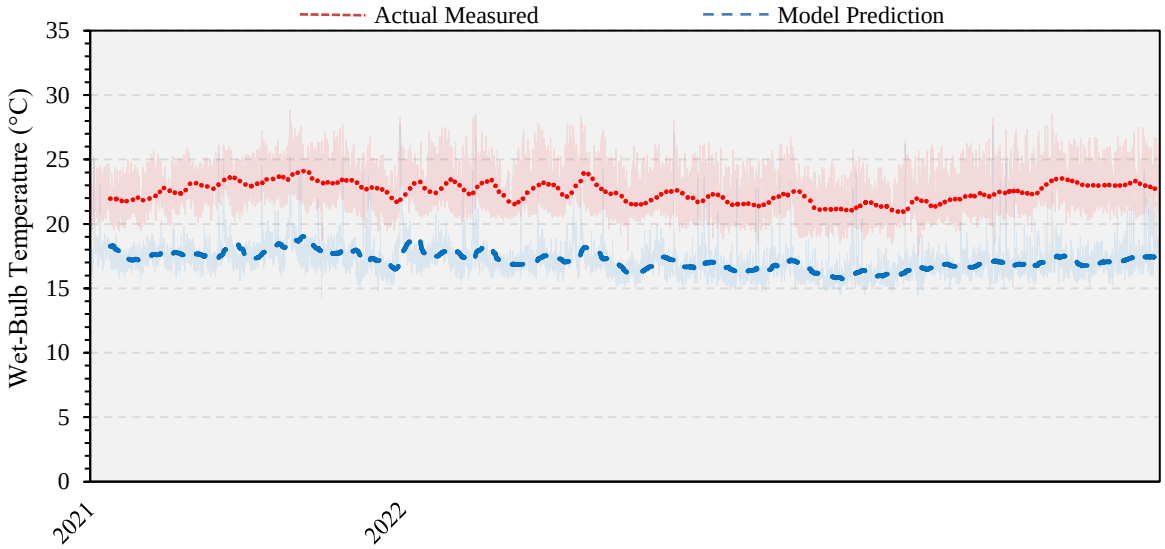
Actual Measured
Model Prediction
Wet-Bulb Temperature (°C)
35
30
25
20
15
10
5
0
2021
2022

FBAC 5

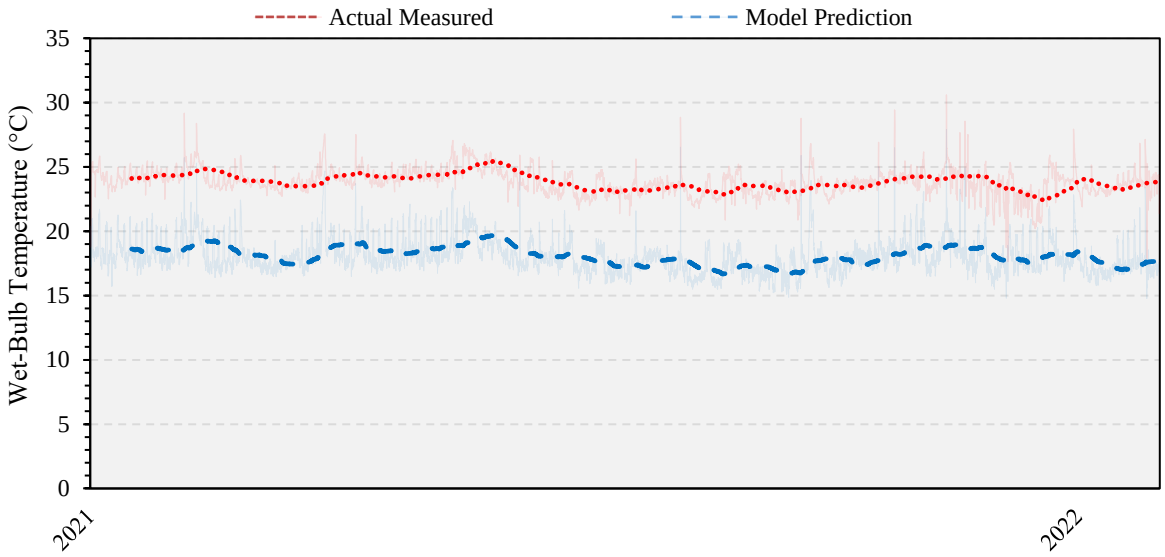
Actual Measured
Model Prediction
Wet-Bulb Temperature (°C)
35
30
25
20
15
10
5
0
2021
2022

FBAC 6

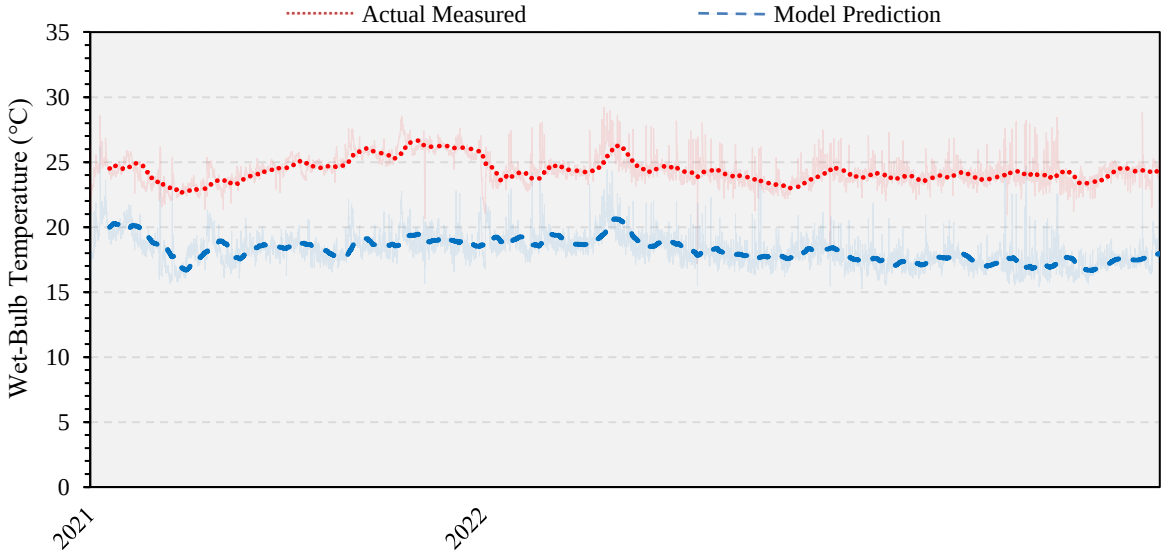
Actual Measured
Model Prediction
Wet-Bulb Temperature (°C)
35
30
25
20
15
10
5
0
2021
2022

FBAC 7

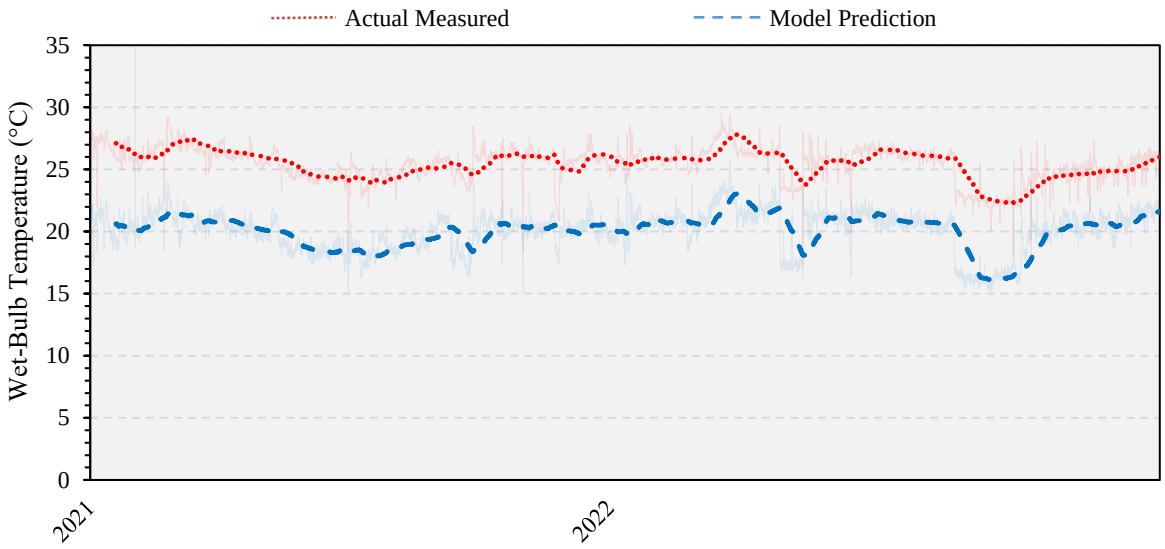

In summary, all FBACs on Mine A were found to deviate from their design condition in some form or another. As discussed in the main body of the dissertation, FBAC 6 showed the largest degree of deviation with an average magnitude of 6.09 °C. FBAC 3 had shown the least amount of average deviation over the evaluation period.

APPENDIX C – OEM DESIGN TABLES

The following section provides all of the OEM design specification tables used to calibrate the prediction model:

Temperature of Water In	***11.4 °C***
Wet Bulb Temperature of Air In	***22.5 °C***
Dry Bulb Temperature of Air In	***24 °C***
Barometric Pressure	***117 kPa***

MANOS
ENGINEERING (PTY.)LTD.

l/s	kPa									
L	ΔP_w	G'►	2	3	4	4.7	5	6	7	8	m^3/s
▼	▼	ΔP_a►	56	113	187	247	275	378	495	625	Pa
4.0	96	q	64.01	85.11	101.17	110.17	113.57	123.3	131.07	137.37	kW
		two	15.22	16.48	17.44	17.98	18.18	18.76	19.23	19.6	°C
		tao	13.88	15	15.92	16.46	16.66	17.28	17.78	18.21	°C
5.0	148	q	65.82	89.14	107.81	118.69	122.89	135.21	145.41	153.93	kW
		two	14.54	15.66	16.55	17.07	17.27	17.86	18.35	18.75	°C
		tao	13.59	14.59	15.43	15.93	16.13	16.72	17.21	17.64	°C
6.0	210	q	66.99	91.85	112.39	124.69	129.5	143.89	156.1	166.55	kW
		two	14.07	15.06	15.87	16.36	16.55	17.13	17.61	18.03	°C
		tao	13.41	14.31	15.08	15.55	15.74	16.3	16.78	17.2	°C
6.1	217	q	67.08	92.07	112.77	125.18	130.05	144.65	157.01	167.65	kW
		two	14.03	15	15.82	16.3	16.49	17.06	17.55	17.96	°C
		tao	13.39	14.29	15.05	15.52	15.71	16.26	16.74	17.16	°C
7.0	283	q	67.81	93.77	115.73	129.12	134.42	150.45	164.33	176.38	kW
		two	13.71	14.6	15.35	15.81	15.99	16.53	17.01	17.42	°C
		tao	13.28	14.11	14.83	15.27	15.45	15.98	16.45	16.85	°C
8.0	367	q	68.42	95.22	118.25	132.5	138.18	155.57	170.78	184.23	kW
		two	13.44	14.24	14.93	15.36	15.53	16.04	16.5	16.9	°C
		tao	13.18	13.96	14.64	15.05	15.22	15.73	16.18	16.57	°C
9.0	460	q	68.89	96.34	120.24	135.17	141.17	159.63	176.01	190.61	kW
		two	13.23	13.96	14.59	14.99	15.15	15.64	16.07	16.46	°C
		tao	13.1	13.85	14.49	14.88	15.04	15.53	15.96	16.34	°C
10.0	564	q	69.26	97.24	121.83	137.34	143.58	162.95	180.3	195.9	kW
		two	13.05	13.72	14.31	14.68	14.83	15.29	15.71	16.08	°C
		tao	13.04	13.75	14.36	14.74	14.9	15.36	15.78	16.15	°C

L = Water flow in l/s
ΔPw = Water pressure drop in kPa
G'► = Air flow in m3/s
ΔPa► = Air pressure drop in Pa
q = Duty of coil in kW
two = Temperature of water leaving coil
tao = Temperature of air leaving coil

Temperature of Water In	***12.5***	***°C***
Wet Bulb Temperature of Air In	***23.5***	***°C***
Dry Bulb Temperature of Air In	***26.5***	***°C***
Barometric Pressure	***117***	***kPa***

MANOS

ENGINEERING (PTY.)LTD.

l/s	kPa									
L ▼	ΔP_w ▼	G'► ΔP_a►	4 186	5 274	6 376	6.2 398	7 492	8 621	9 763	10 918	m^3/s Pa
4.0	96	q	101.13	113.33	122.89	124.54	130.5	136.69	141.77	145.99	kW
		two	18.54	19.27	19.84	19.94	20.29	20.66	20.96	21.22	°C
		tao	17.12	17.85	18.45	18.56	18.94	19.36	19.7	20	°C
5.0	148	q	107.9	122.78	134.91	137.07	144.94	153.34	160.39	166.43	kW
		two	17.65	18.36	18.94	19.05	19.42	19.82	20.16	20.45	°C
		tao	16.64	17.33	17.9	18.01	18.39	18.81	19.16	19.47	°C
5.9	204	q	112.19	128.93	142.95	145.49	154.79	164.9	173.59	181.13	kW
		two	17.04	17.72	18.29	18.39	18.77	19.18	19.53	19.83	°C
		tao	16.33	16.98	17.53	17.63	18.01	18.42	18.77	19.09	°C
6.0	210	q	112.6	129.52	143.72	146.28	155.75	166.03	174.91	182.6	kW
		two	16.98	17.66	18.22	18.32	18.7	19.11	19.46	19.77	°C
		tao	16.3	16.94	17.5	17.6	17.97	18.38	18.73	19.05	°C
7.0	283	q	116.04	134.56	150.4	153.29	164.08	175.97	186.4	195.57	kW
		two	16.46	17.09	17.63	17.73	18.1	18.5	18.86	19.17	°C
		tao	16.04	16.66	17.18	17.28	17.64	18.04	18.39	18.7	°C
8.0	367	q	118.65	138.41	155.61	158.77	170.65	183.91	195.66	206.15	kW
		two	16.04	16.63	17.15	17.24	17.59	17.99	18.34	18.65	°C
		tao	15.85	16.43	16.94	17.03	17.38	17.77	18.11	18.42	°C
9.0	460	q	120.7	141.46	159.75	163.15	175.94	190.38	203.3	214.92	kW
		two	15.7	16.25	16.74	16.83	17.17	17.55	17.9	18.2	°C
		tao	15.7	16.25	16.74	16.83	17.16	17.54	17.88	18.18	°C
10.0	564	q	122.33	143.95	163.15	166.75	180.31	195.75	209.67	222.28	kW
		two	15.42	15.94	16.4	16.48	16.81	17.18	17.51	17.81	°C
		tao	15.58	16.11	16.57	16.66	16.99	17.35	17.68	17.98	°C

L = Water flow in l/s
ΔPw = Water pressure drop in kPa
G'► = Air flow in m3/s
ΔPa► = Air pressure drop in Pa
q = Duty of coil in kW
two = Temperature of water leaving coil
tao = Temperature of air leaving coil

Temperature of Water In	***12.59 °C***
Wet Bulb Temperature of Air In	***23.5 °C***
Dry Bulb Temperature of Air In	***26 °C***
Barometric Pressure	***117 kPa***

MANOS

ENGINEERING (PTY.)LTD.

l/s	kPa										m³/s
L ▼	ΔP_w ▼	G'► ΔP_a►	4 186	5 274	6 376	6.3 410	7 493	8 622	9 764	10 919	Pa
4.0	96	q	100.42	112.5	121.98	124.42	129.54	135.66	140.67	144.86	kW
		two	18.59	19.31	19.87	20.02	20.32	20.69	20.99	21.24	°C
		tao	17.18	17.91	18.5	18.66	18.99	19.4	19.74	20.03	°C
5.0	148	q	107.15	121.9	133.94	137.12	143.88	152.18	159.19	165.18	kW
		two	17.71	18.41	18.99	19.14	19.46	19.86	20.19	20.48	°C
		tao	16.7	17.39	17.96	18.11	18.44	18.85	19.2	19.51	°C
5.4	172	q	109.21	124.85	137.75	141.19	148.55	157.63	165.39	172.04	kW
		two	17.42	18.11	18.68	18.83	19.16	19.56	19.9	20.2	°C
		tao	16.55	17.22	17.78	17.93	18.26	18.67	19.02	19.33	°C
6.0	210	q	111.82	128.62	142.7	146.48	154.62	164.82	173.6	181.23	kW
		two	17.04	17.71	18.27	18.42	18.74	19.15	19.5	19.8	°C
		tao	16.36	17.01	17.55	17.7	18.02	18.43	18.78	19.09	°C
7.0	283	q	115.25	133.61	149.35	153.6	162.91	174.71	185.03	194.15	kW
		two	16.52	17.15	17.69	17.83	18.15	18.55	18.9	19.21	°C
		tao	16.11	16.72	17.24	17.39	17.7	18.09	18.44	18.75	°C
8.0	367	q	117.85	137.47	154.51	159.19	169.44	182.59	194.27	204.65	kW
		two	16.11	16.69	17.2	17.34	17.65	18.04	18.39	18.7	°C
		tao	15.92	16.5	17	17.14	17.43	17.82	18.16	18.46	°C
9.0	460	q	119.89	140.52	158.65	163.68	174.72	189.04	201.84	213.36	kW
		two	15.77	16.32	16.8	16.93	17.23	17.61	17.95	18.25	°C
		tao	15.77	16.32	16.8	16.93	17.22	17.6	17.93	18.23	°C
10.0	564	q	121.52	142.98	162.04	167.34	179.08	194.36	208.16	220.69	kW
		two	15.49	16	16.46	16.59	16.87	17.23	17.56	17.86	°C
		tao	15.65	16.18	16.64	16.77	17.05	17.41	17.73	18.03	°C

L = Water flow in l/s
ΔPw = Water pressure drop in kPa
G'► = Air flow in m3/s
ΔPa► = Air pressure drop in Pa
q = Duty of coil in kW
two = Temperature of water leaving coil
tao = Temperature of air leaving coil

Temperature of Water In	***16.2 °C***
Wet Bulb Temperature of Air In	***23.25 °C***
Dry Bulb Temperature of Air In	***27.5 °C***
Barometric Pressure	***120 kPa***

MANOS

ENGINEERING (PTY.)LTD.

l/s	kPa									
L ▼	ΔP_w ▼	G'► ΔP_a►	4 189	5 279	6 383	7 501	7.2 526	8 632	9 777	10 935	m³/s Pa
4.0	96	q	66.1	73.81	79.84	84.64	85.48	88.53	91.72	94.37	kW
		two	20.15	20.61	20.97	21.25	21.3	21.49	21.68	21.83	°C
		tao	19.24	19.7	20.07	20.37	20.43	20.63	20.85	21.03	°C
5.0	148	q	70.74	80.22	87.91	94.26	95.39	99.55	104.02	107.82	kW
		two	19.58	20.03	20.4	20.7	20.76	20.96	21.17	21.35	°C
		tao	18.93	19.36	19.72	20.03	20.08	20.29	20.51	20.7	°C
6.0	210	q	74	84.82	93.87	101.51	102.89	108.03	113.65	118.52	kW
		two	19.15	19.58	19.94	20.24	20.3	20.5	20.72	20.92	°C
		tao	18.72	19.12	19.47	19.76	19.82	20.02	20.24	20.43	°C
7.0	283	q	76.41	88.27	98.41	107.13	108.73	114.69	121.33	127.15	kW
		two	18.81	19.21	19.56	19.86	19.91	20.11	20.34	20.54	°C
		tao	18.56	18.94	19.27	19.56	19.61	19.8	20.02	20.22	°C
7.2	299	q	76.8	88.86	99.18	108.09	109.73	115.86	122.67	128.67	kW
		two	18.75	19.15	19.49	19.79	19.84	20.04	20.27	20.47	°C
		tao	18.53	18.91	19.24	19.52	19.57	19.77	19.99	20.18	°C
8.0	367	q	78.22	90.94	101.96	111.58	113.36	120.05	127.54	134.22	kW
		two	18.54	18.92	19.24	19.53	19.58	19.78	20.01	20.21	°C
		tao	18.43	18.8	19.12	19.39	19.44	19.63	19.85	20.04	°C
9.0	460	q	79.68	93.08	104.82	115.2	117.13	124.43	132.68	140.09	kW
		two	18.31	18.67	18.98	19.26	19.31	19.5	19.72	19.92	°C
		tao	18.34	18.69	18.99	19.26	19.31	19.49	19.7	19.89	°C
10.0	564	q	80.83	94.8	107.16	118.19	120.25	128.07	136.97	145.04	kW
		two	18.13	18.46	18.76	19.02	19.07	19.26	19.47	19.66	°C
		tao	18.26	18.6	18.89	19.14	19.19	19.37	19.58	19.76	°C

L = Water flow in l/s
ΔPw = Water pressure drop in kPa
G'► = Air flow in m3/s
ΔPa► = Air pressure drop in Pa
q = Duty of coil in kW
two = Temperature of water leaving coil
tao = Temperature of air leaving coil

APPENDIX D – PREDICTION MODEL CHARACTERISTIC EQUATION

For the sake of completeness, the following passages will show how the characteristic equation of the prediction model was obtained from the data sets presented in Figure 44 following Section 2.4.2 and Section 2.4.3 and utilizing a 5th order polynomial curve fit. The empirical equation with the respective calibration factors obtained using the 5th order polynomial curve fit chosen is shown in Equation (3.14) below:

$$\frac{T_{air_{out}} - T_{air_{in}}}{T_{air_{in}} - T_{water_{in}}} = -0.0081\left(\frac{\dot{m}_w}{\dot{m}_a}\right)^5 + 0.0915\left(\frac{\dot{m}_w}{\dot{m}_a}\right)^4 - 0.3907\left(\frac{\dot{m}_w}{\dot{m}_a}\right)^3 + 0.8119\left(\frac{\dot{m}_w}{\dot{m}_a}\right)^2 - 0.936\left(\frac{\dot{m}_w}{\dot{m}_a}\right) - 0.2618 \quad (3.14)$$

Following Section 2.4.3, and rearranging Equation (3.14) for the chosen performance parameter (outlet wet-bulb air temperature), and keeping in mind the simplifications made in Equation (2.9), Equation (3.15) is obtained:

$$T_{air_{out}} = T_{air_{in}} + T_{max}\left[-0.0081\left(\frac{\dot{m}_w}{\dot{m}_a}\right)^5 + 0.0915\left(\frac{\dot{m}_w}{\dot{m}_a}\right)^4 - 0.3907\left(\frac{\dot{m}_w}{\dot{m}_a}\right)^3 + 0.8119\left(\frac{\dot{m}_w}{\dot{m}_a}\right)^2 - 0.936\left(\frac{\dot{m}_w}{\dot{m}_a}\right) - 0.2618\right] \quad (3.15)$$

Equation (3.15) above denotes the final form of the characteristic equation of the prediction model obtained that was used to verify the prediction accuracy of different curve fits, and subsequently used to implement the prediction model on the case study FBACs. Considering the successful verification of the prediction model obtained by applying the method, the prediction model was implemented on the case study FBACs on Mine A, adhering to the guidelines presented in Section 2.5 of the method outline.

APPENDIX E – LITERATURE REVIEW SUMMARY

The following section provides the state-of-the-art tables of the literature review conducted. Table 13 shows the relevancy of the literature considered and reviewed, and Table 14 shows how each study reviewed complied with the set evaluation criteria put forth in Section 1.7.1:

Table 13: Relevance of literature considered for implementation on underground FBACs, showing lack of condition monitoring literature on finned tube heat exchangers applicable in the mining industry.

			Condition Monitoring Method			**Type of Heat Exchanger**			**Applicable Industry**			
Reference	Author	Year	Direct/Destructive	Non-Destructive	Indirect	Plate	Finned Tube	Shell And Tube	Industrial/Power Plants	Housing	Automotive	Mining
[41]	Truong Ba *et. al.*	2021										
[43]	Prakash *et. al.*.	2005										
[42]	Truong Ba *et. al.*	2022										
[35]	Ogbonnaya *et. al.*	2017										
[44]	Gudmundsson *et. al.*	2009										
[45]	Huang *et. al.*.	2016										
[46]	Berce *et. al.*.	2023										
[19]	Addepalli *et. al.*.	2015										
[47]	Qu *et. al.*.	2020										
[48]	Peta *et. al.*.	2018										
[49]	Freund *et. al.*.	2010										

[50]	WallHauber *et. al.*.	2012										
[52]	Merheb *et. al.*.	2007										
[53]	Shvetsov *et. al.*.	2020										
[51]	WallHauber *et. al.*.	2014										
[23]	Van Rooyen *et. al.*.	2019										
[54]	Pang *et. al.*.	2013										
[55]	Astorga *et. al.*.	2007										
[56]	Astorga *et. al.*.	2008										
[34]	Shen *et. al.*.	2014										
[21]	Tang *et. al.*.	2018										
[58]	Pirompugd *et. al.*.	2005										
[57]	Zhou *et. al.*.	2018										
[59]	Jeronimo *et. al.*.	1997										
[64]	SánchezEscalona *et. al.*	2021										
[60]	Lasowski et. al.	2011										

Table 14: Evaluation summary of existing heat exchanger condition monitoring literature for compliance to the evaluation criteria set forth in Section 1.7.1, showing shortcomings of each and the holistic non-compliance to all methods considered.

			EVALUATION CRITERIA										
			Condition Monitoring Method			Continuous Monitoring?	Remote Monitoring?	Operating Conditions?		Detect Multiple Inefficiencies?	Accurate and Reliable for Mines?	**Does method comply with all evaluation criteria?**
Reference	Author	Year	Direct/Destructive	Non-Destructive	Indirect	Yes	Yes	Design	Off-Design	Yes	Yes	
[41]	Truong Ba *et. al.*	2021										
[43]	Prakash *et. al.*.	2005										
[42]	Truong Ba *et. al.*	2022										
[35]	Ogbonnaya *et. al.*	2017										
[44]	Gudmundsson *et. al.*	2009										
[45]	Huang *et. al.*.	2016										
[46]	Berce *et. al.*.	2023										
[19]	Addepalli *et. al.*.	2015										
[47]	Qu *et. al.*.	2020										
[48]	Peta *et. al.*.	2018										
[49]	Freund *et. al.*.	2010										
[50]	WallHauber *et. al.*.	2012										
[52]	Merheb *et. al.*.	2007										
[53]	Shvetsov *et. al.*.	2020										

[51]	WallHauber *et. al.*.	2014											
[23]	Van Rooyen *et. al.*.	2019											
[54]	Pang *et. al.*.	2013											
[55]	Astorga *et. al.*.	2007											
[56]	Astorga *et. al.*.	2008											
[34]	Shen *et. al.*.	2014											
[21]	Tang *et. al.*.	2018											
[58]	Pirompugd *et. al.*.	2005											
[57]	Zhou *et. al.*.	2018											
[59]	Jeronimo *et. al.*.	1997											
[64]	Sánchez-Escalona *et. al.*	2021											
[60]	Laskowski *et. al.*.	2011											